BIOLOGICAL RHYTHMS OF VOCAL BEHAVIOR IN FISH: HORMONAL, NEURONAL, AND GENETIC MECHANISMS

A Dissertation

Presented to the Faculty of the Graduate School

of Cornell University

In Partial Fulfillment of the Requirements for the Degree of

Doctor of Philosophy

by

Ni Ye Feng

February 2016

© 2016 Ni Ye Feng

BIOLOGICAL RHYTHMS OF VOCAL BEHAVIOR IN FISH: HORMONAL, NEURONAL, AND GENETIC MECHANISMS

Ni Ye Feng, Ph. D.

Cornell University 2016

Vocalization is a prominent feature of social communication among vertebrates. For energetically costly vocal-acoustic courtship behaviors, timing across seconds, days, and seasons is critical and can enhance sender-receiver coupling, reproductive success, and reproductive isolation. Many species of fish produce sound to communicate in different social contexts, such as courtship. Here, I investigated hormonal, neuronal, and genetic mechanisms underlying the timing of vocal behavior in the plainfin midshipman fish (*Porichthys* notatus), across timescales spanning milliseconds to seasons. I demonstrated that the robust daily rhythm of midshipman male's nocturnal courtship vocalization is under endogenous, circadian control. Exogenous delivery of melatonin, the nocturnal hormone in vertebrates, rescued the inhibition of courtship vocalization under constant light, which abolishes endogenous melatonin production. Melatonin also rescued the inhibition of neural excitability in the midshipman vocal network under constant light. Furthermore, melatonin receptor 1b mRNA was shown to be expressed in neuroendocrine, sensory (including auditory) and vocal motor pathways. Together, these results support the hypothesis that melatonin plays a central role in timing the nocturnal midshipman courtship vocalization by acting on specific neural pathways. Finally, I used RNA-sequencing to characterize the transcriptome of

the vocal motor nucleus (VMN), the final node of the hindbrain vocal pattern generator that directly determines vocalization temporal characteristics such as duration and frequency. I identified a suite of candidate genes, including ion channels, for shaping the precise and synchronous firing of VMN motor neurons. Many candidate genes showed day-night and seasonal changes in expression. Furthermore, enrichment and high expression of cellular respiration genes in VMN compared to the surrounding hindbrain tissue likely enable midshipman courtship calls that can last up to hours, and suggest that the neural patterning of vocal behavior is energetically costly. Finally, high expression of several antioxidant genes in VMN suggested a high capacity for combating cellular respiration-generated oxidative stress, which may also enable long duration courtship call production. Altogether, these chapters identify mechanisms underlying the timing of vocalization that may be applicable across other lineages of vertebrates, including birds and mammals, which exhibit rhythmic production of vocalization across multiple timescales.

BIOGRAPHICAL SKETCH

Ni was born in Beijing, China, to Feng Chufang and Ye Liang in 1985. She immigrated to the U.S. in 1996 and was naturalized in 2013, when she officially added "Ye" as her middle name. See Acknowledgments for the cast of family members who have contributed significantly to her upbringing and personal development.

Ni earned a Bachelor of Science degree from the University of California, Los Angeles (2003-2007) where she majored in Biology and minored in Art History. During her junior year, she joined Barney Schlinger's laboratory of neuroendocrinology and discovered a passion for basic scientific research and for studying the neural and hormonal basis of behavior. Her senior thesis examined how steroid hormones contribute to the acrobatic courtship display of the Golden-collared manakin (*Manacus vitellinus*), a suboscine bird found in the rainforests of Panama. This work resulted in her first peer-reviewed publication in the journal Endocrinology.

Ni is perpetually fascinated by the "how" questions in biology. For example, how do conserved signaling molecules such as hormones contribute to the expression of diverse behaviors across taxa? How do similarities or differences in hormone receptors carry out similar or different actions? Where are these receptors expressed in the brain, and how do these brain regions control behavior?

In pursuit of some of these questions, Ni joined the Bass lab in the Fall of 2009. In the ensuing years, she became fascinated with the charismatic "singing" fish, the plainfin midshipman (*Porichthys notatus*), as a neuroethological model for studying how hormones and the nervous system work together to pattern vocal-acoustic behavior.

Dedicated to my family, the village who raised me.

ACKNOWLEDGMENTS

I am forever grateful for and indebted to the family, friends, mentors, colleagues, and departmental staff who have made this journey possible. First, I would like to thank Andy Bass and Midge Marchaterre for their incredible support throughout my graduate career. Andy inspires me everyday with his work ethic, scientific rigor, and excitement about the brain and behavior. His passion for science and mentorship is palpable and comes across in even the most mundane conversations. Andy has always been a responsible mentor who is expedient in answering any of my questions or concerns, whether it is getting back to me on a technical question, helping me with a grant application, or editing a manuscript. I am grateful for the many challenges and opportunities Andy has given me, such as being apart of grant writing, starting a more "high-risk" RNA-sequencing project, and contributing to a book chapter. Not only did Andy stand up for my interests, he also extended guidance and resources to help my fellow NBB graduate student and boyfriend, Matt Lewis, during several trying times. Andy is a champion of his students, and I am so grateful for his mentorship, guidance, and support over the past six years.

I am also grateful to Midge for all she has done for me throughout my Ph.D. Over the years, Midge has helped me collect tissue at all hours of the day, spent countless hours trouble-shooting and performing in-situ hybridization that was crucial for one of the chapters presented here, and supported me whenever I struggled with experiments or analyses. I was fortunate to have gone on several field seasons with Midge, where in addition to work, she always made sure each trip was fun and educational, like the time she insisted that we go to the California Academy of

Sciences even though we would then be rushed to catch a flight. There is never a dull moment when you are with Midge! I will treasure memories of the many elaborate lab celebrations and pig roasts she has tirelessly organized, and the warmth and compassion that she showers on the people around her.

I would also like to thank the many Bass lab members who have been my mentors, friends, and fieldwork buddies over the years, including Boris Chagnaud, Kevin Rohmann, Dan Fergus, Irene Ballagh, Joel Tripp, and Raquel Vasconcelos. Boris trained me on electrophysiology, pushed me to persevere and think critically. Kevin not only trained me on a variety of techniques in the lab, but also helped me tremendously outside of lab, especially when I first moved to Ithaca. I am also grateful to Dan for being so patient, funny, and generous. He would always stop anything he is doing to answer a question or help with a problem. I was very fortunate to have him as a mentor and a partner throughout our transcriptome project. Excellent undergraduates such as Rachel Genova, Grace Ahn, Frenda Yip, and Clara Liao have helped me with many crucial aspects of data collection and analysis.

I would like to thank my thesis committee, David Deitcher, Joseph Fetcho, and Ned Place for their support and mentorship over the years. David was a wealth of information for molecular biology; Joe pushed me to think critically and beyond my own scientific interests; Ned was a great resource for the melatonin and circadian rhythm aspects of my project.

I would not have gotten through graduate school without the help and support of Terri Natoli, Dawn Potter, Lori Maine, Kathie Ely, Stacey Coil, Sara Eddleman, Saundra Anderson, and other NBB staff members. I am very thankful to Rich Moore

for his help with keeping the fish alive and healthy. Rich was instrumental in helping me achieve the setup for several behavioral experiments, and has patiently dealt with all the light cycle changes I put the rooms under. I am also grateful to John Howell for keeping our freezers running, lights schedules on track, and Brian Mlodzinski for keeping my licenses up to date and computers running.

I am indebted to many supportive faculty members and colleagues outside of the Bass lab or NBB. Christiane Linster and Tom Cleland have opened their home to me many times for their lab celebrations. Rob Raguso has generously offered emotional support during testing times. Kelly Zamudio and Monica Geber ran an extremely effective course that helped me obtain a NSF DDIG. Cameron Finucane and Matt Einhorn have generously helped with programming and trouble shooting electrical equipment. Bruce Land has helped with Matlab, electrophysiology, and finding talented engineering students to collaborate on projects. Ron Hoy and Gil Menda from the neighboring lab were always friendly and cheerful. Dave Rose and Joseph Sisneros of University of Washington were instrumental in helping Joel and I set up behavior projects at Seabeck, WA.

Many fellow students in NBB and the greater community have made daily life in Ithaca enjoyable. I am grateful to many close friends who have made even the longest and gloomiest winters fun. Matt Lewis has been an amazing and supportive partner to me for the past five or so years. I am thankful to have shared many meals and adventures with some of the most amazing people, including Allie King, Cameron Finucane, Cait McDonald, Cissy Ballen, Emma Greig, Eric Ryan, Hnin Aung, Holly Summers, Jenélle Dowling, Julian Kapoor, Julie Miller, Kat Agres, Kristin Hook,

Kristy Lawton, Maria Modanu, and many others. These friends have built one of the warmest communities I have been apart of.

I am grateful for the generous support from the following funding sources: NSF IOS 1120925, NSF DDIG 1406515, NBB Animal Behavior Grants, Cornell Sigma Xi Research Grants, Cornell's Center for Vertebrate Genomics scholarship, the Ta-Chung & Ya-Chao Liu Memorial Award, and Cornell Graduate School's summer research and conference travel grants.

Lastly, I would like to thank my family. It takes a village to raise a child and this was especially true in my case. My primary care takers have included my mother, father, grandfather, step-grandmother, eryi, eryifu, and sanyi. You have all shaped the person I am today and I am extremely grateful for the sacrifices and hard work you went through in order to give me a better life. To my father and grandfather who are no longer with us: thank you for loving me unconditionally, you will always be in my heart and thoughts. To mom: thank you for your optimism, your perseverance, and your hard work. I know you are proud of me and I am so proud of you. To Eryi, Eryifu, and Lisl: thank you for welcoming me into your home, raising me, and helping my mother and I gain a footing in this country; you are truly my guardian angels. To Sanyi: thank you for all the fun summers Lisl and I spent with you in DC, for continuing to be my emotional support and travel partner; you are my rock. Thanks also to grandma Becky and aunt Lisa for the love and generosity they have shown me. It is difficult to express just how much I appreciate each one of you for the love, support, and care you have given me. You are my life and my inspiration.

TABLE OF CONTENTS

PREFACE

Vocal-acoustic communication is widespread among vertebrates and serves important social and survival functions. The precise timing of vocalizations across the timescales of seasons, days, and even seconds is critical for enhancing sender-receiver coupling, reproductive success, and reproductive isolation. Timing is especially critical for courtship vocalizations that are energetically costly to produce and convey crucial information about the sender's condition and motivation to mate.

Like other vertebrates, many species of fish produce sound to communicate under a variety of social contexts, including courtship. Members of the toadfish family (Batrachoididae) are highly vocal, especially the plainfin midshipman (*Porichthys notatus*) fish that breed throughout the summer in the intertidal zone along the western United States. Males of the type I morph defend rocky nests and acoustically court females by producing long duration "hum" calls that can last up to hours per call. Hums have fundamental frequencies of about 100 Hz in 16°C and exhibit low amplitude and frequency modulation. Important for my dissertation, hums are produced almost exclusively at night during the summer breeding season.

At the start of my Ph.D., I asked the simple question of how midshipman males time their courtship vocalizations to occur at night. A recent study by Tine Rubow and Andy Bass had just been published in 2009 showing that neural excitability of the underlying vocal control network increases during the night in breeding animals, concurrent with the timing of natural vocal behavior. The obvious place to begin was to test whether the nocturnal timekeeping hormone melatonin is involved, as melatonin has been shown to regulate daily and seasonal activity in other

vertebrates. To date, melatonin regulation of vocal behavior has only been investigated in a few species of diurnal birds. I hypothesized that in nocturnally vocal midshipman fish, melatonin stimulates vocal behavior by acting via specific receptors expressed within neural pathways that control vocalization.

In Chapter 1, I investigated whether melatonin stimulates spontaneous humming behavior in captive midshipman fish. This chapter also tested whether midshipman hums follow an endogenous circadian rhythm. In chapter 2, I explored whether melatonin's permissive/stimulating effects on vocal behavior can be explained by increased excitability of the underlying neural network controlling vocalization. In chapter 3, I examined where melatonin is exerting its actions by localizing the mRNA expression of a melatonin receptor subtype. Finally, in chapter 4, I leveraged RNA-sequencing techniques to globally quantify daily, seasonal, and tissue-specific gene expression patterns in the vocal motor nucleus, the last node of the hindbrain vocal pattern generator that directly patterns vocalization.

CHAPTER 1

CIRCADIAN AND MELATONIN CONTROL OF COURTSHIP VOCAL BEHAVIOR IN FISH

Abstract

Endogenous circadian rhythms in behavior and physiology enable animals to anticipate cyclical changes in the 24 h light-dark cycle. For energetically costly vocal-acoustic courtship behaviors, timing across the daily cycle is critical for enhancing sender-receiver coupling. In vertebrates, the nocturnal hormone melatonin is known for playing a central role in entraining locomotor activity, but its control of social behaviors such as vocal communication is less understood. Knowledge of melatonin action in nocturnal vocal species is especially lacking, as diurnal songbirds are the predominant models for studying vocal behavior. Here, we investigated circadian and melatonin regulation of the courtship vocalization ("hums") of a nocturnally active and highly vocal teleost fish, the plainfin midshipman (*Porichthys notatus*). By recording hums from individual males held under normal light-dark (LD) and constant dark (DD) light regimes, we found that courtship vocalization is under circadian control with a free-running period of 25.1±0.4 h under DD, significantly longer than the approximately 24 h entrained period observed under LD. There were no changes in the total duration of humming per day under these light regimes. To test the hypothesis that melatonin stimulates nocturnal courtship vocalization, males were transitioned from LD to constant light (LL), known to inhibit melatonin production. On the first day of LL, males were either left untreated, or implanted with either 2-iodomelatonin (2-Imel; potent melatonin receptor agonist) or vehicle control. Humming was

significantly inhibited under LL in untreated and control-implanted males. In striking contrast, males implanted with 2-IMel maintained hum activity under LL and increased hum duration compared to controls. To our knowledge, the results are collectively the first demonstration of both circadian and melatonin regulation of daily vocal activity in fishes, and one of the few examples aside from birds in vertebrates.

Introduction

Endogenously generated biological rhythms enhance survival and reproduction by synchronizing behavior and physiology to cyclical changes in the external environment, such as light regimes, temperature, and the availability of food and mates. For energetically costly vocal behaviors, such as those used in courtship (Ophir et al., 2010), robust daily vocal rhythms can enhance sender-receiver coupling (Luther, 2008; Roth et al., 2009), reproductive success (Greives et al., 2015), and reproductive isolation (Danley et al., 2007). Direct observations of daily and seasonal rhythms in courtship vocalizations have been made across lineages, including in insects (Fergus and Shaw, 2013), fishes (Ibara et al., 1983; Locascio and Mann, 2008; Rice and Bass, 2009) and birds (Derégnaucourt et al., 2012; Penteriani, 2001; Tramontin and Brenowitz, 2000; Wang et al., 2012; Wood et al., 2013). However, few studies have tested whether vocalizations are under endogenous, circadian control mediated by melatonin, the nocturnal time-keeping hormone in vertebrates (Falcón et al., 2010; Reiter, 1993).

In vertebrates, the hormone melatonin is the chemical expression of darkness and plays a central role in entraining daily activity to the day-night cycle (Ekström and

Meissl, 1997; Falcón et al., 2010; Reiter, 1993). Despite the widely conserved pattern of melatonin release from the pineal gland at night [for exceptions see (Taniguchi et al., 1993; Wikelski et al., 2005)], it remains unclear how vertebrates exhibit large variations in daily activity rhythms categorized broadly as diurnal, nocturnal, or crepuscular (active at dawn and dusk). Furthermore, although melatonin regulation of cyclical patterns of locomotion has been well characterized [e.g. *birds:* (Gwinner and Brandstätter, 2001); *mammals*: (Silver and Kriegsfeld, 2014); *fish*: (Chiu and Prober, 2013; Falcón et al., 2010; Reebs, 2011)], its regulation of social behaviors, including vocal communication, is not well understood. While locomotion is a reliable readout of the circadian clock, vocal activity is a more precise indicator of an animal's affective state (Bradbury and Vehrencamp, 2011). In many species including our study model, the highly vocal midshipman fish (*Poricthys notatus*), call types differ in spectro-temporal properties and function depending on social context (Bradbury and Vehrencamp, 2011; Brantley and Bass, 1994; Ibara et al., 1983).

Surprisingly little research, aside from a few studies in birds (Derégnaucourt et al., 2012; Wang et al., 2012; Wang et al., 2014), has tested for circadian control of vocal behaviors under constant conditions or for its control by melatonin with hormone treatments or pinealectomy. A circadian rhythm in the pre-dawn crowing of roosters was recently demonstrated, but melatonin influences were not investigated (Shimmura and Yoshimura, 2013). In songbirds, circadian regulation of song and call production that is dependent on melatonin action has only recently been shown (Derégnaucourt et al., 2012; Wang et al., 2012; Wang et al., 2014), even though melatonin regulation of the volume of song nuclei (population of neurons controlling

song) and the expression of melatonin receptors in those nuclei had been well documented (Bentley, 2003; Bentley and Ball, 2000; Bentley et al., 2013; Bentley et al., 1999; Cassone et al., 2008; Fusani and Gahr, 2015; Gahr and Kosar, 1996; Jansen et al., 2005; Whitfield-Rucker and Cassone, 1996). Knowledge of melatonin action in nocturnally vocal species is especially lacking, as diurnal songbirds are the predominant models for studying vocal behavior. In summary, melatonin control of daily rhythms in vocal behavior is not well understood, especially in nocturnal animals.

The nocturnal rise in melatonin acts as both an internal "clock" and "calendar" by tracking the duration of the dark phase (night), which is shorter in the summer and longer in the winter (Fig. 1.1A) (Reiter, 1993). Melatonin action would be predicted to have an inhibitory effect on courtship vocal behaviors in diurnal species that breed during the summer, as vocalization occurs during the day when melatonin levels are low and when the nocturnal rise in melatonin is shorter (Fig. 1.1A). In most cases, an inhibitory action of melatonin on song and underlying neurocircuits has been supported (Fig. 1.1A) [(Bentley and Ball, 2000; Bentley et al., 1999; Cassone et al., 2008; Jansen et al., 2005; Whitfield-Rucker and Cassone, 1996) but see (Bentley et al., 2013; Derégnaucourt et al., 2012)]. It is more difficult, however, to predict how nocturnal summer breeders might respond to melatonin, given that they are active during peak melatonin levels at night but experience a relatively short duration of nocturnal melatonin elevation compared to in the winter (Fig. 1.1A).

Here, we investigated circadian and melatonin regulation of daily rhythms in the vocal behavior of a nocturnally active and highly vocal teleost fish, the plainfin

midshipman (*Porichthys notatus*) (Fig. 1.1B). During the late spring-summer breeding season, male midshipman "sing" for long durations at night to attract females to rocky nests along the intertidal zone (Fig. 1.1B) (Brantley and Bass, 1994; McIver et al., 2014). Males contract superfast swim bladder muscles at ~100 Hz (14-16°C) to produce several call types, including long duration (min-h) courtship/advertisement "hums" (Brantley and Bass, 1994; McIver et al., 2014) (Fig. 1.1B). While "singing" in their nests, they are positively buoyant due to inflation of the swim bladder during humming (Bass et al., 2015; Ibara et al., 1983), and are essentially sedentary, i.e. not locomoting. Hence, vocalization rather than locomotion is a better readout of the midshipman's affective state. For example, courtship humming is a direct indicator of a male's motivation level and readiness for reproduction (Brantley and Bass, 1994; McKibben and Bass, 1998).

In most fishes, the daily rhythm in melatonin production persists under constant darkness and thus is under the control of an internal circadian oscillator (Ekström and Meissl, 1997). In some species, such as salmonids, melatonin production is controlled exclusively by light and remains elevated in constant darkness (Ekström and Meissl, 1997). In both cases, constant light is a potent inhibitor of melatonin production, and thus can be considered as a functional pinealectomy (Ekström and Meissl, 1997).

Midshipman fish present an ideal model for investigating melatonin regulation of nocturnal vocal behavior because (1) male courtship hums exhibit dramatic daily and seasonal vocal rhythms (Fig. 1.1B) (Brantley and Bass, 1994; McIver et al., 2014); (2) the neural circuit controlling vocalization is well-characterized and shares

traits with tetrapods (Bass, 2014; Bass et al., 2015); (3) vocal behavior and neural circuitry are exquisitely sensitive to the action of hormones such as steroids and neuropeptides (Forlano et al., 2015); (4) recent *in-vivo* neurophysiology results show that melatonin increases the excitability of the neural pathways that control vocalization (Feng and Bass, 2014). However, photoperiod and melatonin regulation of naturally occurring vocal behavior remain to be demonstrated.

In midshipman and a closely related toadfish of the same family, as well as other sonic species of fish, field and captive recordings have captured robust daily periodicity in vocal behavior that peaks at night (Brantley and Bass, 1994; Ibara et al., 1983; Locascio and Mann, 2008; Rice and Bass, 2009). However, no study to date has recorded fish vocal activity under constant conditions to test for endogenous rhythmicity or investigated melatonin's involvement. We used long-term vocal recordings from individual midshipman fish to characterize circadian rhythmicity and melatonin action in spontaneously vocalizing individuals under laboratory-controlled light regimes (Fig. 1.1C,D). We show that (1) courtship vocal behavior exhibits an endogenous circadian rhythm under constant darkness and (2) that melatonin rescues and stimulates courtship vocal behavior under constant light. Taken together, our results demonstrate for the first time in fishes, and the only example in vertebrates aside from birds, that a circadian clock controls vocal behavior, and that melatonin stimulates nocturnal courtship vocalization.

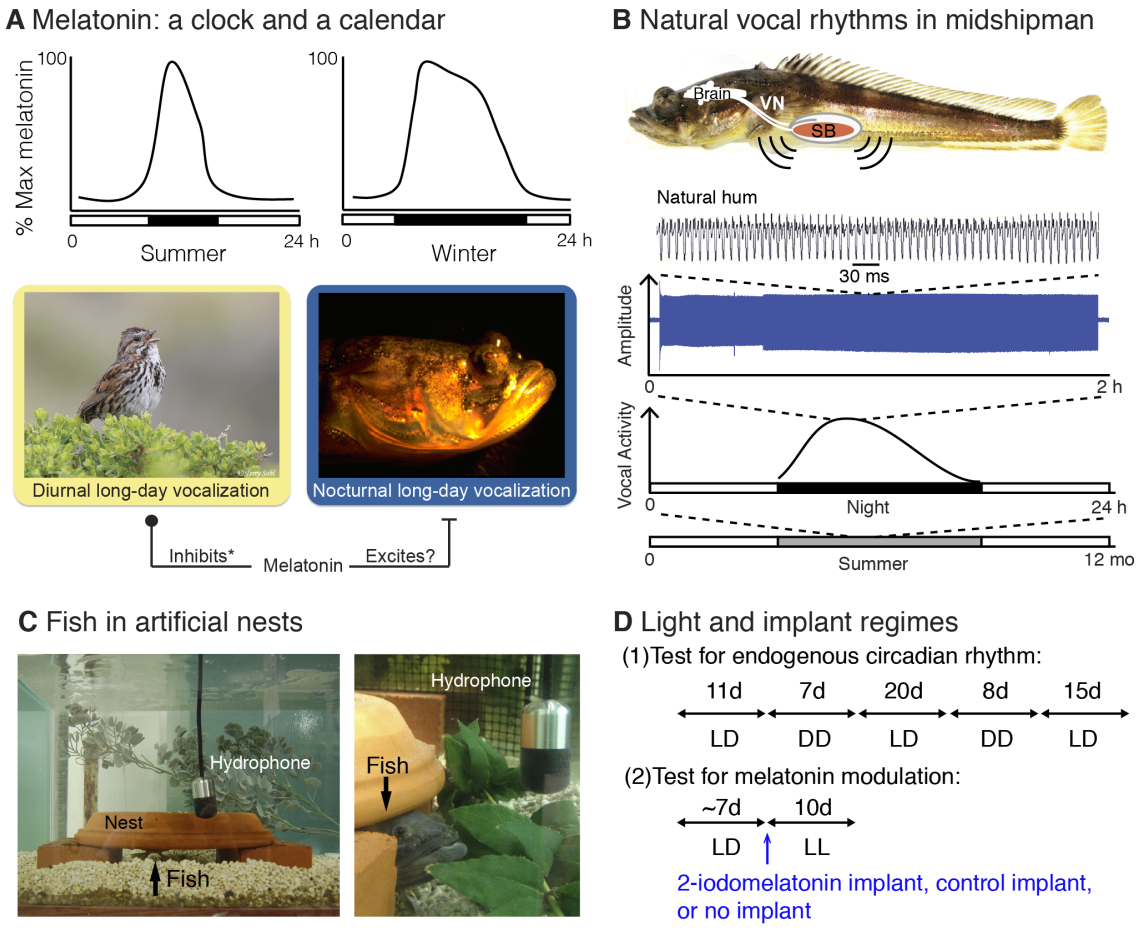

Figure 1.1

A) Melatonin translates the time of day into a hormone message by increasing levels at night and decreasing during the day. Melatonin also acts like a seasonal calendar by tracking the length of the night, which is shorter during the summer and longer during the winter. *See Discussion for melatonin regulation of singing and calling in birds. **B)** Midshipman courtship vocalizations are called "hums" and are produced during the summer almost exclusively at night. A picture of a midshipman (top) with superimposed schematic drawings of the brain, vocal nerve (VN) innervating one pair of vocal muscles (red) attached to the walls of the sonic swimbladder (SB). Continuous hums can last from mins to >1 h, shown by the 1.85 h hum recorded from a captive male (blue trace), and are produced repetitively throughout a night of courtship activity. Adapted from (Feng et al., 2015). **C)** In our captive recording set up, each fish is provided with an artificial nest and recorded by a hydrophone. Arrows point to resident fish under his nest. Note that during the day, fish sometimes expose their eyes to room lighting (right). **D)** Light and treatment regimes used in this study. Room lights are turned from normal light:dark (LD) to constant dark (DD) in the first experiment to test for an endogenous hum rhythm. In the second experiment, fish are first held in LD then transitioned to constant light (LL). On the first day of LL, fish are either implanted with 2-iodomelatonin or vehicle control or left un-implanted.

Results

Many fish readily produced hums under our captive conditions, with documented humming beginning as soon as two days after arriving at Cornell, consistent with previous reports of humming in captivity (Brantley and Bass, 1994; Ibara et al., 1983).

Circadian rhythm of courtship vocalization

Out of 12 fish tested, six hummed throughout at least one normal 15:9 h light:dark (LD) and one period of constant 24 h darkness (DD). Vocal actograms recorded from these fish are shown in Figure 1.2. The individual vocal actograms (Fig. 1.2) and the heatmap showing mean duration hummed per hour by 10 fish (Fig. 1.3A) show that midshipman humming followed a circadian free-running rhythm under DD with a phase delay (Figs. 1.2; 1.3A). However, this rhythm was noisy as hums were produced throughout the subjective day and night under DD. We observed no significant increase in hum duration under DD ($t_{(6)} = 1.17$, $P = 0.28$) (Fig. 1.3B). By calculating half of the distance of the second autocorrelation peak from the center peak (Fig. 1.3Ci), we found that under normal LD, fish humming activity cycled with a period of 23.96±0.05 h (N = 8). Under DD, the estimated free-running period was 25.0±0.4 (N = 6), which is significantly longer than the LD period ($t_{(5)} = 3.42$, $P = 0.019$) (Fig. 1.3Cii). The strength of the free-running rhythm under DD (autocorrelation index 0.19±0.06) was significantly weaker compared to the strength of the LD-driven daily rhythm (autocorrelation index 0.40±0.03; $t_{(5)} = 6.19$, $P = 0.0016$) (Fig. 1.3Ciii). The autocorrelation results support conclusions drawn by visual inspection of the vocal actograms: phase delays in actograms are explained by longer free-running periods;

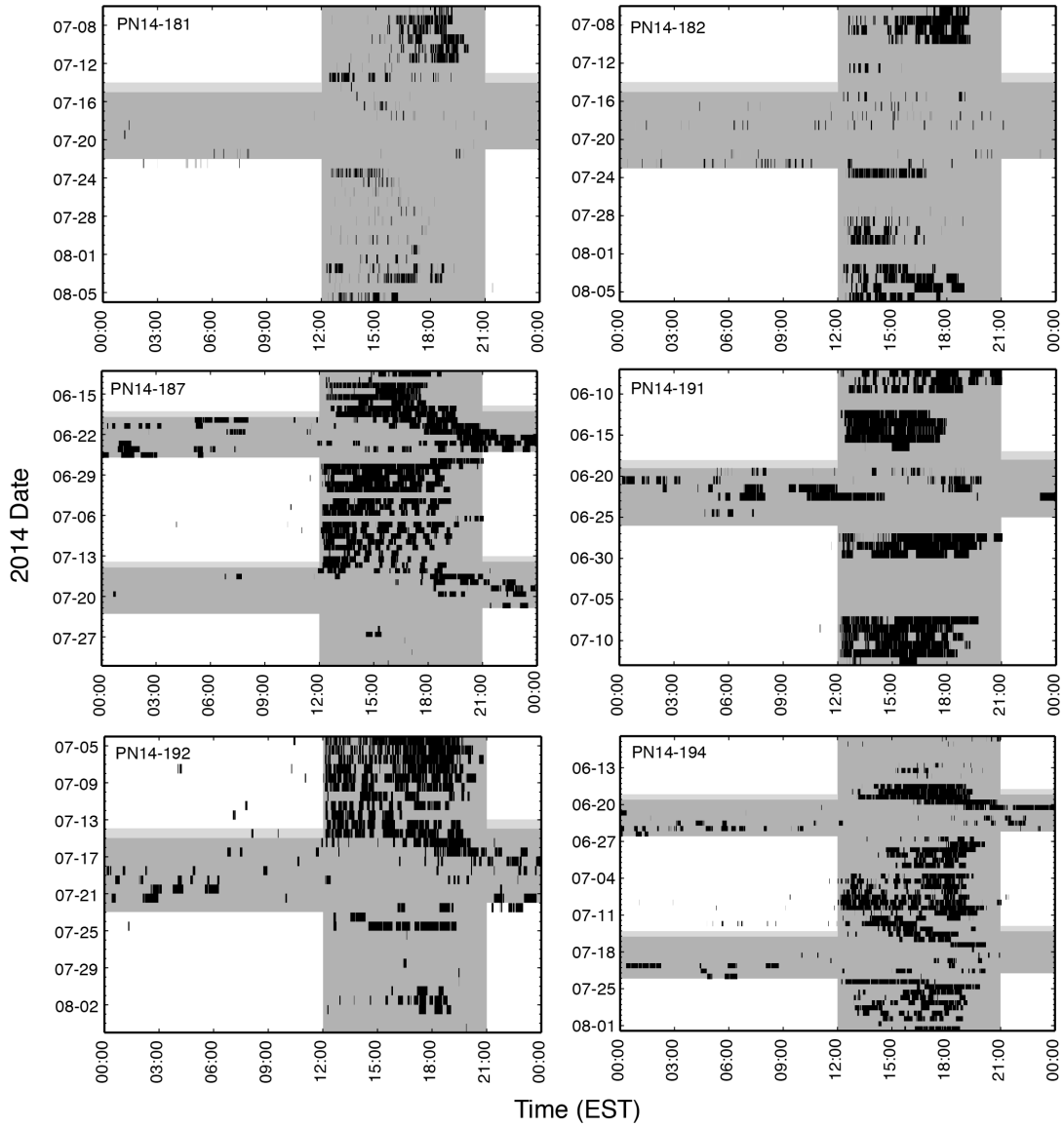

Figure 1.2
Actograms documenting daily humming activity of six individuals across light:dark and continuous 24 h dark light regimes. Black indicates when hums occurred. Dark grey indicates lights-off, and white indicates lights-on. Light grey bars indicate days when main room lights were turned off and only floodlights illuminated the tanks. Fish ID numbers are shown on top left corners.

Figure 1.3
Circadian rhythm of courtship vocalization is revealed under constant darkness (DD). A) Vocal actograms of one fish (left) and mean hum durations binned by hour (right) from 10 fish. Black indicates when hums occurred. Dark grey indicates lights-off, and white indicates lights-on. Light grey bars indicate days when main room lights were turned off and only floodlights illuminated the tanks. **B)** No changes in hum duration per day were observed under DD compared to light:dark (LD). **Ci-iii)** Estimating the period and strength of the free-running hum rhythm under DD. **Ci:** Autocorrelation plots from the same fish whose vocal actogram is shown in A (left). The periods calculated from the second peak from the center peak are displayed. Red x's mark the location of peaks. **Cii:** The length of the free-running period is significantly longer in DD than under LD. **Ciii:** The strength of the free-running circadian rhythm was weaker compared to LD. Asterisks indicate significant differences (* $P = 0.019$; ** $P = 0.0016$).

Figure 1.3 (continued)

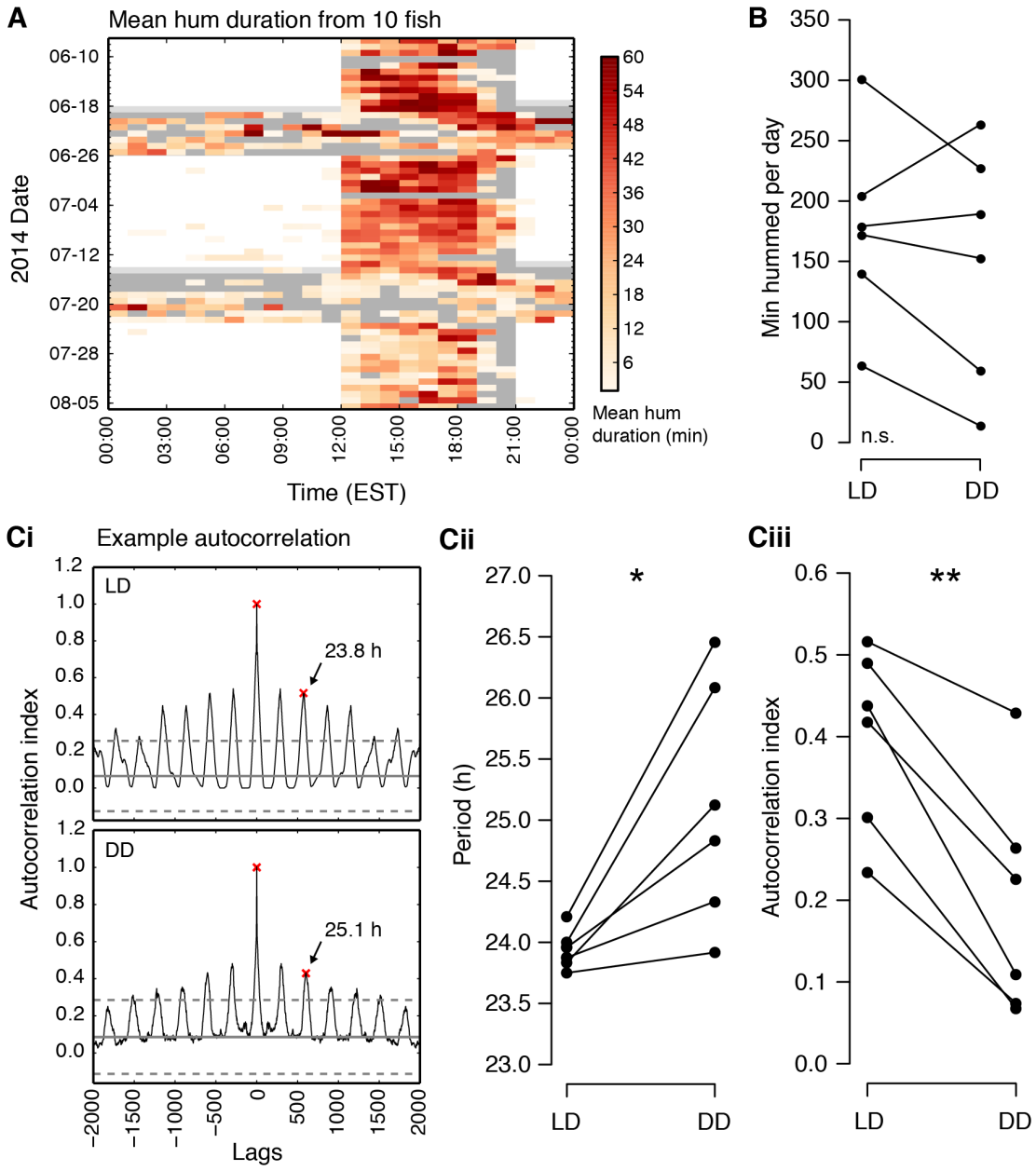

noisy free-running rhythms are reflected in weak autocorrelation indices. We conclude that midshipman courtship vocal behavior follows an endogenous, circadian rhythm with a free-running period of approximately 25 h.

Melatonin regulation of courtship vocalization

If midshipman vocalizations are dependent on melatonin action, we predicted a suppression of hum duration under LL, which has been shown to inhibit melatonin production in vertebrates, including fish (Bayarri et al., 2002; Bhattacharya et al., 2007; Ekström and Meissl, 1997; Porter et al., 1998). Furthermore, we predicted that exogenous melatonin replacement under LL would rescue the occurrence of vocalizations. Vocal actograms for all control fish are shown in Fig. 1.4, and 2-IMel implanted fish in Fig. 1.5.

Supporting our predictions, we found that LL suppressed hum duration in control-implanted (N = 6) and non-implanted fish (N = 2) (Figs. 1.4 & 1.6A). Also supporting our hypothesis that melatonin stimulates courtship vocalization, 2-IMel implanted fish rescued humming activity throughout the LL period (Figs. 1.5 & 1.6A). We observed the following significant fixed effects: treatment ($F_{(1,12.78)} = 16.12$; $P = 0.0015$), days nested within light regime ($F_{(2,211.1)} = 3.59$; $P = 0.029$) and treatment*light regime interaction ($F_{(1,212.9)} = 19.37$, $P < 0.0001$) (Fig. 1.6A). Light regime alone was not significant ($F_{(1,210.8)} = 1.23$, $P = 0.27$)

Similarly, after collapsing the data into mean daily hum duration over days when a fish hummed (Fig. 1.6B), we found a significant treatment effect ($F_{(1,12)} = 20.64$, $P = 0.0007$) and a significant treatment*light regime interaction ($F_{(1,12)} = 5.03$, P

Figure 1.4
Vehicle-implanted and non-implanted control fish vocal actograms under normal light:dark and constant light regimes. White denotes lights-on; grey denotes lights-off; black denotes humming activity. Fish were implanted on the first day of constant light. Fish ID's are in upper left corners. Arrow in PN15-92 point to hum not seen at this resolution.

Figure 1.4 (continued)

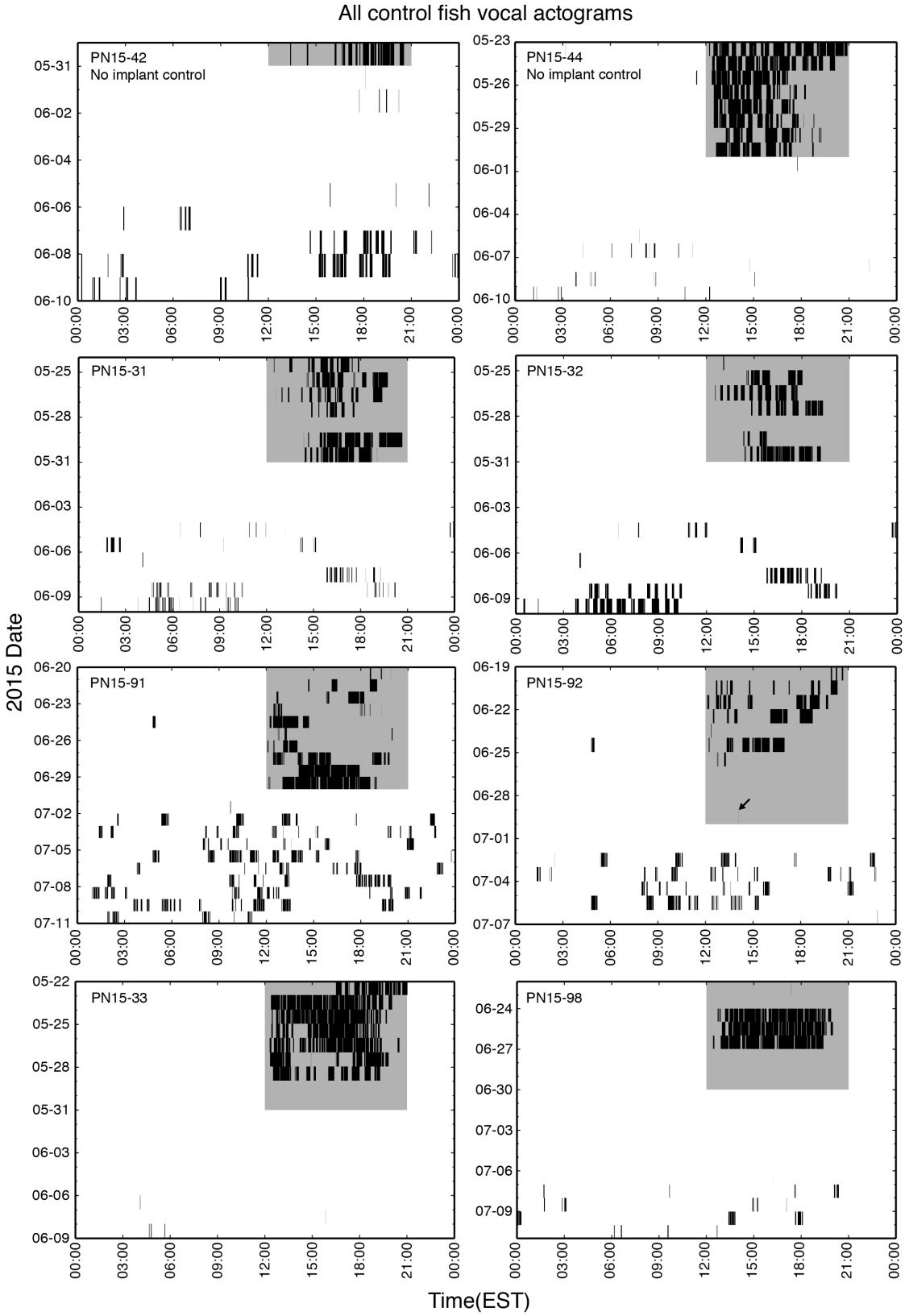

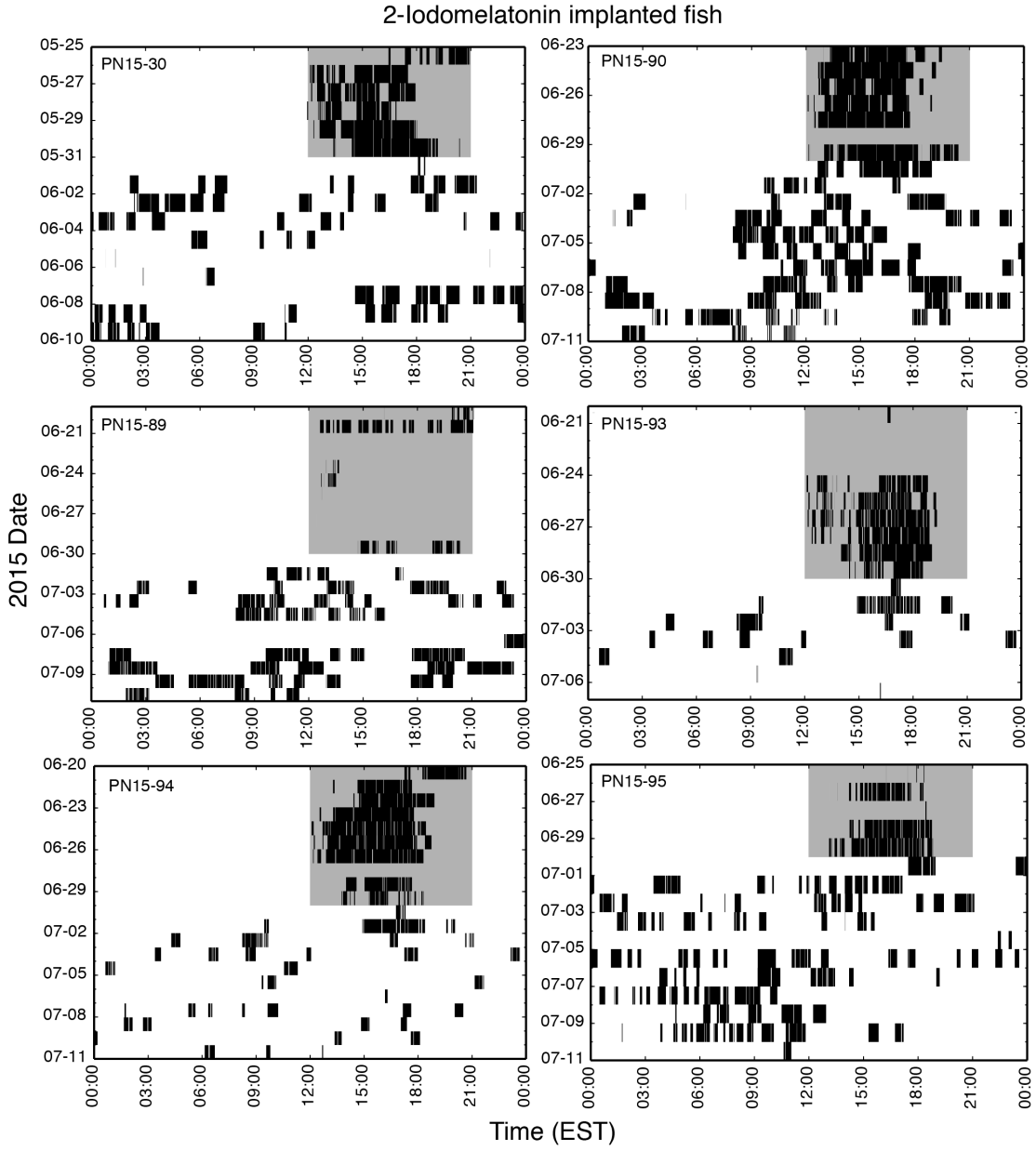

Figure 1.5
2-iodomelatonin-implanted fish vocal actograms under normal light:dark and constant light regimes. White denotes lights-on; grey denotes lights-off; black denotes humming activity. Fish were implanted on the first day of constant light. Fish ID's are in upper left corners.

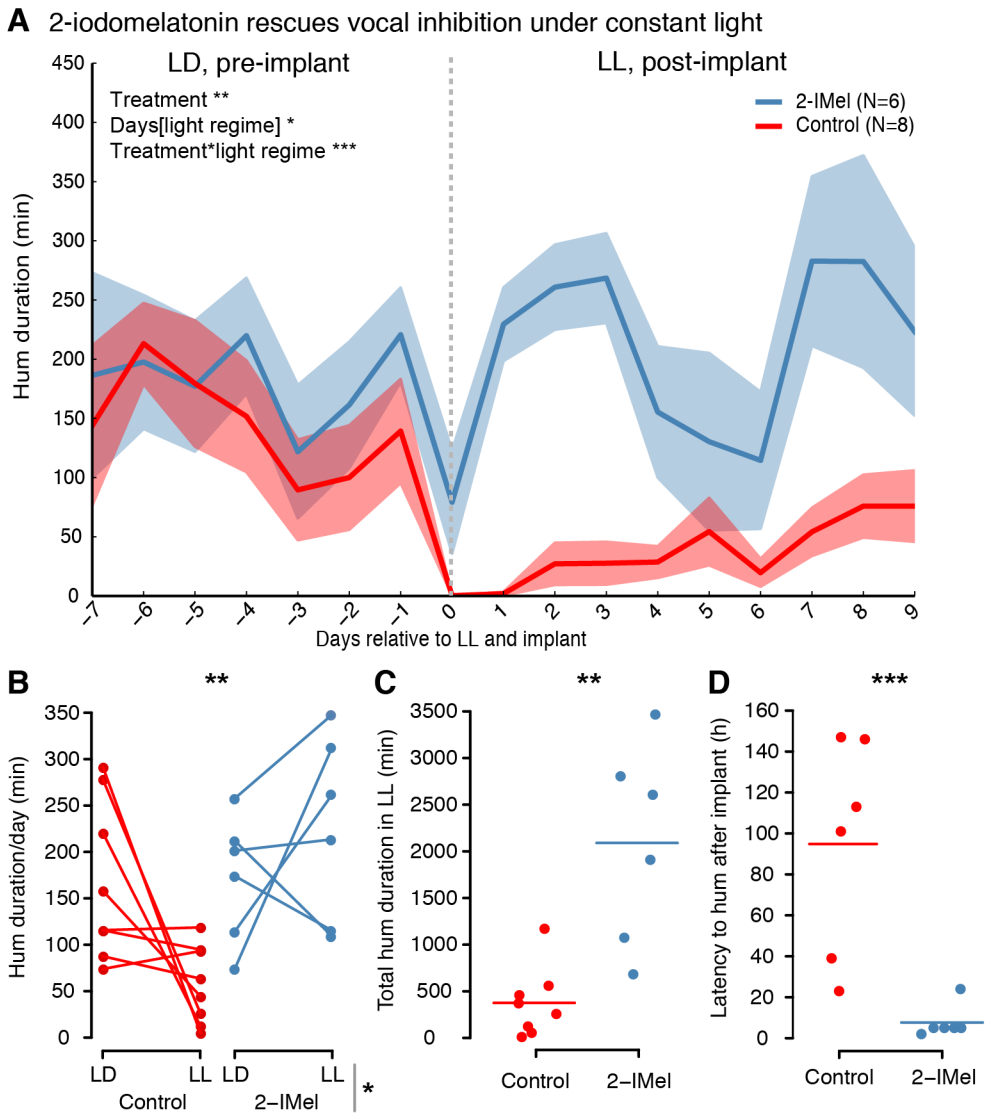

Figure 1.6

Melatonin action rescues courtship vocal activity under constant light (LL). A) Hum duration per day before and after implant and LL. Humming activity was inhibited by LL in control fish, but rescued in 2-IMel-implanted fish. All main effects were significant except for light regime. **B)** Hum duration per day under each light regime differed based on treatment. Asterisks above the graph indicates significant treatment effect and asterisk next to grey bar indicates significant treatment*light regime interaction. **C)** 2-IMel fish hummed for a significantly longer duration than control under the entire LL period. **D)** 2-IMel fish showed shorter latency to hum after implantation than control fish. Asterisks indicate significant differences (*=P<0.05; **=P<0.01; ***=P<0.001).

= 0.0446), with hum duration decreasing under LL in control fish, but increasing in 2-IMel implanted fish, but no light regime effect alone ($F_{(1,12)} = 2.40$, P = 0.1472). The total duration hummed under the entire LL period was also significantly higher in 2-IMel implanted fish compared to control-implanted and non-implanted fish ($t_{(12)} = 4.25$, P = 0.0011) (Fig. 1.6C). Furthermore, the latency to hum, which measured how long the fish began humming after implantation, was significantly shorter in 2-IMel implanted fish ($t_{(10)} = 5.86$, P = 0.0002) (Fig. 1.6D), with one 2-IMel implanted individual resuming hum activity within 2.65 h of implantation.

It is important to note that although 2-IMel implantation maintained and even increased the total amount of hum activity compared to controls under LL, it was not sufficient to induce humming in fish that had not hummed under LD (N = 3). Control-implanted non-hummers also remained silent (N = 3). These result suggest that the external photoperiodic cues and the internal melatonin signal must interact with other internal factors, such as steroid hormone levels (Genova et al., 2012; Remage-Healey and Bass, 2005; Remage-Healey and Bass, 2006) to gate humming behavior.

Similar to the daily humming period observed under LD in the 2014 experiment, fish from the 2015 LD-LL experiment exhibited a period of 23.98±0.11 h under LD (N = 10, data not shown). This diel rhythm was robust, as shown by the high autocorrelation indices of 0.41±0.05. There was no circadian free-running period under LL in either control or 2-IMel treated fish. However, we observed significant autocorrelation peaks corresponding to periods that were too short to be counted as circadian (12.67±1.1 h) and very weak (autocorrelation index 0.16±0.02; N = 9). We conclude that LL masks or abolishes the vocal circadian rhythm of midshipman fish.

Discussion

Given the diversity in circadian rhythms, their dependence on melatonin among vertebrates (Bloch et al., 2013; Zhdanova and Reebs, 2005), and observations of degeneration in the pineal/melatonin axis in nocturnal birds (Quay, 1972; Taniguchi et al., 1993; Van't Hof et al., 1998), it was unclear whether melatonin would have a strong effect on the plainfin midshipman's nocturnal courtship vocalization. Furthermore, circadian and melatonin regulation of vocal behavior has only been studied in a few cases using birds (Derégnaucourt et al., 2012; Wang et al., 2012). Thus, to our knowledge, this study is the first demonstration of both circadian and melatonin regulation of vocal activity in fishes, and one of few in all vertebrates.

Circadian rhythms in courtship vocalization

Our results demonstrated that the nocturnal courtship vocalization is under endogenous circadian control in a species of highly vocal fish. Compared to the entrained rhythm under LD, this free-running circadian rhythm was noisy and weak, commonly observed for teleost fish locomotor rhythms (Reebs, 2011; Zhdanova and Reebs, 2005). Although most organisms have endogenously generated circadian rhythms, this fact cannot be assumed without testing for persistence of daily activity patterns under constant conditions, especially because the strength of circadian rhythms can be highly variable across and within species (e.g. Figs. 1.2 & 1.3) (Bloch et al., 2013; Zhdanova and Reebs, 2005). While mammals are able to keep robust circadian rhythms over months (Moore-Ede et al., 1982), fish species exhibit noisy free-running rhythms that tend to dampen over days to weeks (Reebs, 2011; Zhdanova

and Reebs, 2005). Within a fish species, the presence or absence of overt circadian rhythms under constant conditions is highly variable across individuals (Zhdanova and Reebs, 2005). Furthermore, a diversity in circadian rhythms is observed in vertebrates that reside in or migrate to polar regions during summer or winter solstices, with some sustaining rhythmicity while others becoming arrhythmic under these natural, relatively constant light conditions (Bloch et al., 2013; Steiger et al., 2013). Fundamental differences in neural mechanisms controlling circadian behavior may be responsible for the differences observed between vertebrate lineages, such as the existence of a definitive master clock, the suprachiasmatic nucleus in mammals, versus distributed oscillators found in the brains of fish (Falcón et al., 2010; Reebs, 2011) and birds (Gwinner and Brandstätter, 2001).

Melatonin regulation of vertebrate vocalization

Evidence for melatonin action in songbirds and our work in vocal fish show that it is a direct modulator of vocal behavior and the underlying vocal control neurocircuitry (Bentley, 2003; Bentley and Ball, 2000; Bentley et al., 1999; Bentley et al., 2013; Cassone et al., 2008; Gahr and Kosar, 1996; Jansen et al., 2005; Wang et al., 2012; Whitfield-Rucker and Cassone, 1996). However, to our knowledge, aside from limited studies in songbirds (Derégnaucourt et al., 2012; Wang et al., 2012; Wang et al., 2014), little is known about melatonin effects on vocal behavior.

As mentioned in the Introduction, songbirds are vocally active during the day when melatonin is low, and breed during long days when the duration of nocturnal melatonin release is short, leading to the straightforward prediction that melatonin

inhibits vocal courtship behaviors. Indeed, songbirds sing throughout the 24 h period under constant light (Derégnaucourt et al., 2012), and daily melatonin treatment entrains song and call activity to occur during periods without melatonin replacement in pineal-removed zebra finches housed under constant dim light (Wang et al., 2012). Furthermore, long duration melatonin treatment in songbirds mimics the effect of winter-like short days by decreasing song nuclei volumes (Bentley et al., 1999; Cassone et al., 2008). When melatonin is applied to brain slices, the firing of a premotor song control nucleus is inhibited, further indicating that melatonin can act directly within vocal pathways to affect vocal patterning (Jansen et al., 2005). Melatonin is likely exerting these actions via specific G-protein coupled receptor subtypes localized to specific song control nuclei (Bentley, 2003; Bentley and Ball, 2000; Bentley et al., 1999; Bentley et al., 2013; Cassone et al., 2008; Gahr and Kosar, 1996; Jansen et al., 2005; Whitfield-Rucker and Cassone, 1996). Taken together, sufficient evidence in birds suggests that vocal behaviors and their underlying neural circuitry are under direct melatonin inhibition.

For nocturnally active vertebrates who are also long-day breeders, it is more difficult to predict whether melatonin would be stimulatory or inhibitory. It was especially difficult to predict whether melatonin would have an effect on nocturnal vocal behavior because the evolution of nocturnality in birds may have been accompanied by a degeneration of the melatonin system in some groups, such as in owls that exhibit atrophied pineal glands and low, arrhythmic levels of plasma melatonin (Quay, 1972; Taniguchi et al., 1993; Van't Hof et al., 1998).

Our data suggest that melatonin plays a permissive role in stimulating vocal

behavior, due to the observation that 2-IMel maintained and increased humming activity under LL compared to LD in fish who were already humming, but did not stimulate non-humming fish to hum. However, because of the inhibitory effects of constant light, it is unclear whether administration of exogenous melatonin during LD or DD would be able to induce a non-hummer to hum. It would be interesting to test whether melatonin would be similarly permissive for vocal behavior in nocturnally vocal active songbirds, such as nightingales.

In contrast to the inhibition of humming activity under LL in midshipman, diurnal zebra finches increased singing activity under LL (Derégnaucourt et al., 2012). However, LL decreased the duration of zebra finch song motifs as a result of shortened syllables within each motif (Derégnaucourt et al., 2012). Furthermore, LL effects were recapitulated by pinealectomy and rescued by melatonin replacement (Derégnaucourt et al., 2012). Thus, melatonin appears to regulate nocturnal vs. diurnal vocal behavior in an opposing manner at the daily timescale but in a similar manner at the msec-minute timescale of individual vocalizations. Melatonin's divergent effects on vocalization are likely due to indirect action in neuroendocrine/circadian centers that impact a range of behaviors vs. direct actions in neural centers dedicated to vocal patterning, mediated by melatonin receptors in these brain regions [songbirds: e.g. (Fusani and Gahr, 2015); midshipman fish: unpublished observation, N.Y. Feng, A.H. Bass].

Finally, although many fish hummed under our captive conditions, there were also many who did not. The extent of humming activity can vary widely under both natural (McIver et al., 2014) and captive (Genova et al., 2012) conditions. Presumably,

fish that did not hum consistently lack sufficient levels of motivation/arousal that may be related, in part, to divergent plasma steroid profiles between humming and non-humming males observed in midshipman and related toadfish (Genova et al., 2012; Remage-Healey and Bass, 2005; Remage-Healey and Bass, 2006).

Comparison with in-vivo neurophysiology results

The midshipman brain contains well-defined forebrain, midbrain, and hindbrain nuclei that form a vocal network (Bass et al., 1994; Goodson and Bass, 2002), the output of which is monitored as a vocal motor volley, or fictive call, from vocal nerves that innervate sonic muscles (Bass and Baker, 1990; Goodson and Bass, 2000; Remage-Healey and Bass, 2004; Rubow and Bass, 2009). Fictive calls directly predict natural call duration and pulse repetition rate.

In parallel with the midshipman's natural vocal rhythm, neurophysiology experiments showed a nocturnal increase in vocal network excitability, measured in increased fictive call duration and decreased stimulation threshold, the minimum current required to evoke fictive calls (Rubow and Bass, 2009). Five days of DD or LL exaggerated the increase and decrease in vocal excitability, respectively (Rubow and Bass, 2009), suggesting these light regimes amplify the underlying control mechanisms. In a follow-up study, we reported evidence supporting the hypothesis that an increase or decrease in melatonin action was responsible for the increase and decrease in neural excitability of the vocal network observed under DD and LL, respectively (Feng and Bass, 2014). We found that melatonin treatment reversed the inhibitory effect of LL on the abovementioned metrics of vocal network excitability,

while melatonin receptor antagonists decreased vocal excitability for animals maintained under DD (Feng and Bass, 2014).

Contrary to the neurophysiology results and our hypothesis that DD stimulates vocal behavior (Feng and Bass, 2014), DD did not increase spontaneous humming duration in the current study (Fig. 1.3B). Because fictive calls were elicited artificially by electrical stimulation at the level of midbrain vocal centers, DD may not increase the neural excitability of upstream, forebrain vocal centers, such as the preoptic area, known to regulate vertebrate social behavior and midshipman vocalizations (Goodson and Bass, 2000). In other words, the increase in neural excitability under DD that we observed in downstream vocal centers is not sufficient to initiate courtship vocal behavior. Although there were no significant differences in the total amount of hum activity per day under LD and DD, four fish showed a decrease (Fig. 1.3B). Perhaps DD either reduced basal melatonin levels or mimicked the inhibitory effects of winter-like short-days, warranting future studies that measure melatonin levels throughout the daily cycle under DD. Finally, consistent with melatonin rescuing neural excitability under LL (Feng and Bass, 2014), melatonin replacement also rescued spontaneous humming behavior under LL (Fig. 1.6).

Conclusions

The discovery of a melatonin-sensitive vocal circadian rhythm in fish, together with similar studies in birds (Derégnaucourt et al., 2012; Wang et al., 2012), suggest that melatonin regulation of vocalizations is shared among lineages of vocal vertebrates. This hypothesis is supported by the ubiquity of diel rhythms observed in vertebrate

vocal activity. The cellular and molecular mechanisms by which melatonin inhibits vocal activity in diurnal species but permits or stimulates vocal activity in nocturnal species is a fascinating question that remains to be answered.

Materials and Methods

Animals

There are two reproductive male morphs in midshipman fish: type I males that defend nests and acoustically court females with long duration hums, and type II males that sneak spawn (Brantley and Bass, 1994). We collected nesting type I males from the intertidal zone in Seal Rock Beach (Hood Canal), Washington, in June of 2014 and May through June of 2015. Fish were transported to the Big Beef Creek Field Station in Seabeck, Washington, held overnight in large outdoor aquaria (~6 m^3), and then shipped overnight to Cornell University. At Cornell, fish were housed in an environmental control room in six 125-gallon tanks that were divided in half by a screen divider with each fish having sole access to a single artificial nest. Each artificial nest comprised a clay disk supported by two bricks and gravel as substrate. In 2015, we added two 40-gallon tanks that housed one fish each that also had a single nest, allowing us to record from 14 fish simultaneously. In all experiments, we put at least one female in each tank to stimulate humming, although captive midshipman males hum without females (Brantley and Bass, 1994; Genova et al., 2012; Ibara et al., 1983). The temperature-controlled room in which the experiment took place had an ambient temperature of between 14-16°C. Fish were fed goldfish under LD approximately every week at random times of the day. All methods were approved by

the Cornell Institutional Animal Care and Use Committee.

Light regimes and implants

In all experiments, fish were initially acclimatized to a 15:9 h light:dark (LD) schedule that mimics the natural long day light cycle during the summer, with lights on at 21:00 EST and off at 12:00 EST. In order to test the hypothesis that midshipman vocal behavior is under endogenous circadian control, we recorded hums under LD and constant 24 h dark (DD) that removed external light cues. In 2014, fish were held under LD for 11 days, constant dark (DD) for seven days, LD for 20 days, DD for eight days, and LD for 15 days (Fig. 1.1D). During the experiment, some non-vocal fish were switched out and new ones added. Furthermore, we expanded from initially recording from 8 to 12 channels.

In order to test the hypothesis that melatonin stimulates vocal behavior in the nocturnally active midshipman fish, we recorded vocalizations in May and June of 2015 under LD and constant 24 h light (LL), which has been shown to suppress melatonin synthesis in vertebrates, including fish (Bayarri et al., 2002; Bhattacharya et al., 2007; Ekström and Meissl, 1997; Porter et al., 1998). After fish had been humming for ~7 days under LD, the light cycle was switched to LL. We then implanted fish with either two 12 mm 10mg/ml 2-iodomelatonin (2-IMel) dissolved in coconut oil or coconut oil alone (control). A dose of 0.63±0.07 μg/g 2-IMel per body weight (mean±se; range 0.47-0.94 μg/g) was achieved by the implants, which is less than two fold higher than the dosage used in our in-vivo neurophysiology study of vocal network excitability and well within the range used in other studies [see (Feng and

Bass, 2014)]. In addition, we had 2 non-implanted controls that were active hummers. Because some fish were actively humming and some were not, we had the following treatment groups: (1) 2-IMel-implanted hummers (N = 6); (2) control-implanted hummers (N = 6); (3) non-implanted hummers (N = 2); (4) 2-IMel-implanted non-hummers (N = 3); (5) control-implanted non-hummers (N = 3); (6) non-implanted non-hummers (N = 4). We focused our analyses on the first three groups involving actively humming fish, but briefly mention results from some of the other groups in the Results section. Fish from the same tank always received the same treatment. We discarded data from two fish who died during the experiment.

Sound recording and hum duration analyses

Hum vocalizations from each fish were recorded with either of two types of hydrophones: H1a (Aquarian Audio Products, Anacortes, WA) or HTI-94-SSQ (High Tech Inc., Long Beach, MS). Hydrophones were fed into two MOTU 8pre USB audio interfaces (MOTU, Cambridge, MA) daisy-chained with an ADAT optical cable, which allowed us to record from up to 16 channels, with each channel corresponding to one fish. Using a custom MATLAB script, audio data was collected continuously (6000 Hz sample rate, 16-bit) and written to an external hard drive every hour, usually for 24 h. The experimenter restarted the recording daily to ensure that the equipment was functioning properly. For audio files containing hums, we used Raven Pro 1.5 sound analysis software (The Cornell Lab of Ornithology, Ithaca, NY) to extract the date, duration, start times, and end times of each hum into a table format. Hums produced simultaneously by fish housed in the same aquarium were disambiguated by

amplitude and acoustic beating. Custom Python scripts, employing packages such as pandas and timbre, were used to compile selection tables for each fish and to plot vocal activity across the daily cycle into actograms. In order to show the general pattern of humming activity pooled from all individuals, we first binned hum duration by hour, calculated the mean duration hummed for each hour by all individuals who vocalized, which was then plotted as an actogram (Fig. 1.3A). Finally, we calculated mean hum duration binned per day under LD vs DD for each fish to test the hypothesis that DD stimulates vocal behavior (Fig. 1.3B).

For the LD-LL implant experiment, we first evaluated treatment effects over time by binning hum duration by day for seven days pre-implant and 10 days post-implant (Fig. 1.6A). We also looked at the mean duration hummed per day under each light regime (LD vs LL) in control (vehicle-implanted and non-implanted) and 2-IMel implanted fish (Fig. 1.6B). Furthermore, we compared the total duration hummed under LL for each treatment group (Fig. 1.6C). Lastly, we compared the latency to start humming after implant across treatment (Fig. 1.6D).

Estimating the period and strength of daily and free-running rhythms

Six fish hummed throughout at least one LD and one DD light regime. For fish that hummed under LD but stopped humming before DD or hummed fewer than 3 days under DD, we used their data only for estimating the LD period. To estimate period lengths for each fish, we binned data by 5 min and calculated the autocorrelations under each light regime using matplotlib.pyplot.acorr with the detrend option (Hunter, 2007). We then estimated the period by taking the difference between the second peak

to the center peak (Levine et al., 2002; Stoddard et al., 2007). In a few cases where the second peak was below but the third peak was above the 95% confidence interval, we used data from the third peak instead. For fish tested in 2015 in LD-LL experiments, we estimated LD periods using the same methods as above, but because the rhythms were weak and noisy under LL, we first lowpass-filtered the LL data with a 0.05 Hz cutoff using a two-pole butterworth filter (scipy.signal.butter). For DD and LL free-running rhythms, we only included data with least two autocorrelation peaks above the upper 95% confidence interval.

Statistics

For the LD-DD experiment, we averaged hum duration per day over LD and DD periods for each fish, which were then subjected to a paired t-test to assess whether hum duration changed across light regimes (Fig. 1.3B). In order to estimate the free-running period under DD, we calculated the distance between the second autocorrelation peak and the center peak (Fig. 1.3Ci, Cii) [see (Levine et al., 2002; Stoddard et al., 2007)]. To estimate the strength of the free-running rhythm, we obtained the autocorrelation value at the second peak (Fig. 1.3Ciii) [see (Levine et al., 2002; Stoddard et al., 2007)]. The paired t-test was also used for comparing period and strength of the rhythms under LD and DD.

For the LD-LL implant experiment, we performed a linear mixed model with the following fixed effects: light regime, days (relative to day of implant) nested within light regime, treatment, and treatment*light regime interaction. Fish nested within treatment was included as a random effect (Fig. 1.6A; JMP Pro 11, SAS

Institute Inc., Cary, NC, USA). There were no observable differences in the distribution of residuals across parameters such as tank position on a rack (top vs. bottom), rack, compartment position within a tank (left vs. right), or experiment (May vs. June 2015) so we excluded these as random effects. For examining the effect of light regime and treatment on hum duration per given day of humming, we performed a repeated measures ANOVA with effects of light regime, treatment, and their interaction (Fig. 1.6B). We used the Student's t tests for assessing treatment effect on free-running period, total duration hummed under LL (Fig. 1.6C), and latency to hum, which was first log transformed (Fig. 1.6D).

Acknowledgments

We would like to thank Grace Ahn, Frenda Yip, and Clara Liao for their help analyzing raw sound files. Joel Tripp and Ian Pengra generously helped with fish collection; Dave Rose helped tremendously with tank setup at Big Beef Creek; Raquel Vasconcelos, Bret Pasche, and Aaron Rice provided advice on recording methods; Irene Ballagh helped with restarting recordings and lent her iPhone for photos and videos; We thank Margaret Marchaterre for feeding the animals and Rich Moore for tank set up. Statistical analyses were done in consultation with Dr. Kevin Packard at the Cornell Statistical Consulting Unit. This work was generously supported by the NSF IOS 1120925, NSF DDIG 1406515, NBB Animal Behavior Grants, and Cornell Sigma Xi Research Grants.

References

Bass, A. H. (2014). ScienceDirectCentral pattern generator for vocalization: is there a vertebrate morphotype? *Current Opinion in Neurobiology* **28**, 94–100.

Bass, A. H. and Baker, R. (1990). Sexual dimorphisms in the vocal control system of a teleost fish: Morphology of physiologically identified neurons. *Journal of Neurobiology* **21**, 1155–1168.

Bass, A. H., Chagnaud, B. P. and Feng, N. Y. (2015). Comparative Neurobiology of Sound Production in Fishes. In *Sound Communication in Fishes*, pp. 35–75. Vienna: Springer Vienna.

Bass, A. H., Marchaterre, M. A. and Baker, R. (1994). Vocal-acoustic pathways in a teleost fish. *Journal of Neuroscience* **14**, 4025–4039.

Bayarri, M. J., Madrid, J. A. and Sánchez-Vázquez, F. J. (2002). Influence of light intensity, spectrum and orientation on sea bass plasma and ocular melatonin. *J. Pineal Res.* **32**, 34–40.

Bentley, G. E. (2003). Melatonin receptor density in Area X of European starlings is correlated with reproductive state and is unaffected by plasma melatonin concentration. *General and Comparative Endocrinology* **134**, 187–192.

Bentley, G. E. and Ball, G. F. (2000). Photoperiod-dependent and -independent regulation of melatonin receptors in the forebrain of songbirds. *J. Neuroendocrinol.* **12**, 745–752.

Bentley, G. E., Perfito, N. and Calisi, R. M. (2013). Season- and context-dependent sex differences in melatonin receptor activity in a forebrain song control nucleus. *Hormones and Behavior* **63**, 829–835.

Bentley, G. E., Van't Hof, T. J. and Ball, G. F. (1999). Seasonal neuroplasticity in the songbird telencephalon: a role for melatonin. *Proc Natl Acad Sci USA* **96**, 4674–4679.

Bhattacharya, S., Chattoraj, A. and Maitra, S. K. (2007). Melatonin in the Regulation of Annual Testicular Events in Carp Catla catla: Evidence from the Studies on the Effects of Exogenous Melatonin, Continuous Light, and Continuous Darkness. *Chronobiol Int* **24**, 629–650.

Bloch, G., Barnes, B. M., Gerkema, M. P. and Helm, B. (2013). Animal activity around the clock with no overt circadian rhythms: patterns, mechanisms and adaptive value. *Proc. Biol. Sci.* **280**, 20130019.

Bradbury, J. W. and Vehrencamp, S. L. (2011). *Principles of Animal Communication*. Sinauer Associates Incorporated.

Brantley, R. K. and Bass, A. H. (1994). Alternative Male Spawning Tactics and Acoustic Signals in the Plainfin Midshipman Fish Porichthys notatus Girard (Teleostei, Batrachoididae). *Ethology* **96**, 213–232.

Cassone, V. M., Bartell, P. A., Earnest, B. J. and Kumar, V. (2008). Duration of melatonin regulates seasonal changes in song control nuclei of the house sparrow, Passer domesticus: independence from gonads and circadian entrainment. *Journal of Biological Rhythms* **23**, 49–58.

Chiu, C. N. and Prober, D. A. (2013). Regulation of zebrafish sleep and arousal states: current and prospective approaches. *Front. Neural Circuits* **7**, 58.

Danley, P. D., deCarvalho, T. N., Fergus, D. J. and Shaw, K. L. (2007). Reproductive Asynchrony and the Divergence of Hawaiian Crickets. *Ethology* **113**, 1125–1132.

Derégnaucourt, S., Saar, S. and Gahr, M. (2012). Melatonin affects the temporal pattern of vocal signatures in birds. *J. Pineal Res.* **53**, 245–258.

Ekström, P. and Meissl, H. (1997). The pineal organ of teleost fishes. *Reviews in Fish Biology and Fisheries* **7**, 199–284.

Falcón, J., Migaud, H., Muñoz-Cueto, J. A. and Carrillo, M. (2010). Current knowledge on the melatonin system in teleost fish. *General and Comparative Endocrinology* **165**, 469–482.

Feng, N. Y. and Bass, A. H. (2014). Melatonin action in a midbrain vocal-acoustic network. *Journal of Experimental Biology* **217**, 1046–1057.

Feng, N. Y., Fergus, D. J. and Bass, A. H. (2015). Neural transcriptome reveals molecular mechanisms for temporal control of vocalization across multiple timescales. *BMC Genomics* **16**, 417.

Fergus, D. J. and Shaw, K. L. (2013). Circadian rhythms and period expression in the Hawaiian cricket genus Laupala. *Behav. Genet.* **43**, 241–253.

Forlano, P. M., Sisneros, J. A., Rohmann, K. N. and Bass, A. H. (2015). Neuroendocrine control of seasonal plasticity in the auditory and vocal systems of fish. *Frontiers in Neuroendocrinology* **37**, 129–145.

Fusani, L. and Gahr, M. (2015). Differential expression of melatonin receptor subtypes MelIa, MelIb and MelIc in relation to melatonin binding in the male songbird brain. *Brain Behav Evol* **85**, 4–14.

Gahr, M. and Kosar, E. (1996). Identification, distribution, and developmental changes of a melatonin binding site in the song control system of the zebra finch. *J. Comp. Neurol.* **367**, 308–318.

Genova, R. M., Marchaterre, M. A., Knapp, R., Fergus, D. and Bass, A. H. (2012). Glucocorticoid and androgen signaling pathways diverge between advertisement calling and non-calling fish. *Hormones and Behavior* **62**, 426–432.

Goodson, J. L. and Bass, A. H. (2000). Forebrain peptides modulate sexually polymorphic vocal circuitry. *Nature* **403**, 769–772.

Goodson, J. L. and Bass, A. H. (2002). Vocal–acoustic circuitry and descending vocal pathways in teleost fish: Convergence with terrestrial vertebrates reveals conserved traits. *J. Comp. Neurol.* **448**, 298–322.

Greives, T. J., Kingma, S. A., Kranstauber, B., Mortega, K., Wikelski, M., van Oers, K., Mateman, A. C., Ferguson, G. A., Beltrami, G. and Hau, M. (2015). Costs of sleeping in: circadian rhythms influence cuckoldry risk in a songbird. *Funct Ecol* **29**, 1300–1307.

Gwinner, E. and Brandstätter, R. (2001). Complex bird clocks. *Philos. Trans. R. Soc. Lond., B, Biol. Sci.* **356**, 1801–1810.

Hunter, J. D. (2007). Matplotlib: A 2D Graphics Environment. *Computing in Science & Engineering* **9**, 90–95.

Ibara, R. M., Penny, L. T., Ebeling, A. W., van Dykhuizen, G. and Cailliet, G. (1983). The mating call of the plainfin midshipman fish, Porichthys notatus. In *Predators and prey in fishes*, pp. 205–212. Dordrecht: Springer Netherlands.

Jansen, R., Metzdorf, R., van der Roest, M., Fusani, L., Maat, ter, A. and Gahr, M. (2005). Melatonin affects the temporal organization of the song of the zebra finch. *FASEB J.* **19**, 848–850.

Levine, J. D., Funes, P., Dowse, H. B. and Hall, J. C. (2002). Signal analysis of behavioral and molecular cycles. *BMC Neuroscience* **3**, 1.

Locascio, J. V. and Mann, D. A. (2008). Diel Periodicity of Fish Sound Production in Charlotte Harbor, Florida. *Transactions of the American Fisheries Society* **137**, 606–615.

Luther, D. A. (2008). Signaller: receiver coordination and the timing of communication in Amazonian birds. *Biology Letters* **4**, 651–654.

McIver, E. L., Marchaterre, M. A., Rice, A. N. and Bass, A. H. (2014). Novel underwater soundscape: acoustic repertoire of plainfin midshipman fish. *J. Exp. Biol.* **217**, 2377–2389.

McKibben, J. R. and Bass, A. H. (1998). Behavioral assessment of acoustic parameters relevant to signal recognition and preference in a vocal fish. *J. Acoust. Soc. Am.* **104**, 3520–3533.

Moore-Ede, M. C., Sulzman, F. M. and Fuller, C. A. (1982). *The clocks that time us*. Cambridge: Harvard University Press.

Ophir, A. G., Schrader, S. B. and Gillooly, J. F. (2010). Energetic cost of calling: general constraints and species-specific differences. *Journal of Evolutionary Biology* **23**, 1564–1569.

Penteriani, V. (2001). The annual and diel cycles of Goshawk vocalizations at nest sites. *Journal of Raptor Research* **35**, 24–30.

Porter, M. J. R., Randall, C. F., Bromage, N. R. and Thorpe, J. E. (1998). The role of melatonin and the pineal gland on development and smoltification of Atlantic salmon (Salmo salar) parr. *Aquaculture* **168**, 139–155.

Quay, W. B. (1972). Infrequency of Pineal Atrophy among Birds and Its Relation to Nocturnality. *The Condor* **74**, 33–45.

Reebs, S. G. (2011). SENSORY SYSTEMS, PERCEPTION, AND LEARNING | *Circadian Rhythms in Fish*. Elsevier.

Reiter, R. J. (1993). The melatonin rhythm: both a clock and a calendar. *Experientia* **49**, 654–664.

Remage-Healey, L. and Bass, A. H. (2004). Rapid, hierarchical modulation of vocal patterning by steroid hormones. *J. Neurosci.* **24**, 5892–5900.

Remage-Healey, L. and Bass, A. H. (2005). Rapid elevations in both steroid hormones and vocal signaling during playback challenge: a field experiment in Gulf toadfish. *Hormones and Behavior* **47**, 297–305.

Remage-Healey, L. and Bass, A. H. (2006). From social behavior to neural circuitry: Steroid hormones rapidly modulate advertisement calling via a vocal pattern generator. *Hormones and Behavior* **50**, 432–441.

Rice, A. N. and Bass, A. H. (2009). Novel vocal repertoire and paired swimbladders of the three-spined toadfish, Batrachomoeus trispinosus: insights into the diversity of the Batrachoididae. *Journal of Experimental Biology* **212**, 1377–1391.

Roth, T., Sprau, P., Schmidt, R., Naguib, M. and Amrhein, V. (2009). Sex-specific timing of mate searching and territory prospecting in the nightingale: nocturnal life of females. *Proceedings of the Royal Society B: Biological Sciences* **276**, 2045–2050.

Rubow, T. K. and Bass, A. H. (2009). Reproductive and diurnal rhythms regulate vocal motor plasticity in a teleost fish. *Journal of Experimental Biology* **212**, 3252–3262.

Shimmura, T. and Yoshimura, T. (2013). Circadian clock determines the timing of rooster crowing. *Curr. Biol.* **23**, R231–3.

Silver, R. and Kriegsfeld, L. J. (2014). Circadian rhythms have broad implications for understanding brain and behavior. *European Journal of Neuroscience* **39**, 1866–1880.

Steiger, S. S., Valcu, M., Spoelstra, K., Helm, B., Wikelski, M. and Kempenaers, B. (2013). When the sun never sets: diverse activity rhythms under continuous daylight in free-living arctic-breeding birds. *Proc. Biol. Sci.* **280**, 20131016.

Stoddard, P. K., Markham, M. R., Salazar, V. L. and Allee, S. (2007). Circadian rhythms in electric waveform structure and rate in the electric fish Brachyhypopomus pinnicaudatus. *Physiol. Behav.* **90**, 11–20.

Taniguchi, M., Murakami, N., Nakamura, H., Nasu, T., Shinohara, S. and Etoh, T. (1993). Melatonin release from pineal cells of diurnal and nocturnal birds. *Brain Research* **620**, 297–300.

Tramontin, A. D. and Brenowitz, E. A. (2000). Seasonal plasticity in the adult brain. *Trends in Neurosciences* **23**, 251–258.

Van't Hof, T. J., Gwinner, E. and Wagner, H. (1998). A highly rudimentary circadian melatonin profile in a nocturnal bird, the barn owl (Tyto alba). *Naturwissenschaften* **85**, 402–404.

Wang, G., Harpole, C. E., Paulose, J. and Cassone, V. M. (2014). The role of the pineal gland in the photoperiodic control of bird song frequency and repertoire in the house sparrow, Passer domesticus. *Hormones and Behavior* **65**, 372–379.

Wang, G., Harpole, C. E., Trivedi, A. K. and Cassone, V. M. (2012). Circadian Regulation of Bird Song, Call, and Locomotor Behavior by Pineal Melatonin in the Zebra Finch. *Journal of Biological Rhythms* **27**, 145–155.

Whitfield-Rucker, M. G. and Cassone, V. M. (1996). Melatonin binding in the house sparrow song control system: sexual dimorphism and the effect of photoperiod. *Hormones and Behavior* **30**, 528–537.

Wikelski, M., Tarlow, E. M., Eising, C. M., Groothuis, T. G. G. and Gwinner, E. (2005). Do night-active birds lack daily melatonin rhythms? A case study comparing a diurnal and a nocturnal-foraging gull species. *J Ornithol* **147**, 107–111.

Wood, W. E., Osseward, P. J., Roseberry, T. K. and Perkel, D. J. (2013). A daily oscillation in the fundamental frequency and amplitude of harmonic syllables of zebra finch song. *PLoS ONE* **8**, e82327.

Zhdanova, I. V. and Reebs, S. G. (2005). Circadian rhythms in fish. *Fish Physiology* **24**, 197–238.

CHAPTER 2

MELATONIN ACTION IN A MIDBRAIN VOCAL-ACOUSTIC NETWORK

Abstract

Melatonin is a well-documented time-keeping hormone that can entrain an individual's physiology and behavior to the day-night cycle, though surprisingly little is known about its influence on the neural basis of social behavior, including vocalization. Male midshipman fish (*Porichthys notatus*) produce several call types distinguishable by duration and by daily and seasonal cycles in their production. We investigated melatonin's influence on the known nocturnal- and breeding season-dependent increase in excitability of the midshipman's vocal network (VN) that directly patterns natural calls. VN output is readily recorded from the vocal nerve as a "fictive call." Five days of constant light significantly increased stimulus threshold levels for calls electrically evoked from vocally active sites in the medial midbrain, supporting previous findings that light suppresses VN excitability, while 2-iodomelatonin (2-IMel; a melatonin analogue) implantation decreased threshold. 2-IMel also increased fictive call duration evoked from medial sites as well as lateral midbrain sites that produced several-fold longer calls irrespective of photoregime or drug treatment. When stimulus intensity was incrementally increased, 2-IMel increased duration only at lateral sites, suggesting melatonin action is stronger in the lateral midbrain. For animals receiving five days of constant darkness, known to increase VN excitability, systemic injections of either of two mammalian melatonin

* Previously published as Feng NY, Bass AH. 2014. *Journal of Experimental Biology* 217: 1046–1057.

receptor antagonists increased threshold and decreased duration for calls evoked from medial sites. Our results demonstrate melatonin modulation of vocal network excitability and suggest that social context-dependent call types differing in duration may be determined by neuro-hormonal action within specific regions of a midbrain vocal-acoustic network.

Introduction

Conserved features of vertebrate vocal-acoustic communication include the production of context-dependent vocal call types, occurrence over predictable daily and seasonal cycles, and the ability of neuro-hormones to modulate vocal motor output by acting upon dedicated neural networks (Bass and Remage-Healey, 2008; Goodson and Bass, 2001; Tramontin and Brenowitz, 2000). Most studies to date on fish circadian rhythms have investigated the effects of photoperiod and the time-keeping pineal hormone, melatonin, on locomotor or feeding activity, while little attention has been paid to melatonin's action on courtship behaviors such as vocalization, or more generally on underlying neural circuitry (Azpeleta et al., 2010; López-Olmeda et al., 2006; Piccinetti et al., 2010; Pinillos et al., 2001; Zhdanova et al., 2001). In songbirds, a melatonin-sensitive circadian rhythm in song and call behaviors has only recently been shown (Wang et al., 2012), even though melatonin influence on song nuclei volume and expression of song nuclei-specific melatonin receptors has been well-documented (Bentley, 2003; Bentley and Ball, 2000; Bentley et al., 1999; Bentley et al., 2013; Cassone et al., 1995; Cassone et al., 2008; Gahr and Kosar, 1996; Jansen et al., 2005; Whitfield-Rucker and Cassone, 1996). Additionally, melatonin inhibited the

spontaneous firing rate of a vocal premotor nucleus in the zebra finch, suggesting that it can act directly on vocal circuits to influence vocal patterning (Jansen et al., 2005). Here, we use a fish model to investigate melatonin influence on the temporal patterning of a brainstem neural circuit dedicated to sound production.

Male plainfin midshipman (*Porichthys notatus*) contract sonic swim bladder muscles at ~100Hz to produce several call types distinguishable mainly by their duration and the social context under which they are produced (Brantley and Bass, 1994; Bass et al., 1999). Nest-guarding males produce very long duration (mins-h) advertisement/courtship "hums" or short duration agonistic "grunts" (~50-200 ms) (e.g., Fig. 2.1A) (Bass et al., 1999; Bass and McKibben, 2003; Brantley and Bass, 1994). Well-defined forebrain, midbrain, and hindbrain nuclei form a vocal-acoustic network (Bass et al., 1994; Goodson and Bass, 2002), the output of which is readily recorded *in-vivo* from paired vocal occipital nerves that innervate the sonic muscles and are considered homologues of hypoglossal nerve roots (Fig. 2.1B) (Bass et al., 2008). The spike-like vocal nerve motor volley is referred to as a fictive call in the absence of muscle activation because each nerve spike directly translates into a single muscle contraction and, in turn, one sound pulse (Fig. 2.1A) (Bass and Baker, 1990; Cohen and Winn, 1967). Each spike reflects the synchronous firing of vocal motor neurons whose activity is patterned by hindbrain premotor nuclei (Bass and Baker, 1990; Chagnaud et al., 2011; Chagnaud et al., 2012). Hence, fictive calls are a reliable proxy for assessing hormonal influences mediated by specific receptors on a discrete vocal network that directly determines natural call properties (Forlano et al, 2005; Forlano et al., 2010; Goodson and Bass, 2000a; Goodson and Bass, 2000b; Goodson

et al., 2003; Fergus and Bass, 2013; Remage-Healey and Bass, 2004; Remage-Healey and Bass, 2007). Given the importance of day length on regulating reproductive physiology, melatonin's role as the main time-keeping hormone among vertebrates, and evidence of its interaction with the hypothalamo-pituitary-gonadal axis (Azpeleta et al., 2010; Bhattacharya et al., 2007; Falcón et al., 2007; Falcón et al., 2010), the midshipman presents a tractable model for investigating potential melatonin action on the excitability of neural networks regulating courtship behaviors.

Midshipman courtship vocalization follows dramatic daily and seasonal rhythms, occurring at night during the summer breeding season (Brantley and Bass, 1994; Ibara et al., 1983). Field and captive studies of fish vocal behavior report robust daily periodicity, with activity peaking during nighttime in most species identified, including closely related toadfish (Locascio and Mann, 2008; Rice and Bass, 2009). Directly complementing behavioral studies, *in-vivo* neurophysiology in midshipman demonstrates a nocturnal increase in vocal network excitability, measured in increased duration and decreased stimulation threshold of midbrain evoked fictive calls (Rubow and Bass, 2009). Constant light conditions abolish the nocturnal rise in excitability, while constant dark substantially increases excitability (Rubow and Bass, 2009). Although these studies support the existence of either daily or circadian rhythms in fish vocal behavior and neural circuit plasticity, potential control mechanisms remain unknown.

Given the ability of constant light to abolish pineal melatonin production and constant dark to increase baseline melatonin in many species of fish (Bayarri et al., 2002; Bhattacharya et al., 2007; Falcón et al., 2010), we tested the hypothesis that the

stimulatory effects of constant darkness on vocal excitability were due, in part, to an increase in melatonin action in discrete vocal nuclei. Within the midshipman vocal network, the midbrain periaqueductal gray (PAG) and surrounding midbrain tegmentum play a crucial role in vocalization initiation, consistent with other vertebrates (Kittelberger and Bass, 2013). We report that, compared to medial stimulation sites, lateral midbrain sites produce longer duration calls comparable to natural advertisement/mate calls that are more sensitive to the stimulatory effects of melatonin than brief calls evoked from medial sites. We propose the existence of a neuroendocrine center located laterally within the previously described midbrain vocal-acoustic network that contributes to the generation of social context-dependent calls. To our knowledge, this study is the first demonstration of melatonin effects on the excitability of a neural network underlying vocal behavior in fishes, and one of few such studies in all of vertebrates (Jansen et al., 2005).

Results

We used two electrical microstimulation regimes in the midbrain to probe vocal network excitability. The first regime evoked fictive responses at ten time points over 120 min, following Rubow and Bass (2009). The second stimulation regime, referred throughout as a stimulus-response curve (**SRC**), assessed fictive call responses to increasing stimulus current levels. Prior to each time point in 120 min sessions and each SRC, we measured the minimum stimulus current required to elicit responses (threshold). Figure 2.1C and D provide schematics of photoperiod, drug treatment, and neurophysiology stimulation regimes used in this study.

Figure 2.1
(A) Natural (adapted from Rubow and Bass, 2009) and fictive calls of male midshipman fish. Long-duration advertisement hums are produced in the summer at nighttime. Short-duration agonistic grunt trains can be produced at any time of day or year. **(B)** A schematic saggital view of the midshipman brain showing the vocal control network (adapted from Chagnaud et al., 2011). Stimulation in the midbrain vocal-acoustic complex (mVAC) evokes readily recorded fictive calls from the vocal nerve. mVAC receives input from forebrain vocal-acoustic complex (fVAC), from which fictive calls can also be evoked. mVAC drives the hindbrain vocal pattern generator, which provides a precise and synchronous code for sonic muscle contraction and consists of vocal pre-pacemaker nucleus (VPP), vocal pacemaker nucleus (VPN), and vocal motor nucleus (VMN). **(C-D)** Schematic of photoperiod, drug treatment, and neurophysiology stimulation regimes used in this study. **(C)** 5LL fish were implanted with 2-IMel or vehicle before subjective lights-off and moved to constant light (LL) for 5 days (d). Light grey boxes represent subjective night. 5DD fish were held in 5 days of constant darkness (DD) and injected daily around subjective lights-off with vehicle, luzindole, or 4PPDOT. Dark grey boxes represent subjective day. Black arrows indicate time of treatment, and gray arrow indicates time of neurophysiology for both 5LL and 5DD fish. 120 min sessions consisted of stimulation at indicated times after fish acclimated on the rig for 1 h. 40 stimuli were delivered at each time point except for 120 min when an additional 60 stimuli for a total of 100 was delivered (highlighted by *). 10 min later, a stimulus response curve (SRC) was collected without moving the electrode, where stimulus intensity was increased to indicated % of baseline threshold, recording 10 fictive calls every 5 min. The stimulus electrode was then immediately moved to a lateral site in the midbrain to collect another SRC. **(D)** LD fish were tested for medial and lateral midbrain stimulation comparisons and were housed in 9 h of darkness (D) and 15 h of light (L). The neurophysiology stimulation regime followed that of 5LL and 5DD animals except only 40 stimuli were delivered at the 120 min trial, and only one SRC was collected after 120 min sessions without moving the electrode.

Figure 2.1 (continued)

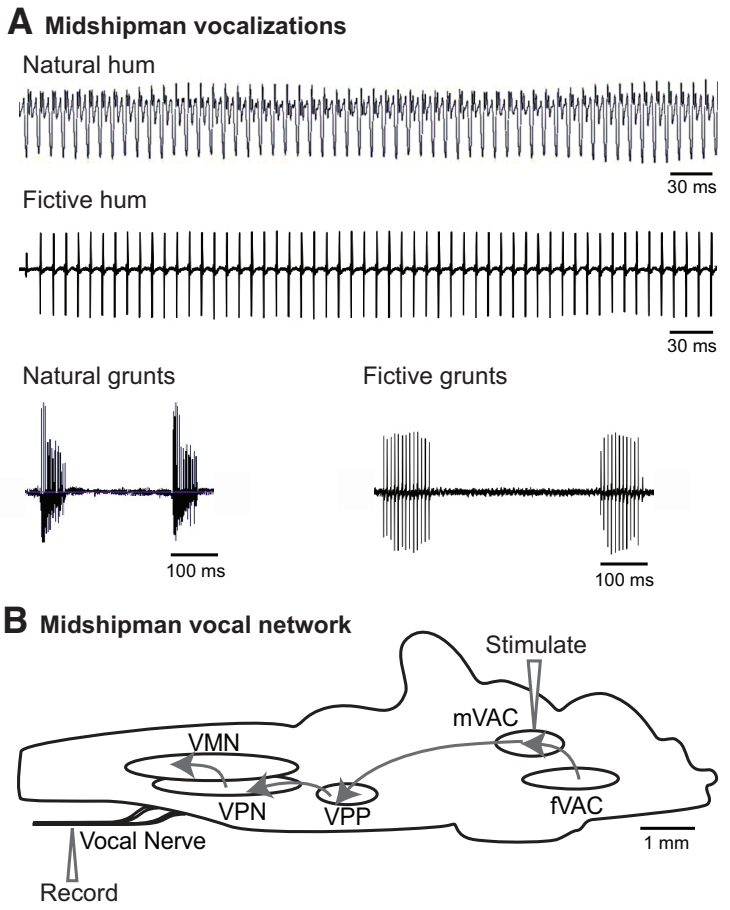

Although earlier studies were suggestive that more robust vocal stimulation sites could be found in lateral portions of the midbrain PAG and portions of the surrounding tegmentum in comparison to medial sites (Goodson and Bass, 2000b), no study systematically compared vocal output between midbrain regions or examined their neuroendocrine control. In addition to eliciting vocal output from medial sites in the medial PAG and nearby tegmentum (Kittelberger and Bass, 2013), we also stimulated sites in the lateral midbrain that could reliably elicit up to a magnitude longer duration output. We first provide evidence of photoregime effects and melatonin modulation in medial and lateral midbrain regions followed by detailed comparisons of their excitability.

Effects of photoperiod on vocal excitability inferred from control animals

Fish were held under three different photoregimes: one group was maintained on a 15:9h L:D cycle (**LD**), consistent with their breeding season photoperiod during late spring-summer. Another group was moved from LD to 24h of light for five days **(5LL)**. Constant light conditions have been equated to "functional pinealectomy", which in fish, as in mammals, abolishes the nocturnal increase in melatonin secretion from the pineal (Bayarri et al., 2002; Bhattacharya et al., 2007; Carter et al., 1982; Porter et al., 1999). A third group was moved from LD to 24h of darkness for five days (**5DD**). In constant darkness, the pineal of most teleosts exhibits endogenous cycling of melatonin production albeit at higher daytime levels than under normal light-dark cycles, with the exception of some that show constant up-regulation of melatonin production within the duration of darkness (Ekström and Meissl, 1997;

Oliveira et al., 2009). Either 5LL or 5DD was chosen because these regimes exaggerate the observed natural decrease or increase in vocal excitability associated with daytime and nighttime, respectively (Rubow and Bass, 2009).

We first compared vocal output in control animals from each of the photoperiod groups (see above and Results sections below) to examine effects of photoperiod manipulation alone and to validate previous findings that 5LL decreased and 5DD increased vocal excitability, respectively (Rubow and Bass, 2009). For 120 min sessions and medial site SRC comparisons (Fig. 2.2A-C), data were from animals tested at medial stimulation sites, including 5LL implant controls for testing effects of a melatonin agonist on excitability (n=10, Fig. 2.3), 5DD vehicle-injected controls for testing effects of melatonin antagonists on excitability (n=6, Fig. 2.4), and LD animals for comparing vocal motor output from medial vs. lateral midbrain sites (n=5, Fig. 2.5). For lateral SRCs (Fig. 2.2D), data were from the same 5LL and 5DD control animals as above, as well as LD animals that first received lateral stimulation over 120 min sessions (n=5, Fig. 2.5). We present the following results with the caveat that although all were control animals, differences in treatment methods (no treatment, implant, injection) could have contributed to variation in vocal excitability.

For the medial midbrain, we observed a strong trend of photoregime effect on call duration recorded over 120 min, with 5DD animals having the longest fictive calls (Fig. 2.2A) (P=0.06). There was a significant effect of photoregime on stimulus threshold over the 120 min session (Fig. 2.2B) ($F_{(2,18.0)}$=6.02, P=0.01) and a significant photoregime*time interaction ($F_{(18,161)}$=2.68, P=0.0005), with 5LL animals having the highest thresholds (Tukey-HSD: 5LL vs 5DD: P=0.018; 5LL vs LD: P=0.043). These

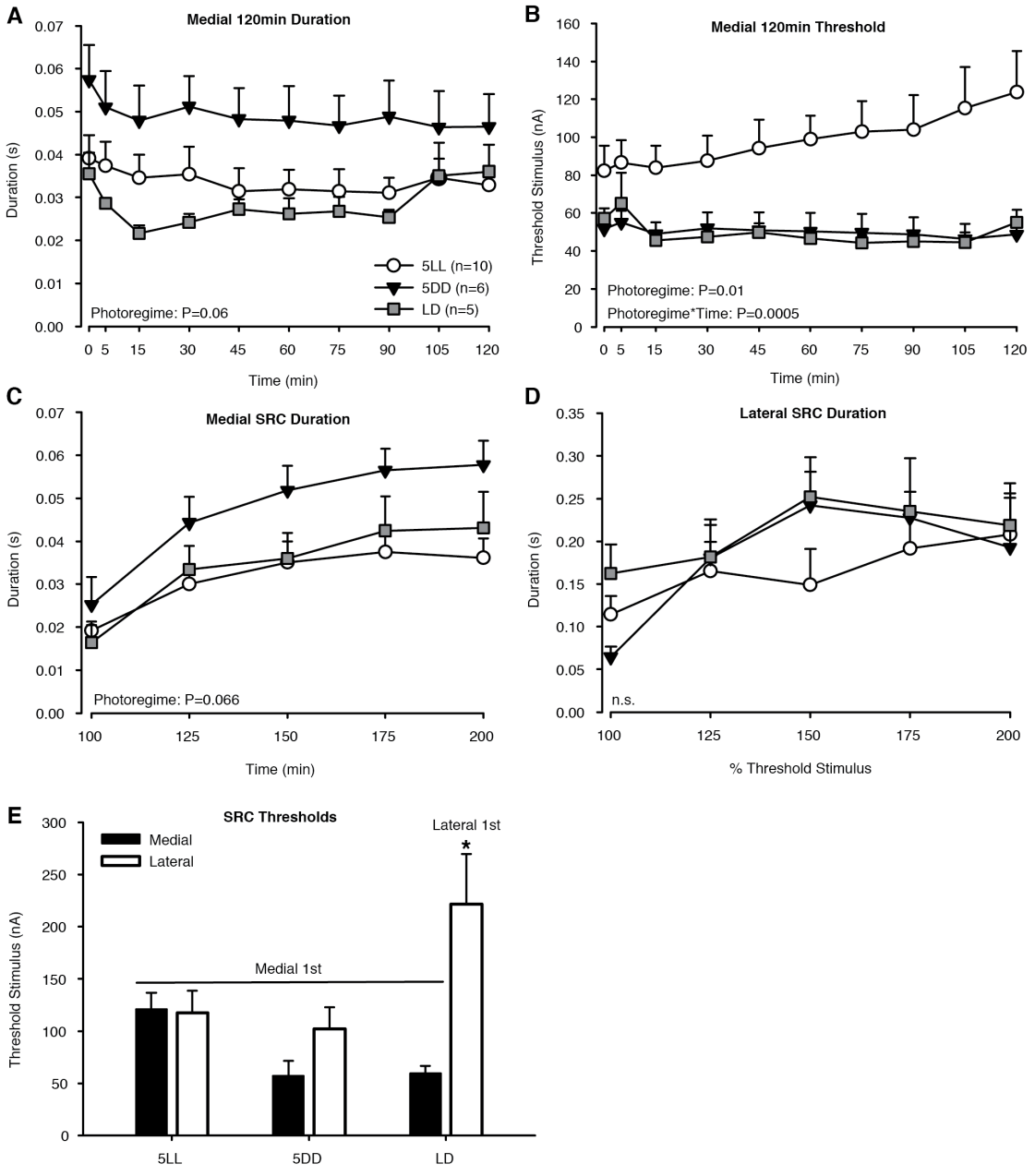

Figure 2.2

Effects of photoperiod on vocal excitability inferred from control animals. Fictive call duration **(A)** and threshold **(B)** over 120 min sessions, as well as medial **(C)** and lateral **(D)** SRCs recorded from control fish of each photoregime/treatment group: LD, 5LL, and 5DD (see legend in **A**). **(E)** Threshold levels at baseline trials of medial and lateral SRCs. For LD fish that received lateral midbrain stimulation only, lateral SRCs were recorded without prior medial SRCs (Lateral 1st). All other groups received medial stimulation first (Medial 1st). Data are presented as mean±standard error. n.s., non-significant. * indicates P<0.042.

results for medial sites suggested that 5DD increased and 5LL suppressed vocal excitability, as best revealed by threshold levels.

There was a similar strong trend for a photoregime effect on medial site SRC burst duration (P=0.066), with 5DD animals having the highest duration (Fig. 2.2C). For lateral site SRC (Fig. 2.2D), we detected no significant photoregime effect (P=0.73). There was no photoregime*stimulus-intensity interaction for either medial (P=0.12) or lateral (P=0.17) SRCs.

Finally, we compared medial vs. lateral site excitability by examining SRC thresholds in control animals (Fig. 2.2E). When we examined the effects of photoregime, stimulus site, and their interaction on SRC thresholds, we found a near-significant photoregime effect (P=0.061), significant stimulus site effect ($F_{(1,1)}$=12.48, P=0.001), and photoregime*stimulus site interaction ($F_{(2,2)}$=6.41, P=0.004). Post-hoc Tukey-HSD showed that the lateral SRC threshold of LD animals who did not receive prior medial stimulation was significantly higher than all others who received medial stimulation first (P<0.042) (Fig. 2.2E). These results imply that stimulation at medial sites first with a 120 min session disinhibits lateral sites by decreasing threshold, but stimulation at lateral sites first does not.

We concluded that photoregime had a significant influence on vocal excitability. This was most strikingly revealed by threshold comparisons (Fig. 2.2B), consistent with the results of Rubow and Bass (2009) and our hypothesis that constant light inhibits vocal excitability.

2-Iodomelatonin treatment in 5LL animals

To test the prediction that melatonin replacement can rescue the decreased vocal motor excitability seen in 5LL animals (Rubow and Bass, 2009), fish held in 5LL received an implant for five days of either a vehicle or 2-iodomelatonin (2-IMel), a high affinity melatonin analogue that acts on both MT1/Mel1a and MT2/Mel1b receptor subtypes in mammals (Dubocovich et al., 2010; Boutin et al., 2005; Stankov et al., 1993).

For 120 min recording sessions at medial sites, 2-IMel significantly increased fictive call duration in a time-dependent manner (Fig. 2.3A). There was a significant effect of time ($F_{(10,200)}$=2.9, P=0.002) and time*treatment interaction ($F_{(10,200)}$=2.0; P=0.038), but no treatment effect alone (P=0.09). Additionally, 2-IMel significantly decreased overall stimulus threshold in 5LL males across 120 min sessions (Fig. 2.3B) ($F_{(1,20)}$=4.3, P=0.0514) and there was a significant treatment*time interaction ($F_{(9,180)}$=2.17, P=0.026). In sum, 120 recording sessions revealed that 2-IMel increased vocal excitability at medial stimulation sites in 5LL fish.

For SRCs, 2-IMel exerted a site-dependent effect on duration with a significant stimulatory effect at lateral, but not medial, stimulation sites (Fig. 2.3C,D). At lateral sites, 2-IMel treatment significantly increased duration ($F_{(1,20)}$=4.8, P=0.041), with a significant treatment*stimulus-intensity interaction ($F_{(4,80)}$=5.6, P=0.0005). At medial sites, we observed no treatment (P=0.59) or treatment*stimulus-intensity interactions (P=0.91). We also compared the threshold stimulus levels for SRCs (Fig. 2.3E). There was a significant treatment effect of 2I-Mel for decreasing threshold ($F_{(1,40)}$=5.28, P=0.027), but no stimulus-site effect (P=0.44) or stimulus-site*treatment interaction (P=0.33).

Figure 2.3
Characterization of fictive calls elicited from animals kept under five days of continuous light (5LL) and implanted with 2-iodomelatonin (2-IMel) or vehicle control. (A) 2-IMel treatment increased fictive call duration in a time-dependent manner during the 120 min stimulus trial and decreased stimulus threshold **(B)** (see legend in **A**). **(C-D)** 2-IMel increased fictive call duration in stimulus response curves (SRC) only when lateral midbrain was stimulated. **(E)** 2I-Mel decreased stimulus threshold measured at the onset of SRCs. All fish were stimulated at a medial site first for the 120 min session and SRC, followed by recording a second SRC at a lateral site. Data are presented as mean±standard error. Abbreviations: Stim, stimulus intensity; n.s., non-significant. Note for 120 min session duration, the means from the first 40 responses were separated from the last 60 fictive call responses (displaced to the right), hence the two data points at 120 min.

Figure 2.3 (continued)

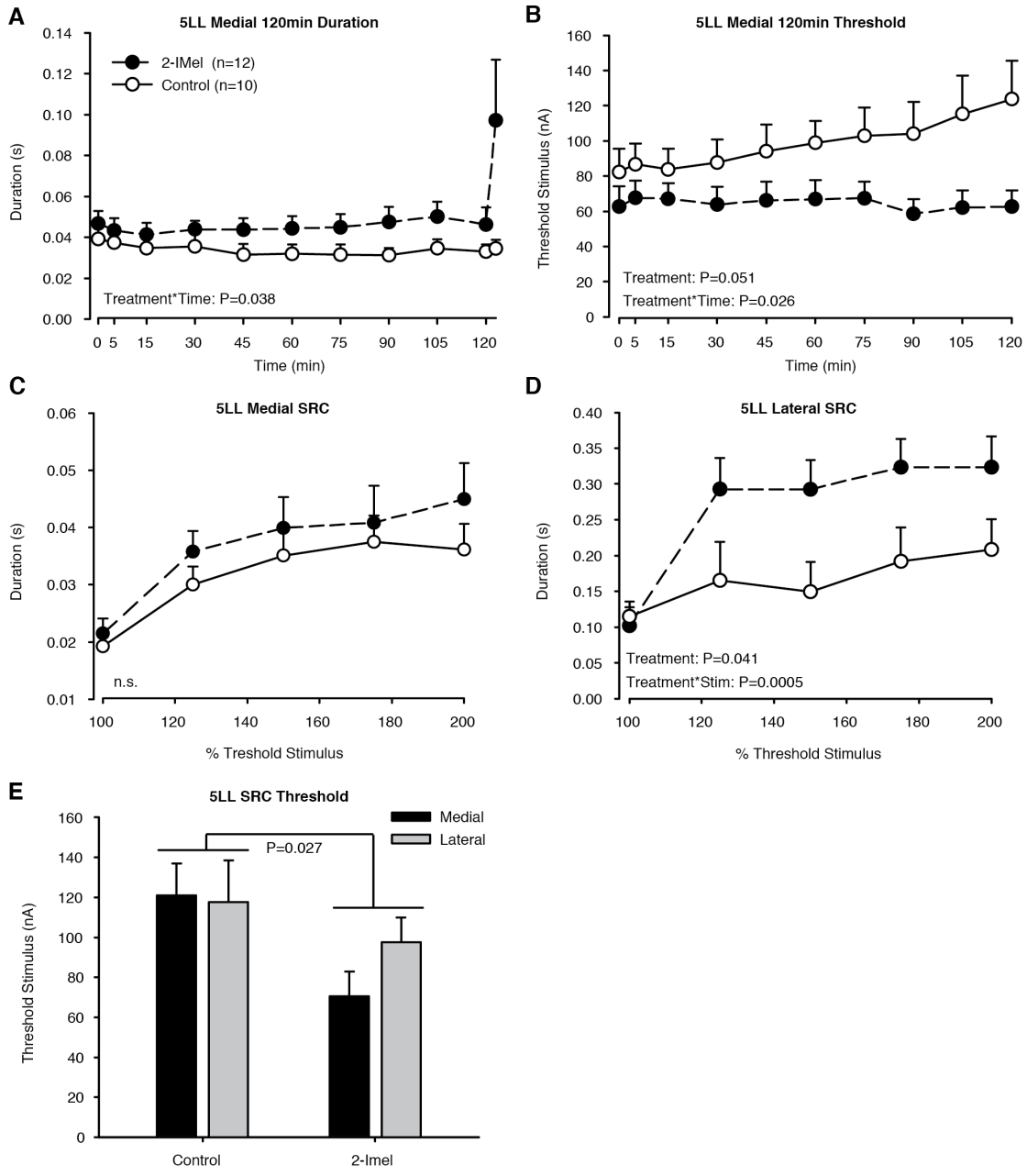

Taken together, the results indicated that 2-IMel increased excitability at vocal midbrain sites, irrespective of stimulating electrode location. However, the SRC paradigm revealed a particularly robust stimulatory effect of melatonin on call duration specific to lateral midbrain sites.

Melatonin receptor antagonist treatment in 5DD animals

We set out to test the hypothesis that melatonin action on specific receptor subtypes could explain the increased vocal excitability observed in 5DD males. Since our comparisons of control groups showed that 5DD decreased threshold levels at medial sites (Fig. 2.2B), we predicted that treatment with melatonin receptor antagonists would reverse this effect. Fish held in 5DD received daily intramuscular injections for five days of a receptor antagonist or vehicle (Fig. 2.1C). The antagonists used were luzindole, a general Mel1a/b antagonist, or 4-phenyl-2-propionamidotetralin (4P-PDOT), a Mel1b specific antagonist (Dubocovich et al., 2010).

For 120 min sessions, although luzindole values for duration were generally lower at all time points, there was no significant effect (P=0.16) or treatment*time interaction (P=0.58) when compared to animals injected with vehicle control. No treatment (P=1.00) or treatment*time interaction (P=0.76) on duration were observed between vehicle and 4P-PDOT (Fig. 2.4A). For vehicle to luzindole stimulus threshold comparisons, there was no effect of treatment (P=0.84) or treatment*time interaction (P=0.74). For vehicle to 4P-PDOT threshold comparisons, we found no effect of treatment (P=0.18) alone, but there was a significant treatment*time interaction (Fig. 2.4B) ($F_{(9,90)}$=4.34, P=0.0001). In sum, 4P-PDOT increased threshold in a time-

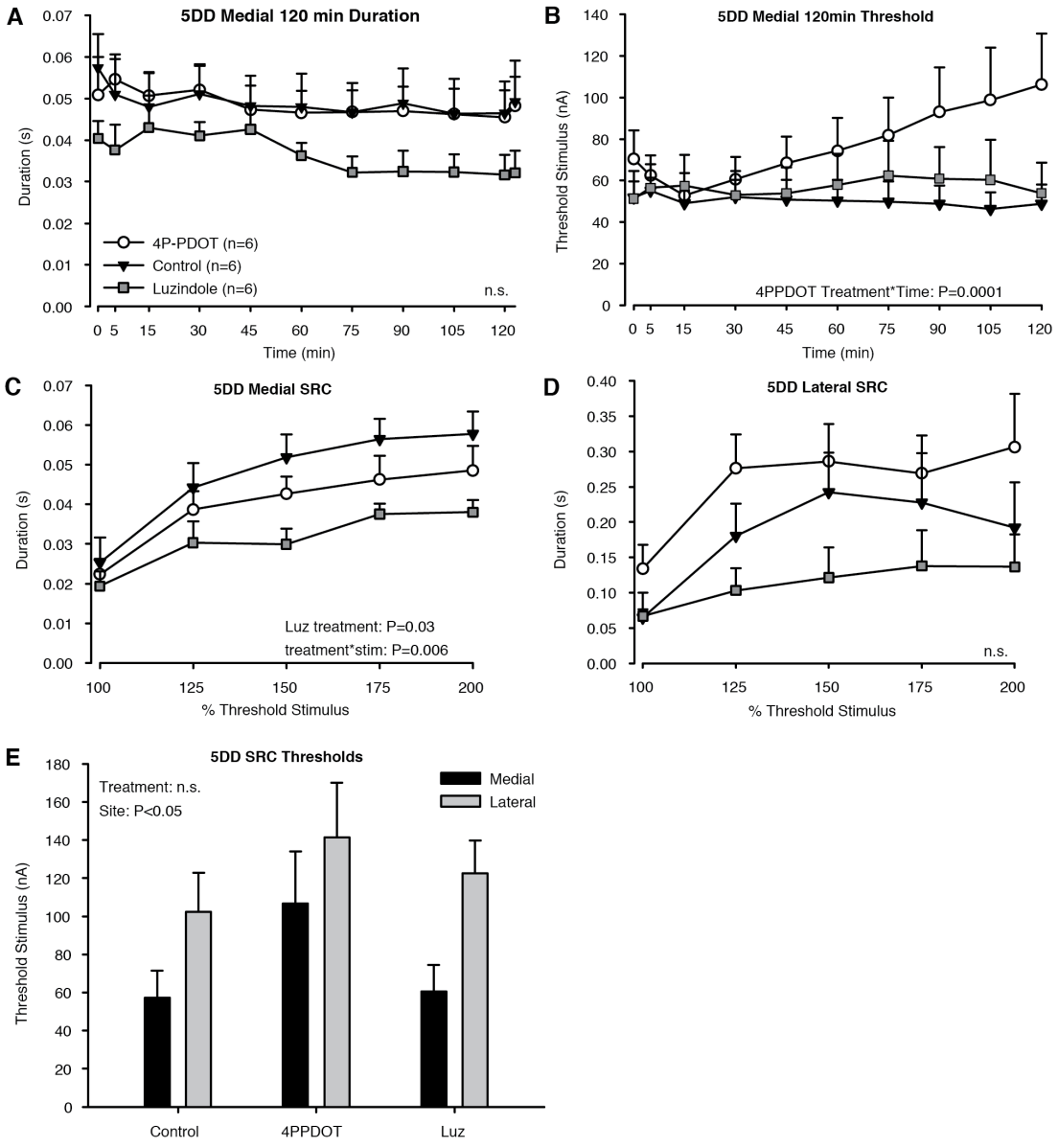

Figure 2.4

Melatonin receptor antagonists luzindole (luz) and 4P-PDOT have mixed effects on fictive call 120 min session duration **(A)**, 120 min session threshold **(B)**, medial SRC duration **(C)**, and lateral SRC duration **(D)** in fish kept under five days of constant dark (5DD) (see legend in **A**). **(E)** Treatments had no effect on SRC threshold levels, which were higher at lateral sites. Data are presented as mean±standard error. stim, stimulus intensity; n.s., non-significant. Note for 120 min session duration measurements the means from the first 40 responses were separated from the last 60 fictive call responses (displaced to the right), hence the two data points at 120 min.

dependent manner, suggesting that disrupting Mel1b-mediated melatonin action impacts vocal excitability at medial sites in 5DD animals.

For SRCs evoked at medial sites, luzindole significantly decreased fictive call duration ($F_{(1,10)}$=6.42, P=0.03) with a significant treatment*stimulus-intensity interaction ($F_{(4,40)}$=4.23, P=0.006); 4P-PDOT had no effect (P=0.32) (Fig. 2.4C). In lateral SRCs, treatment with either luzindole (P=0.21) or 4P-PDOT (P=0.25) had no effect on duration (Fig. 2.4D). Thus, luzindole, like 4P-PDOT, inhibited vocal excitability at medial sites in 5DD animals. Finally, there was no significant treatment effect on SRC threshold levels (luzindole: P=0.56; 4P-PDOT: P=0.11) or treatment*stimulus-site interaction (Fig. 2.4E) (luzindole: P=0.75; 4P-PDOT: P=0.59), but there was a stimulus-site effect of lateral sites having significantly higher thresholds (Fig. 2.4E) (luzindole: $F_{(1,9.4)}$=14.5; P=0.004; 4P-PDOT: $F_{(1,10)}$=5.0; P=0.048).

In summary, for calls evoked from medial sites, antagonizing Mel1b receptors (4P-PDOT) increased threshold in 120 min sessions, while antagonizing Mel1a/b receptors (luzindole) decreased duration in SRCs. This was consistent with our predication that the increased vocal excitability seen in 5DD control animals was due to melatonin action on specific melatonin receptors.

Medial vs. lateral midbrain vocal sites

We wanted to ensure that the several fold longer duration calls consistently elicited from stimulation sites in the lateral compared to the medial midbrain (Figs. 2.2C,D; 2.3C,D; 2.4C,D) were not due to a priming effect of stimulating for 120 min at a

medial site first. We tested non-treated LD males at either (1) only a medial or only a lateral site for a 120 min session delivering only 40 stimuli at the 120 min trial, followed by one SRC at the same site (Figs. 2.1D; 2.5) or (2) a lateral site for a 120 min session and SRC followed by a second SRC at a medial site (Fig. 2.6).

Stimulation at lateral midbrain sites often led to several-fold longer duration fictive calls than those elicited from medial sites (e.g., Fig. 2.5Ai,ii; Bi,ii). Examination of fictive call frequency, measured in inter-pulse intervals (IPIs), of all fictive calls taken from one pair of representative medial and lateral SRCs revealed no significant site-dependent differences (P=0.14) (e.g. Fig. 2.5Aiii, Biii). For 120 min trials, lateral-evoked calls had a significantly longer duration (Fig. 5C) ($F_{(1,7.9)}$=217.6, P<0.0001), higher threshold (Fig. 2.5D) ($F_{(1,7.9)}$=14.0, P=0.006), and longer latency (Fig. 2.5E) ($F_{(1,8.0)}$=316.8, P<0.0001). Medial site stimulation successfully evoked fictive calls for 98.8±1.0% (mean±s.e.m, 120 min trial means) of the 40 stimuli delivered in each trial, whereas lateral stimulation was less reliable at 65.0±2.2% (data not shown).

Similar to the results for 120 min trials (Fig. 2.5C), lateral site SRCs had significantly longer calls (Fig. 2.5F) ($F_{(1,8.0)}$=68.4, P<0.0001). In a pilot study (n=3), we found the same response patterns when first stimulating in a lateral site for a 120 min session and SRC and then moving to a medial site for a second SRC (Fig. 2.6) ($F_{(1,18)}$=138.9, P<0.0001).

Taken together, although calls elicited from lateral sites were longer duration than those from medial sites, they required more stimulus current to initiate and exhibited longer latencies.

Figure 2.5
(A-B) Five representative fictive vocal responses evoked by medial (**Ai**) and lateral (**Bi**) midbrain stimulation at 200% SRC, taken from a fish that was treated with 2-IMel. Fictive vocal traces outlined in grey boxes were enlarged in (**Aii**) and (**Bii**). Grey carat signs point to stimulus artifacts. From the same fish and stimulation trial, fictive call firing frequency, measured in inter-pulse intervals (IPI), taken from 200% threshold medial SRC trial (**Aiii)** and lateral SRC trial **(Biii)** showed no significant site-dependent differences. **(C-F)** Quantification of fictive call duration **(C)**, stimulus threshold **(D)**, latency **(E)**, and stimulus response curves **(F)** resulting from either medial or lateral midbrain stimulation in non-treated fish held in normal light:dark (LD) cycles (n=5/group). Data are presented as mean±standard error. All stimulus-site comparisons shown in **C-F** are statistically significant ($P<0.006$).

Figure 2.5 (continued)

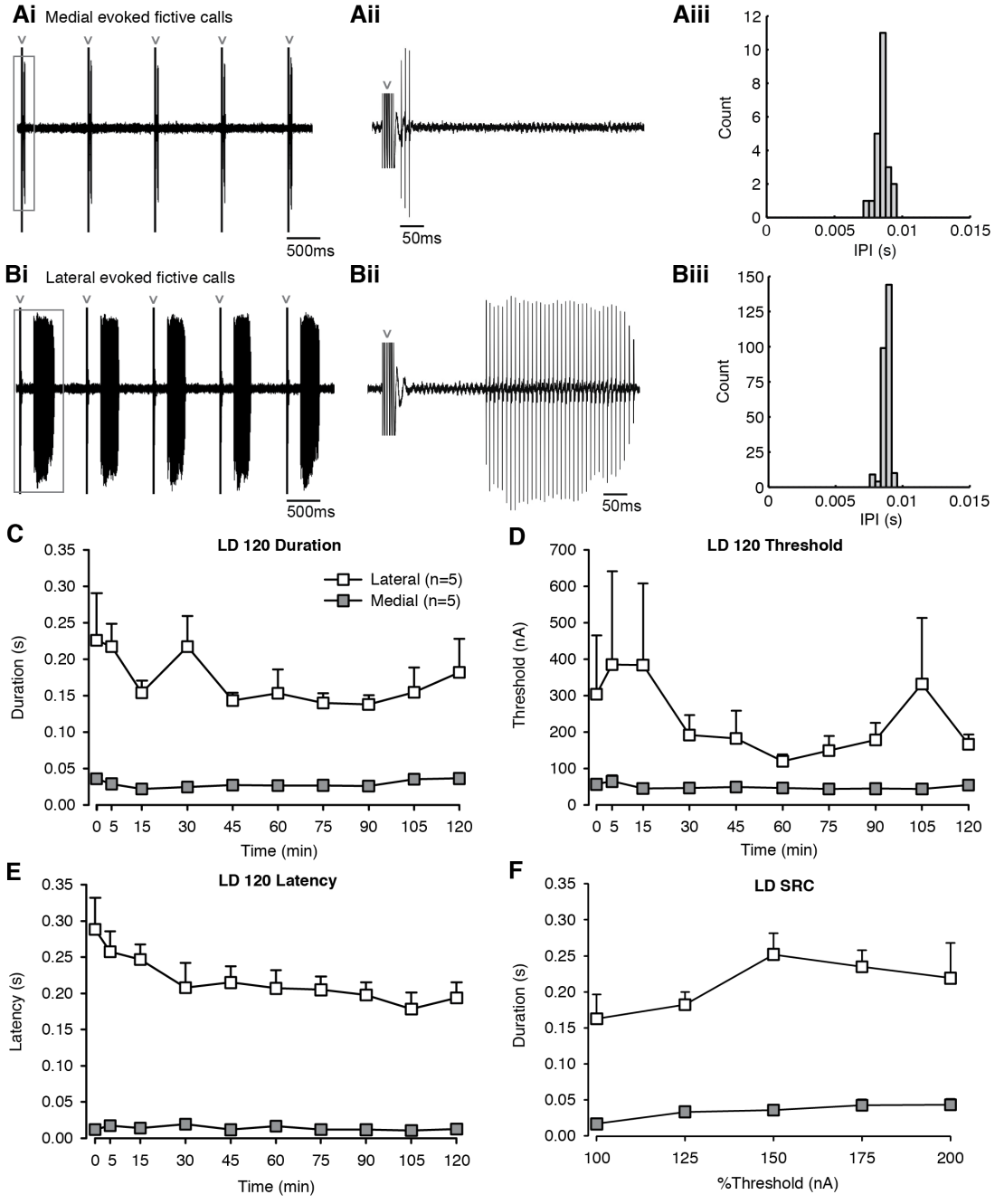

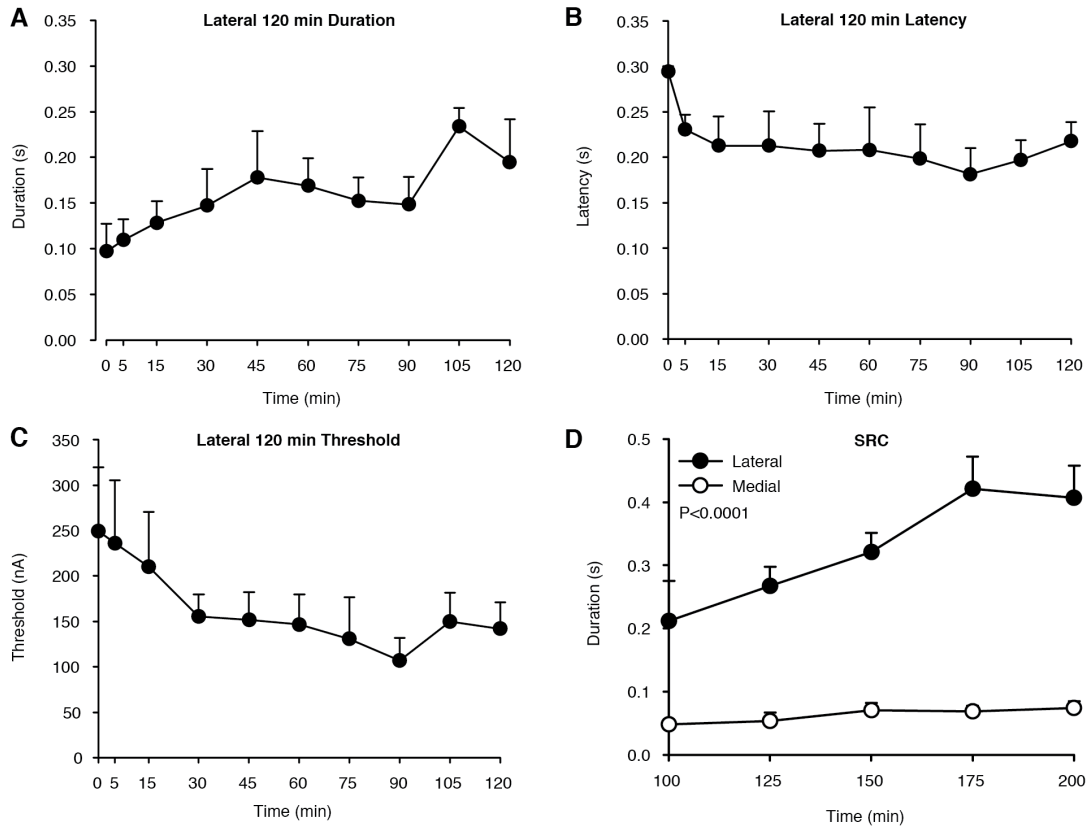

Figure 2.6
Medial sites evoked shorter fictive calls, even after lateral stimulation. Three males held in normal 15 h light:9 h dark cycle were tested at the lateral site first for a 120 min session and a SRC at the same site, followed by recording a second SRC at the medial site. **(A)** Fictive call duration recorded over 120 min from the lateral site. **(B)** Fictive call latency recorded over 120 min from the medial site. **(C)** Threshold stimulus required to elicit fictive calls over 120 min sessions. **(D)** Fictive calls elicited during lateral SRC are significantly longer than medial SRC, demonstrating that regardless of stimulus order, lateral midbrain stimulation reliably elicits longer duration calls. P value is shown for the fixed effect of stimulus-site. Data are presented as mean±standard error.

Electrolytic lesions in a subset of animals, including those from drug treatment experiments, localized medial (n=11) and lateral (n=10) midbrain stimulation sites. Fictive call duration was highly dependent upon the site of stimulation segregated along the medial-lateral midbrain axis (Fig. 2.7). Medial sites were located in the midbrain tegmentum and the medial PAG. Lateral sites were in the paratoral tegmentum (PTT), deep layer of the torus semicircularis (TSd), and just below and within the ventral aspect of the paralemniscal tegmentum (PL).

Discussion

Our results support the hypothesis that nocturnal melatonin action contributes to increased vocal excitability during the midshipman breeding season. The SRC stimulation paradigm highlighted the lateral midbrain vocal-acoustic network as a potential neuroendocrine node that contributes to the production of distinct social context-dependent vocal outputs. We propose that these findings apply to other lineages of vocal vertebrates given wide occurrence of daily and seasonal cyclicity in vocal behaviors and conserved vocal network organization.

Melatonin regulation of vocal excitability

We found that in control animals, constant light (5LL) inhibited vocal excitability by increasing stimulus threshold at the medial site compared to fish held in constant dark (5DD) and normal light-dark cycles, consistent with previous findings (Rubow and Bass, 2009). This inhibitory effect was rescued by melatonin agonist (2-IMel) implants in fish held under 5LL (Fig. 2.3B). 2-IMel implant also led to increased call

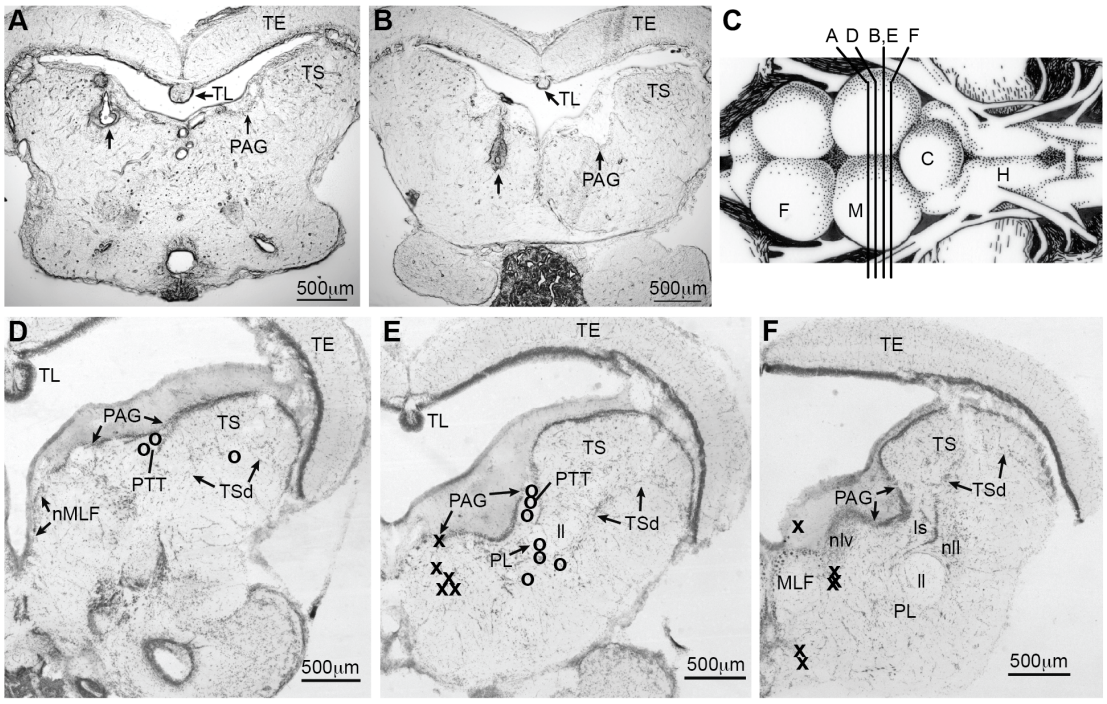

Figure 2.7

Localization of lateral and medial midbrain lesion sites. Sample lateral **(A)** and medial **(B)** lesions are indicated by arrows. **(C)** Dorsal view of the midshipman brain, showing relative midbrain levels at which coronal sections in D-F were taken. Abbreviations: F, forebrain; M, midbrain; C, cerebellum; H, hindbrain. **(D-F)** The relative positions of medial (x) and lateral (o) lesion sites were mapped onto midbrain sections at three transverse levels adapted from Kittelberger and Bass (2013). Of the medial lesions, seven fell within the midbrain tegmentum adjacent to the medial longitudinal fasciculus (MLF) that connects the vocal midbrain with the hindbrain vocal pattern generator (E,F), one was on the medial edge of the PAG (E), one was within the MLF (F), and two were below the MLF (F). Of the lateral lesions, five were in the paratoral tegmentum (PTT) that lies below the lateral periaqueductal gray (PAG) (D,E), one within the deep layer of the torus semicircularis (TSd) (D), and four just below or along ventral aspect of the paralemniscal tegmentum (PL) that borders the lateral lemniscus (ll) (E). Abbreviations: Is, isthmal nucleus; nll, nucleus of the ll; nMLF, nucleus of the MLF; nlv, nucleus lateralis valvulae; TE, midbrain tectum; TL, torus longitudinalis.

duration across 120 min sessions in a time-dependent manner. Interestingly, 2IMel increased duration in SRCs only at lateral, but not medial, midbrain stimulation sites (Fig. 2.3C-E). For 5DD fish, daily injections of 4P-PDOT, a Mel1b-specific receptor antagonist, increased thresholds across 120 min sessions in a time dependent manner; luzindole, a general Mel1a/b antagonist, resulted in consistently low call durations in both 120 min sessions and SRCs, but these effects were only significant in SRCs (Fig. 2.4). These mammalian-specific antagonists may be less effective in fish (Dubocovich et al., 2010), though some fish studies have effectively antagonized melatonin effects on locomotor and feeding activity via peripheral delivery of luzindole (Pinillos et al., 2001; Zhdanova et al., 2001). Together, our results support the hypothesis that a nocturnal melatonin action increases vocal network excitability in male midshipman fish during the breeding season.

Our experimental design was inspired by a previous study where 5DD and 5LL manipulations either significantly increased or decreased vocal network excitability, respectively (Rubow and Bass, 2009). Surprisingly at first, we found that medial midbrain stimulation in 5DD fish did not readily evoke the grunt-hums observed in the prior study that are structurally comparable to natural amplitude-modulated growls (see Rubow and Bass, 2009). Rather, we consistently elicited long duration fictive calls reminiscent of non-amplitude-modulated hum advertisement calls (see Fig. 2.1A), but only from the lateral midbrain. Our comparisons of control groups showed that although a 5DD effect on duration was apparent, it was only near significant (Fig. 2.2A). Two prominent methodological differences could explain this inconsistency. First, Rubow and Bass (2009) noted that an increase in stimulus intensity in

conjunction with the 100 stimulus presentation at 120 min was needed to evoke the grunt-hums, whereas in the current study stimulus intensity was kept low and consistent across the 120 min sessions. Second, the long duration fictive calls reported by Rubow and Bass (2009) were only readily evoked in males that were held in captivity for less than one month (Rubow, 2010; A. Bass, personal communication). Most fish used in the current study were first tested after being held captive for at least one month and did not produce long calls either at baseline or with repeated stimulation at the medial site, consistent with our earlier studies.

Results from control animal comparisons (Fig. 2.2) may shed light on the apparent conundrum that midshipman are both long-day and nocturnal breeders. The short duration of nocturnal melatonin experienced under long-days would lead to the prediction that melatonin is inhibitory to courtship behaviors, while being nocturnally active during peak diel levels of melatonin would lead to the inverse prediction. In support for an inhibitory role of melatonin in vocalization of diurnally active species, melatonin treatment in songbirds mimics the effect of short days by decreasing song nuclei volumes (Bentley et al., 1999; Cassone et al., 2008). Furthermore, daily melatonin treatment in pinealectomized zebra finches kept in constant dim light entrained song and call activity to occur during periods without melatonin (Wang et al., 2012). Our results in nocturnally active midshipman showed that fictive call duration was increased in 5LL+2-IMel animals, especially in the lateral midbrain (Fig. 2.3D), but not for vehicle-injected 5DD animals (Fig. 2.2D). One feasible explanation is that the combination of melatonin treatment and long durations of light experienced by 5LL+2-IMel animals increases vocal excitability by increasing melatonin

sensitivity in the lateral midbrain, perhaps in the form of a higher density of melatonin receptors. On the other hand, in fish that have experienced long durations of darkness (5DD), sensitivity to melatonin could have been diminished at the lateral midbrain, leading to no change in vocal excitability in response to constant darkness when melatonin levels are putatively high. However we did observe significantly lower threshold levels at medial midbrain sites in 5DD animals (Fig. 2.2B), suggesting 5DD does increase aspects of vocal excitability. These are testable hypotheses to be investigated in future studies on melatonin levels in 5DD animals, as well as photoperiod regulation of receptor density and localization.

Alternatively, increases in midshipman vocal excitability at night may rely on an increase in peak nocturnal melatonin levels during the summer breeding season. In some fish species, it has been found that although the duration of a nocturnal rise in circulating melatonin levels is shortened in response to long-day lengths, the amplitude of the rise is higher during the spring/summer breeding season and is positively correlated with water temperature (García-Allegue et al., 2001; Iigo and Aida, 1995; Vera et al., 2007). If this is also true for the midshipman, as males migrate from wintering in deeper, colder waters to shallow, warmer intertidal zones for breeding (see Bass, 1996), a higher nocturnal peak in melatonin levels could lead to increased vocal excitability at night.

Melatonin has been shown to interact with neuropeptide and steroid pathways in many vertebrates, including teleost fishes (Falcón et al., 2010; Maitra and Chattoraj, 2006), frogs (Lutterschmidt and Wilczynski, 2012), and birds (Chowdhury et al., 2010; Ubuka et al., 2005). Unlike nonapeptides and steroid hormones (Goodson and

Bass, 2000a; Remage-Healey and Bass, 2004), pilot studies showed that acute melatonin injections did not rapidly (5-120 min) change the output of the midshipman vocal system under our testing conditions (N. Feng, personal observations). Hence, the effects of melatonin on vocal excitability documented here were likely via slower, transcriptionally dependent events. Melatonin may interact with multiple neurotransmitter and neuromodulatory systems synergistically to stimulate the full expression of nocturnal behavior. In other words, melatonin could increase baseline vocal network excitability at night so that in the presence of other activating factors such as neuro-hormones and social cues, the vocal system is capable of responding by producing long duration calls.

A potential mechanism for melatonin to influence network excitability is through the inhibitory neurotransmitter gamma-aminobutyric acid (GABA). Acute melatonin application to mammalian brain slices increases or decreases GABAergic currents via Mel1a or Mel1b receptors, respectively (Wan et al., 1999). Supporting a stimulatory role for Mel1b-mediated action, antagonizing Mel1b receptors in zebra finches (which are specifically expressed in song control nuclei) at night decreased song duration the following day (Jansen et al., 2005). Song nucleus-specific Mel1b mRNA expression is also positively correlated with immediate early gene expression (Bentley et al., 2013), suggesting melatonin action contributes to increased neural activity in vocal centers. Our result of 4P-PDOT (mammalian Mel1b antagonist) increasing threshold during the 120 min session is consistent with Mel1b-mediated events as stimulatory on the vocal system. Given GABA's essential role in midshipman vocal network function (Chagnaud et al., 2011; Chagnaud et al., 2012),

melatonin might alter vocal network excitability via GABA.

Medial versus lateral midbrain vocal excitability

How the brain generates social context-dependent calls, distinguishable by vocal attributes such as duration, is still largely unresolved. Together with evidence from some mammalian species (Bandler and Carrive, 1988; Fenzl and Schuller, 2007), our study supports the possibility that vocal-acoustic centers in the midbrain contribute to modulation of different call types. We showed that activation of medial and lateral midbrain regions led to either short or long duration calls, respectively. The vocally active sites identified here are inclusive of those anatomically mapped in prior studies of midshipman (Goodson and Bass, 2002; Kittelberger et al., 2006; Kittelberger and Bass, 2013). Whether medial and lateral sites represent two parallel subdivisions of the descending vocal system or the lateral midbrain feeds into the medial to activate the hindbrain vocal central pattern generator (CPG) is beyond the scope of this study and requires further investigation of midbrain microcircuitry. We propose, for vertebrates in general, that the neural control of vocal attributes is sculpted by differential activation of midbrain populations given that (1) call duration is a salient trait distinguishing natural call types in midshipman (Bass and McKibben, 2003), and vertebrates in general (Bradbury and Vehrencamp, 2011), and (2) midbrain vocal sites are present in tetrapods (see Kittelberger et al., 2006).

Specifically, we showed that the duration of fictive calls elicited from lateral midbrain sites was up to an order of magnitude longer than those elicited from medial sites, regardless of stimulus order. In some experiments, medial stimulation may have

directly activated the MLF that also evokes brief calls (Kittelberger et al., 2006). Calls elicited from lateral sites also exhibited higher stimulus thresholds and longer latencies than medial-elicited calls, suggesting that the lateral site is overall less excitable and/or is part of a multi-synaptic pathway that eventually leads to activation of the hindbrain vocal CPG (see below). Strikingly, the latency of lateral midbrain-evoked fictive calls are comparable to the latency of the hum component in medial-midbrain evoked "grunt-hums"/growls (Rubow and Bass, 2009), suggesting that this component could have been produced by a disinhibited lateral site. Importantly, glutamate injection into the lateral midbrain elicits long duration responses like those we report here (Weeg et al., 2005), suggesting stimulation of local neuronal populations. A more complete investigation using, for example, focal glutamate injection can more precisely map vocally active sites in the midbrain. We propose that divergent medial versus lateral midbrain responses is reliant on differential patterns of vocal-acoustic connectivity and/or neuroendocrine modulation.

In midshipman, the midbrain PAG is a crucial node in vocalization initiation and highly interconnected with auditory centers, consistent with its role in sensorimotor integration and vocal initiation in birds and mammals (Jürgens, 2009; Holstege 1989; Kingsbury et al., 2011; Kittelberger and Bass, 2013). Recent studies reveal that the midshipman lateral PAG is more extensively connected than medial PAG to auditory-recipient nuclei including the TSd (Kittelberger and Bass, 2013), consistent with our finding that TSd stimulation can elicit longer calls (Fig. 2.7). The lateral PAG also shows greater connectivity to other brainstem vocal sites, as well as the anterior, ventral tuberal (vT) hypothalamus that is directly connected to and

activates the PAG (Goodson and Bass, 2000b; Goodson and Bass, 2002; Kittelberger et al., 2006; Kittelberger and Bass, 2013). The latency (Fig. 2.5E) and percentage of successfully evoked fictive calls from lateral midbrain sites recorded here (~65%, see Results) closely resemble values for calls evoked from vT, providing a neurophysiological complement to anatomical evidence showing stronger vT input to lateral than medial PAG (Kittelberger et al., 2006; Kittelberger and Bass, 2013). However, our lateral sites evoked notably longer calls than those reported for vT stimulation (Kittelberger et al., 2006), suggesting that while we stimulated the vT-PAG pathway, we were also activating a more extensive network. Furthermore, lateral PAG has stronger connections with the anterior tuberal hypothalamus (AT), a stimulation site that elicits calls similar to those from the lateral midbrain and PL (see Goodson and Bass, 2000b Fig. 4), so both AT and vT inputs into the lateral midbrain could be important for generating long calls. Rostromedial PAG, by contrast, has stronger connections to downstream hindbrain auditory-recipient nuclei that are absent from lateral PAG output (Kittelberger and Bass, 2013). Together, these results support a functional separation of the medial and lateral PAG/midbrain tegmentum in eliciting context-dependent call types, e.g., brief agonistic grunts vs. longer advertisement calls, dependent on sensory inputs and local neuroendocrine influences.

Vocal and acoustic structures in the midbrain such as the PAG, torus semicircularis, paratoral tegmentum (PTT), and paralemniscal tegmentum (PL) are highly interconnected and have been described together as the midbrain vocal-acoustic complex (mVAC) (Bass et al., 2000; Goodson and Bass, 2002). Anatomical studies of neuropeptide input and steroid receptor distribution in the midshipman midbrain

support potential medial versus lateral nodes of neuroendocrine action. Isotocin expressing fibers and terminals originating from the POA show dense expression in the mVAC, including the PTT that receives dense input from the lateral PAG and is a stimulation site resulting in long calls (Fig. 2.7D,E) (Goodson et al., 2003; Weeg et al., 2005; Kittelberger and Bass, 2013). Sparse labeling of isotocin was also found in the TSd, another site for eliciting long fictive calls (Fig. 2.7D). A dorsal bundle of AVT expressing fiber and terminals, also originating from the POA, can be found in the PTT. Unlike the diffuse expression of isotocin throughout the caudal midbrain, AVT immunoreactivity was concentrated in a dense band within the midbrain paralemniscal tegmentum (PL) (Goodson and Bass, 2000b; Goodson et al., 2003). Although Goodson and Bass (2000b) report no effects of AVT on fictive call duration following AVT injections in the PL (unlike in POA, Goodson and Bass, 2000a), the one illustration of a stimulation site (their Fig. 5A, comparable to our Fig. 2.7F) suggests that injections were at sites caudal and medial to the majority identified in our study (Fig. 2.7E).

Previous *in-vivo* physiology experiments are suggestive of steroid action at midbrain levels, where sustained (>30 min) stimulatory effects of steroids on fictive call duration are dependent on descending midbrain input into the hindbrain CPG (Remage-Healey and Bass, 2004). Subsequent studies show androgen and estrogen receptor subtypes in the PAG (Forlano et al., 2010; Fergus and Bass, 2013), and high concentrations of the estrogen-synthesizing enzyme aromatase in the medial PAG (see Forlano et al., 2005). Presumably, endogenous steroids could act upon midbrain specific receptors to increase vocal network excitability. However, since these studies

used systemic steroid injections, medial vs. lateral midbrain specific effects cannot be parsed out.

Taken together, the available evidence strongly suggests that further investigation is warranted to assess differential peptidergic and steroid control of specific midbrain vocal-acoustic regions.

Concluding remarks

Vertebrates occupy divergent temporal niches (Challet, 2007; Helfman, 1993; Reebs, 2002; Steiger et al., 2013) despite sharing a highly conserved and predictable pattern of melatonin secretion from the pineal at night (but see Wikelski et al., 2005). Thus, species-typical patterns of melatonin-dependent circadian and diel behaviors must rely on divergent downstream molecular and physiological events to interpret the melatonin signal accordingly at a particular time of day and year for a given species. Evidence for such plasticity is found in the varying distribution and abundance of melatonin receptors within neural pathways of songbirds across species, sex, development, and seasons (Bentley et al., 1999; Bentley et al., 2013; Cassone et al., 1995; Gahr and Kosar, 1996; Whitfield-Rucker and Cassone, 1996), the pro- or anti-gonadal effects of exogenous melatonin treatment in fishes (Maitra and Chattoraj, 2006), and the differential effects of melatonin on locomotor activity in nocturnal vs. diurnal fishes (López-Olmeda et al., 2006). Results presented here suggest that differential melatonin sensitivity exists within subregions of a central vocal motor network to regulate the production of seasonal and nocturnal-dependent advertisement calling. Comparative approaches studying behaviors with different daily and seasonal

expression patterns at the level of specific neural pathways, such as the vocal network controlling midshipman nocturnal vocalization, will contribute to a more predictive mechanistic model for melatonin regulation of behavior.

Materials and methods

Animals

Midshipman fish have two male reproductive morphs: type I males that acoustically court females and are the focus of this study, and type II males that sneak spawn (Brantley and Bass, 1994). Nesting type I males (standard length 15.1±0.24cm) were hand collected from rocky intertidal zones in northern California between May 2011 and August 2012. Fish were temporarily (1-7 d) held in large outdoor tanks with running seawater at the University of California Bodega Marine Laboratory before shipping overnight to Cornell University where they were housed in individual tanks under 15 h light (L) : 9 h dark (D) for at least two weeks before experimentation. To better simulate sunrise and sunset, a small lamp turned on at 02:00 EST, half an hour before room lights turned on, which turned off half an hour before the small lamp at 17:00 EST. Visual inspection of the gonads and swim bladder muscles at the time of sacrifice confirmed type I male status (Bass, 1996). All methods were approved by the Institutional Animal Care and Use Committee at Cornell.

Drug treatment

Fish held in 5LL received either a control implant (coconut oil vehicle) or a 50 mM 2-IMel implant (Santa Cruz Biotechnology Inc, CA, USA) for five days (Fig. 2.1C). 2-

IMel was dissolved to 2 μg/μl in heat-liquefied coconut oil, sonicated to homogeneity, pipetted into 10 mm plastic tubing with 1 mm inner diameter (BD Infusion Therapy Systems Inc., Sandy, UT, USA) and stored at -20°C in parafilm sealed Eppendorf tubes until use. After normalization by body weight (bw) of implanted males (n=12), implant dosages were 0.36±0.05 μg/g bw, well within reported doses used in fishes and tetrapods that range from 0.1μg/g bw to 300 μg/g bw (Aarseth et al., 2010; Alvariño et al., 2001; Amano et al 2000; Dubocovich et al., 1998; Handeland et al., 2013; López-Olmeda et al., 2006; Pinillos et al., 2001; Porter et al., 1998; Rubio et al., 2004; Stankov et al., 1993). Following general anesthesia in 0.025% benzocaine (Sigma, St. Louis, MO, USA), implants were inserted into the abdominal cavity of males through a small incision, which was closed by suture and Vetbond Tissue Adhesive (3M Animal Care Products, St. Paul, MN, USA). Fish were observed to fully recover within approximately 15 min after surgical procedure.

Fish held in 5DD received daily intramuscular injections for five days via 27 gauge butterfly needles (BD Infusion Therapy Systems Inc.) of 2 μg/g bw of a receptor antagonist or only the vehicle (dimethyl sulfoxide, DMSO; J.T. Baker, Phillipsburg, NJ, USA) (Fig. 2.1C). Stocks of 50 mM luzindole and 4P-PDOT were dissolved in DMSO and stored at -20°C in parafilm-sealed Eppendorf tubes until use. On the first day of injection, fish were anesthetized under 0.025% benzocaine and weighed in order to calculate the appropriate volume of luzindole, 4P-PDOT, or DMSO to reach 2 μg/g bw, to be added to 5 μl/g bw teleost saline solution or water as an injection carrier. Subsequently, daily injections were done within 1 h before subjective lights off, between 16:00-17:00 EST except for the day of neurophysiology

(Fig. 2.1C). We chose to use 2 μg/g bw for luzindole and 4P-PDOT because this dose was within the range used in studies looking at locomotion or feeding (Dubocovich et al., 1998; Pinillos et al., 2004). Treatment groups were staggered to ensure that fish were tested under similar conditions, such as total time spent in captivity.

In-vivo neurophysiology

The *in-vivo* fictive call (defined in Introduction) preparation used here follows Rubow and Bass (2009). Briefly, a dorsal craniotomy exposed the brain, rostral spinal cord, and vocal/occipital nerves after general anesthesia with 0.025% benzocaine and local injection of 0.25% Bupivacaine (Hospira, Inc., Lake Forest, IL, USA), a long-lasting local anesthetic. After surgery, fish were immobilized with an intramuscular injection of pancuronium bromide (0.5 mg/kg; MP Biomedicals, LLC, Solon, OH, USA) and stabilized on a platform within a Plexiglas tank with chilled saltwater (15 -17°C) perfused through the mouth. After 1 h of acclimation, an insulated tungsten electrode (125 μm diameter, 8° tip angle, 5 MΩ impedance, 20 μm exposed tips; A-M Systems, Sequim, WA, USA) was used to evoke fictive calls from midbrain sites using well documented surface landmarks and depth measurements as guidance for electrode placement (Goodson and Bass, 2002; Kittelberger et al., 2006). Fictive calls were recorded from vocal nerve roots unilaterally (reflects synchronous bilateral activity; Bass and Baker, 1990) with an extracellular Teflon coated silver electrode with an exposed ball tip (50-100 μm diameter) and digitized using MATLAB software designed by Dr. Bruce R. Land (School of Electrical and Computer Engineering, Cornell).

In 120 min sessions, each stimulation trial consisted of 40 brief stimulus trains delivered to midbrain sites. Baseline (0 min) and subsequent recording trials were performed at 5, 15, 30, 45, 60, 75, 90, 105, and 120 min (Fig. 2.1C,D). For 5LL and 5DD animals (Fig. 2.1C), we delivered 100 stimulus trains instead of 40 at the time of the 120 min trial because Rubow and Bass (2009) found that the additional 60 stimuli evoked longer duration responses resembling natural calls in 5DD and 14:10 h L:D males. We generated a SRC at the end of the 120 min recording session to measure the relationship between stimulus intensity and fictive call duration (Fig. 2.1C,D). At 10 min after the 120 min recording session and without moving the stimulating electrode, we recorded 10 fictive calls evoked by 100%, 125%, 150%, 175% and 200% of threshold stimulus, with each recording separated by 5 min. For some animals (see Fig. 2.1C,D) the stimulating electrode was immediately moved to a lateral midbrain site and another SRC was recorded. Each stimulus train consisted of 5 square pulses (0.1 ms pulse width, 200 Hz), with inter-train intervals of 1 s were delivered via a stimulus isolation unit (SIU; Model A350D-A, World Precision Instruments, Sarasota, FL, USA). SIU current output (ηA) was interpolated from a linear relationship between SIU dial level and current output derived using the Ohms Law by measuring voltage across a resistor.

All animals were tested 1 h post surgery starting between 17:00 EST to 18:00 EST under darkness with experimenter wearing a red head lamp (except for 5LL animals who were tested under light). 5DD fish experienced approximately 15 min of exposure to low-level scope light during craniotomy.

Medial vs. lateral midbrain lesions

At the end of the experiments in a subset of animals including fish from drug treatment experiments that received stimulation at medial and/or lateral sites, electrolytic lesions were made by passing 10 μA of current with 50% duty cycle for 4–15 s through the stimulus electrode to mark the stimulation site. Fish were then deeply anesthetized under 0.025% benzocaine and perfused transcardially with teleost Ringer followed by 4% paraformaldehyde in 0.1M phosphate buffer (pH 7.2). Prior to sectioning, brains were cryoprotected in 30% sucrose solution overnight, frozen in Cryo-M-Bed (Hacker Instruments, Huntington, UK), sectioned at 30 μm in the transverse plane on a crysostat, and mounted onto Superfrost Plus slides (Erie Scientific, Portsmouth, NH, USA). Photomicrographs were taken of selected sections using the Spot FLEX imaging system (Diagnostics Instruments, Inc, Sterling Heights, MI, USA) on a Nikon Eclipse E800 compound microscope.

Neurophysiological and statistical analysis

Measurements of fictive call duration, latency (delay from end of stimulus to first fictive pulse), and IPI were performed by a customized MATLAB program designed by Dr. Bruce Land, Cornell University. In some cases where more than one fictive burst was elicited from the lateral midbrain, we combined the total duration of all bursts for analysis.

All statistical analyses were performed in JMP 9 (SAS Institute Inc., Cary, NC, USA) using means obtained from individual recording trials and in consultation with the Cornell University Statistical Consulting Unit. Log or square root transformations

were performed whenever assumptions of normality were violated. We used a linear mixed model with appropriate fixed effects (details below) and fish nested within treatment as a random effect.

In order to examine effects of photoperiod manipulation, we first compared data taken from 5LL and 5DD control animals (oil-implanted or vehicle-injected) and LD non-treated animals used in medial vs. lateral comparisons. For 120 min trial and SRC measurements, our fixed effects were photoregime, time, and photoregime*time interaction. Three-way ANOVA followed by Tukey-HSD post-hoc comparison was performed on SRC stimulus thresholds.

For 5LL and 5DD 120 min sessions, we looked for effects of treatment, time, and treatment*time interaction on fictive call duration and threshold. Since luzindole and 4P-PDOT act on melatonin receptors with different affinities (Dubocovich et al., 2010), we performed separate analyses for each. The 100 stimuli delivered on the 120 min trial in 5LL and 5DD animals were split into the first 40 and last 60 calls for analyses. We combined data from 2011 and 2012 5LL animals since year was not a significant factor (120 min session duration: P=0.34; 120 min session threshold: P=0.27; medial SRC duration: P=0.80; lateral SRC duration: P=0.76). For SRC duration comparisons, fixed effects were treatment, stimulus-intensity, and treatment*stimulus-intensity. To compare SRC threshold levels across treatment groups, we performed a three-way ANOVA for each antagonist.

In LD groups used for medial vs. lateral comparisons, we looked for effects of stimulus-site, time, and stimulus-site*time interaction on duration, stimulus threshold, and latency of fictive responses in 120 min sessions. The fixed effects for SRCs were

stimulus-site, stimulus-intensity, and their interaction. Additionally, we performed a *Student's t-test* on a total of 116 IPIs from medial SRC and 1149 IPIs from lateral SRC in one individual to assess potential site-dependent differences in call frequency.

Acknowledgments

We sincerely thank Margaret Marchaterre for support with fish collection and neuroanatomy, Boris Chagnaud for help with neurophysiology and comments on the manuscript, Dan Fergus and Kevin Rohmann for statistical advice, and Bruce Land for programming support. This was supported by NSF IOS 1120925, Cornell Research in Animal Behavior grant, and Cornell Sigma Xi research grant.

References

Aarseth, J. J., Froiland, E. and Jorgensen, E. H. (2010). Melatonin implantation during spring and summer does not affect the seasonal rhythm of feeding in anadromous arctic charr (*Salvelinus alpinus*). *Polar Biol.* **33**, 379-388.

Alvariño, J. M. R., Rebollar, P. G., Olemdo, M., Alvarez-Blázquez, B. and Peleteiro, J. B. (2001). Effects of melatonin implants on reproduction and growth of turbot broodstock. *Aquacult. Int.* **9**, 477-487.

Amano, M., Iigo, M., Ikuta, K., Kitamura, S., Yamada, H. and Yamamori, K. (2000). Roles of melatonin in gonadal maturation of underyearling precocious male masu salmon. *Gen. Comp. Endocrinol.* **120**, 190-197.

Azpeleta, C., Martínez-Álvarez, R. M., Delgado, M. J., Isorna, J., Isorna, E. and Pedro, N. D. (2010). Melatonin reduces locomotor activity and circulating cortisol in goldfish. *Horm. Behav.* **57**, 323-329.

Bandler, R., and Carrive, P. (1988). Integrated defense reaction elicited by excitatory amino acid microinjection in the midbrain periaqueductal grey region of the unrestrained cat. *Brain Res.* **439**, 95-106.

Bass, A. H. (1996). Shaping brain sexuality. *Am. Sci.* **84**, 352-363.

Bass, A. H. and Baker, R. (1990). Sexual dimorphisms in the vocal control system of a teleost fish: morphology of physiologically identified neurons. *J. Neurobiol.* **21**, 1155-1168.

Bass, A. H. and McKibben, J. R. (2003). Neural mechanisms and behaviors for acoustic communication in teleost fish. *Prog. Neurobiol.* **69**, 1-26.

Bass, A. H. and Remage-Healey, L. (2008). Central pattern generators for social vocalization: Androge-dependent neurophysiological mechanisms. *Horm. Behav.* **53**, 659-672.

Bass, A. H., Marchaterre, M. A. and Baker, R. (1994). Vocal-acoustic pathways in a teleost fish. *J. Neurosci.* **14**, 4025-4039.

Bass, A. H., Bodnar, D.A. and Marchaterre, M. A. (1999) Complementary explanations for existing phenotypes in an acoustic communication system. In: *Neural mechanisms of communication* (ed. M. Hauser, M. Konishi), pp. 493–514. Cambridge, MA: MIT.

Bass, A. H., Gilland, E. H. and Baker, R. (2008). Evolutionary origins for social vocalization in a vertebrate hindbrain-spinal compartment. *Science* **321**, 417-421.

Bayarri, M. J., Madrid, J. A. and Sánchez-Vázquez, F. J. (2002). Influence of light intensity, spectrum and orientation on sea bass plasma and ocular melatonin. *J. Pineal Res.* **32**, 34-40.

Bentley, G. E. (2003) Melatonin receptor density in Area X of European starlings is correlated with reproductive state and is unaffected by plasma melatonin concentration. *Gen. Comp. Endocrinol.* **134**, 187-192.

Bentley, G. E. and Ball, G. F. (2000). Photoperiod-dependent and -independent regulation of melatonin receptors in the forebrain of songbirds. *J. Neuroendocrinol.* **12**, 745-752.

Bentley, G. E., Van't Hof, T. J. and Ball, G. F. (1999). Seasonal neuroplasticity in the songbird telencephalon: A role for melatonin. *Proc. Natl. Acad. Sci. USA* **96**, 4674-4679.

Bentley, G. E., Perfito, N. and Calisi, R. M. (2013). Season- and context-dependent sex differences in melatonin receptor activity in a forebrain song control nucleus. *Horm. Behav.* **63**, 829-835.

Bhattacharya, S., Chattoraj, A. and Maitra, S. K. (2007). Melatonin in the regulation of annual testicular events in carp *Catla catla*: evidence from the

studies on the effects of exogenous melatonin, continuous light, and continuous darkness. *Chronobiol. Int*. **24**, 629-650.

Boutin, J. A., Audinot, V., Ferry, G. and Delagrange, P. (2005). Molecular tools to study melatonin pathways and actions. *Trends Pharmacol. Sci*. **26**, 412-419.

Bradbury, J. W. and Vehrencamp, S. L. (2011). Principles of Animal Communication. Sunderland, MA: Sinauer Associates.

Brantley, R. K. and Bass, A. H. (1994). Alternative male spawning tactics and acoustic signals in the plainfin midshipman fish *Porichthys notatus* Girard (Teleostei, Batrachoididae). *Ethology* **96**, 213-232.

Carter, D. S., Hall, V. D., Tamarkin, L. and Goldman, B. D. (1982). Pineal is required for testicular maintenance in Turkish hamster (*Mesocricetus brandti*). *Endocrinol.* **111**, 863-871.

Cassone, V. M., Brooks, D. S. and Kelm, T. A. (1995). Comparative distribution of 2[^{125}I]iodomelatonin binding in the brains of diurnal birds: outgroup analysis with turtles. *Brain Behav. Evol.* **45**, 241-256.

Cassone, V. M., Bartell, P. A., Earnest, B. J. and Kumar, V. (2008). Duration of melatonin regulates seasonal changes in song control nuclei of the house sparrow, *Passer domesticus*: Independence from gonads and circadian entrainment. *J. Biol. Rhythm.* **23**, 49-58.

Chagnaud, B. P., Baker, R. and Bass, A. H. (2011). Vocalization frequency and duration are coded in separate hindbrain nuclei. *Nat. Commun.* **2**, 346.

Chagnaud, B. P., Zee, M. C., Baker, R. and Bass, A. H. (2012). Innovations in motoneuron synchrony drive rapid temporal modulations in vertebrate acoustic signaling. *J. Neurophysiol.* **107**, 3528-3542.

Challet, E. (2007). Minireview: entrainment of the suprachiasmatic clockwork in diurnal and nocturnal mammals. *Endocrinol.* **148**, 5648-5655.

Chowdhury, V. S., Yamamoto, K., Ubuka, T., Bentley, G. E., Hattori, A. and Tsutsui, K. (2010). Melatonin stimulates the release of gonadotropin-inhibitory hormone by the avian hypothalamus. *Endocrinol.* **151**, 271-280.

Cohen, M. J. and Winn, H. E. (1967). Electrophysiological observations on hearing and sound production in the fish, *Porichthys notatus*. *J. Exp. Zool*. **165,** 355-369.

Dubocovich, M. L., Yun, K., Al-Ghoul, W. M., Benloucif, S. and Masana, M. I. (1998) Selected MT_2 melatonin receptor antagonists block melatonin-mediated

phase advances of circadian rhythms. *FASEB J.* **12**, 1211-1220.

Dubocovich, M. L., Delagrange, P., Krause, D. N., Sugden, D., Cardinali, D. P. and Olcese, J. (2010). International union of basic and clinical pharmacology. LXXV. Nomenclature, classification, and pharmacology of G protein-coupled melatonin receptors. *Pharmacol. Rev*. **62,** 343-380.

Ekström, P. and Meissl, H. (1997). The pineal organ of teleost fishes. *Rev. Fish Biol. Fisher.* **7**, 199-284.

Falcón, J., Besseau, L., Sauzet, S. and Boeuf, G. (2007). Melatonin effects on the hypothalamo-pituitary axis in fish. *Trends. Endocrin. Met.* **18**, 81-88.

Falcón, J., Migaud, H., Muñoz-Cueto, J. A. and Carrillo, M. (2010). Current knowledge on the melatonin system in teleost fish. *Gen. Comp. Endocrinol.* **165**, 469-482.

Fenzl, T., and Schuller, G. (2007). Dissimilarities in the vocal control over communication and echolocation calls in bats. *Behav. Brain Res.* **182**,173-179.

Fergus, D. J. and Bass, A. H. (2013) Localization and divergent profiles of estrogen receptors and aromatase in the vocal and auditory networks of a fish with alternative mating tactics. *J. Comp. Neurol.* **521**, 2850-2869.

Forlano, P. M., Deitcher, D. L. and Bass, A. H. (2005). Distribution of estrogen receptor alpha mRNA in the brain and inner ear of a vocal fish with comparisons to sites of aromatase expression. *J. Comp. Neurol.* **483**, 91-113.

Forlano, P. M., Marchaterre, M. Deitcher, D. L. and Bass, A. H. (2010). Distribution of androgen receptor mRNA expression in vocal, auditory, and neuroendocrine circuits in a teleost fish. *J. Comp. Neurol.* **518**, 493-512.

Gahr, M. and Kosar, E. (1996). Identification, distribution, and developmental changes of a melatonin binding site in the song control system of the zebra finch. *J. Comp. Neurol.* **367**, 308-318.

García-Allegue, R., Madrid, J. A. and Sánchez-Vázquez, F. J. (2001). Melatonin rhythms in European sea bass plasma and eye: influence of seasonal photoperiod and water temperature. *J. Pineal Res.* **31**, 68-75.

Goodson, J. L. and Bass, A. H. (2000a). Forebrain peptide modulation of sexually polymorphic vocal circuitry. *Nature* **403**, 769-772.

Goodson, J. L. and Bass, A. H. (2000b). Vasotocin innervation and modulation of vocal-acoustic circuitry in the teleost *Porichthys notatus*. *J. Comp Neurol.* **422**,

363-379.

Goodson, J. L. and Bass, A.H. (2001). Social behavior functions and related anatomical characteristics of vasotocin/vasopressin systems in vertebrates. *Brain Res. Rev.* **35**, 246-265 [plus 36: 91-94].

Goodson, J. L. and Bass, A. H. (2002). Vocal-acoustic circuitry and descending vocal pathways in teleost fish: convergence with terrestrial vertebrates reveals conserved traits. *J. Comp. Neurol.* **448**, 298-322.

Goodson, J. L., Evans, A. K. and Bass, A. H. (2003). Putative isotocin distributions in sonic fish: relation to vasotocin and vocal-acoustic circuitry. *J. Comp. Neurol.* **462**, 1-14.

Handeland, S. O., Imsland, A. K., Björnsson, B. Th., Stefansson, S. O. and Porter, M. (2013). Physiology during smoltification in Atlantic salmon: effect of melatonin implants. *Fish Physiol. Biochem.* **39**, 1079-1088.

Helfman, G. S. (1993). Fish behaviour by day, night and twilight. In *Behaviour of Teleost Fishes, 2nd edition* (ed. T. J. Pitcher), pp. 479–512. London: Chapman and Hall.

Holstege, G. (1989). Anatomical study of the final common pathway for vocalization in the cat. *J. Comp. Neurol.* **284**, 242-252.

Ibara, R. M., Penny, L. T., Ebeling, A.W., van Dykhuizen, G. and Cailliet, G. (1983). The mating call of the plainfin midshipman fish, *Porichthys notatus*. In *Predators and prey in fishe*s (ed. D. L. G. Noakes, D. G. Lindquist, G. S. Helfman and J. A. Ward), pp. 205-212. The Hague, Netherlands: Dr. W. Junk Pubs.

Iigo, M. and Aida, K. (1995). Effects of season, temperature, and photoperiod on plasma melatonin rhythms in the goldfish, *Carassius auratus*. *J. Pineal Res.* **18**, 62-68.

Jansen, R., Metzdorf, R., van der Roest, M., Fusani, L., ter Maat, A. and Gahr, M. (2005). Melatonin affects the temporal organization of the song of the zebra finch. *FASEB J.* **19**, 848-850.

Jürgens, U. (2009). The neural control of vocalization in mammals: a review. *J. Voice* **23**, 1-10.

Kingsbury, M. A., Kelly, A. M., Schrock, S. E. and Goodson, J. L. (2011). Mammal-like organization of the avian midbrain central gray and a reappraisal of the intercolliculuar nucleus. *PLoS One.* **6**, e20720.

Kittelberger, J. M. and Bass, A. H. (2013). Vocal-motor and auditory connectivity of the midbrain periaqueductal gray in a teleost fish. *J. Comp. Neurol.* **521**, 791-812.

Kittelberger, J. M., Land, B. R. and Bass, A. H. (2006). Midbrain periaqueductal gray and vocal patterning in a teleost fish. *J Neurophysiol.* **96**, 71-85.

Locascio, J. V. and Mann, D. A. (2008). Diel periodicity of fish sound production in Charlotte Harbor, Florida. *T. Am. Fish. Soc.* **137**, 606-615.

López-Olmeda, J. F., Madrid, J. A. and Sánchez-Vázquez, F. J. (2006). Melatonin effects on food intake and activity rhythms in two fish species with different activity patterns: Diurnal (goldfish) and nocturnal (tench). *Comp. Biochem. Phys. A*. **144**, 180-187.

Lutterschmidt, D. I. and Wilczynski, W. (2012). Sexually dimorphic effects of melatonin on brain arginine vasotocin immunoreactivity in Green treefrogs (*Hyla cinerea*). *Brain Behav. Evolut.* **80**, 222-232.

Maitra, S. K. and Chattoraj, A. (2006). Photoperiod, pineal photoreceptors and melatonin as the signal of photoperiod in the regulation of reproduction in fish. *J. Endocrinol. Reprod.* **10**, 73-87.

McKibben, J. R. and Bass, A. H. (1998). Behavioral assessment of acoustic parameters relevant to signal recognition and preference in a vocal fish. *J. Acoust. Soc. Am.* **104**, 3520-3533.

Oliveira, C., Garcia, E. M., López-Olmeda, J. F. and Sánchez-Vázquez, F. J. (2009). Daily and circadian melatonin release *in vitro* by the pineal organ of two nocturnal teleost species: Senegal sole (*Solea senegalensis*) and tench (*Tinca tinca*). *Comp. Biochem. Phys. A.* **153**, 297-302.

Piccinetti, C. C., Migliarini, B., Olivotto, I., Coletti, G., Amici, A. and Carnevali, O. (2010). Appetite regulation: The central role of melatonin in *Danio rerio*. *Horm. Behav.* **58**, 780-785.

Pinillos, M. L., De Pedro, N., Alonso-Gómez, A. L., Alonso-Bedate, M. and Delgado, M. J. (2001). Food intake inhibition by melatonin in goldfish (*Carassius auratus*). *Physiol. Behav.* **72**, 629-634.

Porter, M. J. R., Randall, C. F., Bromage, N. R. and Thorpe, J. E. (1998) The role of melatonin and the pineal gland on development and smoltification of Atlantic salmon (*Salmo salar*) parr. *Aquaculture* **168**, 139-155.

Porter, M. J. R., Duncan, N. J., Mitchell, D. and Bromagea, N. R. (1999). The use of cage lighting to reduce plasma melatonin in Atlantic salmon (*Salmo salar*) and its effects on the inhibition of grilsing. *Aquaculture* **176**, 237-244.

Reebs, S. G. (2002). Plasticity of diel and circadian activity rhythms in fishes. *Rev. Fish Biol. Fisher.* **12**, 349-371.

Remage-Healey, L. and Bass, A. H. (2004). Rapid, hierarchical modulation of vocal patterning by steroid hormones. *J. Neurosci.* **24**, 5892-5900.

Remage-Healey, L. and Bass, A. H. (2007). Plasticity in brain sexuality is revealed by the rapid actions of steroid hormones. *J. Neurosci.* **27**, 1114-1122.

Rice, A. N. and Bass, A. H. (2009). Novel vocal repertoire and paired swimbladders of the three-spined toadfish, *Batrachomoeus trispinosus*: insights into the diversity of the Batrachoididae. *J. Exp. Biol.* **212**, 1377-1391.

Rubio, V. C., Sánchez-Vázquez, F. J. and Madrid, J. A. (2004). Oral administration of melatonin reduces food intake and modifies macronutrient selection in European sea bass (*Dicentrarchus labrax,* L.). *J. Pineal Res.* **37**, 42-47.

Rubow, T. K. (2010). Seasonal and diel rhythms regulate multistability in a teleost vocal pattern generator. *Dissertation,* Cornell University

Rubow, T. K. and Bass, A. H. (2009). Reproductive and diurnal rhythms regulate vocal motor plasticity in a teleost fish. *J. Exp. Biol.* **212**, 3252-3262.

Stankov, B., Gervasoni, M., Scaglione, F., Perego, R., Cova, D., Marabini, L. and Fraschini, F. (1993). Primary pharmaco-toxilogical evaluations of 2-iodomelatonin, a potent melatonin agonist. *Life Sci.* **53**, 1357-1365.

Steiger S. S., Valcu, M., Spoelstra, K., Helm, B., Wikelski, M. and Kempenaers, B. (2013). When the sun never sets: diverse activity rhythms under continuous daylight in free-living arctic-breeding birds. *P. R. Soc. B.* **280**, 20131016.

Tramontin, A. D. and Brenowitz, E. A. (2000). Seasonal plasticity in the adult brain. *Trends Neurosci.* **23**, 251-258.

Ubuka, T., Bentley, G. E., Ukena, K., Wingfield, J. C. and Tsutsui, K. (2005). Melatonin induces the expression of gonadotropin-inhibitory hormone in the avian brain. *Proc. Natl. Acad. Sci. USA* **102**, 3052-3057.

Vera, L. M., De Oliveira, C., López-Olmeda, J. F., Ramos, J., Mañanós, E., Madrid, J. A. and Sánchez-Vázquez, F. J. (2007). Seasonal and daily plasma melatonin rhythms and reproduction in Senegal sole kept under natural

photoperiod and natural or controlled water temperature. *J. Pineal Res.* **43**, 50-55.

Wan, Q., Man, H-Y., Liu, F., Braunton, J., Niznik, H. B., Pang, S. F. Brown, G. M. and Wang, Y. T. (1999). Differential modulation of $GABA_A$ receptor function by Mel_{1a} and Mel_{1b} receptors. *Nat. Neurosci.* **2**, 401-403.

Wang, G., Harpole, C. E., Trivedi, A. K. and Cassone, V. M. (2012). Circadian regulation of bird song, call, and locomotor behavior by pineal melatonin in the zebra finch. *J. Biol. Rhythm.* **27**, 145-155.

Weeg, M. S., Land, B. R. and Bass, A. H. (2005). Vocal pathways modulate efferent neurons to the inner ear and lateral line. *J. Neurosci.* **25**, 5967-5974.

Wikelski, M., Tarlow, E. M., Eising, C. M., Groothuis, T. G. G. and Gwinner, E. (2005). Do night-active birds lack daily melatonin rhythms? A case study comparing a diurnal and a nocturnal-foraging gull species. *J. Ornithol.* **147**, 107-111.

Whitfield-Rucker, M. G. and Cassone, V. M. (1996). Melatonin binding in the house sparrow song control system: sexual dimorphism and the effect of photoperiod. *Horm. Behav.* **30**, 528-537.

Zhdanova, I. V., Wang, S. Y., Leclair, O. U. and Danilova, N. P. (2001). Melatoin promotes sleep-like state in zebrafish. *Brain Res.* **903**, 263-268.

CHAPTER 3

MELATONIN RECEPTOR 1B IS ABUNDANT IN SENSORY, AUDIO-VOCAL, AND NEUROENDOCRINE CENTERS IN A HIGHLY VOCAL FISH

Abstract

Melatonin plays a central role in entraining activity to the day-night cycle in vertebrates, including humans. Little is known about melatonin's modulation of social behavior. To date, such studies have focused on the vocal-acoustic behavior of diurnal songbird species, with little research on nocturnally vocal species. Here, we investigate the neural substrates of melatonin-dependent vocal-acoustic behavior in the nocturnally active and highly vocal teleost fish, the plainfin midshipman (*Porichthys notatus*). Previous studies in midshipman show that constant light inhibits courtship vocalization, known generally to abolish endogenous melatonin production, and that melatonin action can rescue such behavior. Consistent with these results, melatonin can increase the excitability of the neural circuitry that controls vocalization. Here, we used *in-situ* hybridization to map the mRNA distribution of melatonin receptor subtype 1B (mel1b). Robust mel1b expression was found in neuroendocrine regions with abundant steroid receptor and nonapeptide expression, including the preoptic area and major nodes of the expansive central audio-vocal network. The results support the hypothesis that melatonin's stimulatory effects on midshipman nocturnal vocalization and vocal network excitability are mediated, in part, by mel1b receptors.

Introduction

Melatonin is a conserved molecule that carries out diverse physiological functions, including being a potent antioxidant and the main time-keeping hormone in vertebrates (Reiter et al., 2014). In the latter function, melatonin exerts its actions via membrane bound G protein-coupled receptors to regulate daily/circadian and seasonal cycles in physiology and behavior, including feeding, thermoregulation, and reproduction (Dubocovich et al., 2010; Falcón et al., 2010; Li et al., 2013). In vertebrates, melatonin is mainly produced by the pineal gland at night (Dubocovich et al., 2010; Ekström and Meissl, 1997). Due to its lipophilicity, melatonin diffuses well through cell membranes, acting as a synchronizing signal that entrains central and peripheral targets to the external light-dark cycle (Dubocovich et al., 2010). Because the length of nights are shorter during the summer and longer during the winter, the duration of nocturnal melatonin release serves both as a daily "clock" and a seasonal "calendar", synchronizing behavior and physiology to the external photoperiodic environment (Ekström and Meissl, 1997; Reiter, 1993). Although melatonin entrainment of locomotor activity is well characterized (Moore-Ede et al., 1982), its regulation of social behaviors such as vocal-acoustic communication is not well understood. Furthermore, despite the widely prevalent pattern of melatonin release from the pineal gland at night [for exceptions see (Taniguchi et al., 1993; Wikelski et al., 2005)], it remains relatively unexplored how vertebrates exhibit large variations in daily activity rhythms broadly categorized as diurnal, nocturnal, or crepuscular (active at dawn and dusk).

Recently, we characterized melatonin regulation of courtship vocal behavior and the excitability of the underlying neural network in a highly vocal teleost fish, the

plainfin midshipman (*Porichthys notatus*) (Feng and Bass, 2014; Feng and Bass, in preparation). Midshipman fish breed during the late spring-summer breeding season, when males "sing" for long durations almost exclusively at night in order to attract females to rocky nests in the intertidal zone along the west coast (Brantley and Bass, 1994; Ibara et al., 1983; McIver et al., 2014). Males contract superfast swim bladder muscles at ~100 Hz (14-16°C) to produce several call types, including long duration (min-h) courtship/advertisement "hums" (Brantley and Bass, 1994; McIver et al., 2014), among the longest continuous vocalizations known in the animal kingdom and especially in fish (Ibara et al., 1983; McIver et al., 2014).

Previously, we showed that holding midshipman fish under constant light (LL), known to inhibit melatonin synthesis (Ekström and Meissl, 1997), decreased both courtship vocal behavior (Feng and Bass, in preparation) and neural excitability of the vocal network (Feng and Bass, 2014). Intraperitoneal implants filled with 2-iodomelatonin, a potent melatonin analogue (Boutin et al., 2005; Dubocovich et al., 2010; Reppert et al., 1996), rescued both vocal behavior (Feng and Bass, in preparation) and vocal neuron excitability (Feng and Bass, 2014) in fish held under the inhibitory LL. From these results, we concluded that the neural circuitry controlling vocal behavior is sensitive to melatonin action, which is permissive for the expression of nocturnal vocal courtship behavior. The logical question that follows is where melatonin receptors are located within the midshipman brain, and whether these locations include specific nodes within the vocal network that could mediate melatonin's effects on vocal behavior.

Two subtypes of melatonin receptors are found in mammals: melatonin receptor

1A (mel1a) and melatonin receptor 1B (mel1b). In non-mammalian vertebrates, a third receptor, 1C (mel1C) has been characterized in fish, amphibians, and birds (Reppert et al., 1995). In addition, likely due to whole-genome duplication events in teleost fish (Hoegg et al., 2004), at least two isoforms of mel1a have been characterized (Ikegami et al., 2009a; Ikegami et al., 2009b; Mazurais et al., 1999; Reppert et al., 1995). Here, we used *in-situ* hybridization to localize a predicted mel1b in the brain of midshipman fish. We found that mel1b mRNA expression is abundant in diverse sensory, motor, sensori-motor integration, and neuroendocrine sites. Me1b expression in relation to regulation of vocal behaviors is discussed.

Results

Our transcriptome-predicted mel1b sequence (GenBank accession number KT878765) was verified by PCR amplification and sequencing. In general, we observed that mel1b was expressed in all major divisions of the brain within discrete and diverse motor, sensory, and neuroendocrine regions. Labeled cells are neuronal in appearance and mel1b distribution is consistent between individuals. The plainfin midshipman has two male reproductive morphs, type I and type II males that follow alternative reproductive tactics (Brantley and Bass, 1994; Lee, 2006). No obvious differences were observed between the brains of the three reproductive morphs (type I and II males, female), though future studies should more thoroughly address sex and morph differences. A list of neuroanatomical abbreviations is provided in Table 3.1 and a summary of mel1b expression by brain region is provided in Table 3.2, which also highlights regions

Table 3.1
Abbreviations

ac	anterior commissure
AT	anterior tuberal nucleus
CA	cerebral aqueduct
Cc	cerebellar crest
Cg	granular layer of the corpus of the cerebellum
Cm	molecular layer of the corpus of the cerebellum
CP	central posterior nucleus of the thalamus
D	area dorsalis of the telencephalon
Dc	central zone of D
Dd	dorsal zone of D
Dl	dorsolateral zone of D
Dm	medial zone of D
Dm-cm	central medial division of Dm
Dm-p	posterior division of Dm
Dp	posterior zone of D
F	forebrain
G	nucleus glomerulosus
GC	griseum centrale
H	hindbrain
Hd	dorsal periventricular hypothalamus
HoCo	horizontal commissure
Hv	ventrolateral nucleus of the hypothalamus
III	third ventricle
IP	isthmal peraventricular nucleus
IS	ismthal nucleus
IV	fourth ventricle
ll	lateral lemniscus
M	midbrain
MED	cell plate of medial octavolateralis nucleus
MLF	medial longitudinal fasciculus
nll	nucleus of the lateral lemniscus
nlv	nucleus lateralis valvulae
nMLF	nucleus of the medial longitudinal fasciculus
OB	olfactory bulb
P	medial pretoral nucleus of the pretectum
PAG	periaqueductal gray
PCo	posterior commissure
Pe	periventricular cell layer of the torus semicircularis
PGl	lateral division of nucleus preglomerulosus
PGm	medial division of nucleus preglomerulosus
PL	paralemniscal midbrain tegmentum
PMg	gigantocellular division of PM
PPa	anterior parvocellular preoptic nucleus
PPd	nucleus pretectalis periventricularis, pars dorsalis
PPp	posterior parvocellular preoptic nucleus
RF	reticular formation
ri	descending octaval nucleus, rostral intermediate division
T	telencephalon
Te	optic tectum
TL	torus longitudinalis
TP	posterior tuberal nucleus
TPp	periventricular posterior tuberal nucleus
TS	torus semicircularis
TSd	deep layer of the torus semicircularis
Vc	central nucleus of V
Vd	dorsal nucleus of V
Vg	granular layer of the valvula
Vi	intermediate nucleus of V
VL	vagal lobe
Vm	molecular layer of the valvula
VM	nucleus ventromedialis
VMN	vocal motor nucleus
VPN	vocal pacemaker neurons
VPP	vocal prepacemaker nucleus
Vs	supracommissural nucleus of V
Vse	trigeminal sensory nucleus
vT	ventral tuberal hypothalamus
VT	vocal tract
Vv	ventral nucleus of V
Xm	vagal motor nucleus

Table 3.2
Mel1b expression compared to known steroid receptor and enzyme expression.
AR: androgen receptor mRNA (Forlano et al., 2010); ARO: aromatase protein (Forlano et al., 2001); ERα: estrogen receptor alpha mRNA (Forlano et al., 2005). ERβ: estrogen receptor beta protein (Fergus and Bass, 2013).

Table 3.2 (continued)

Anatomical location	Mel1b	AR	ARO	ER α	ER β1	ER β2
Ventral telencephalon						
Olfactory bulb (OB)	+	-	+	+	-	-
Ventral nucleus (Vv) **AUDITORY**	+	-	+	+	-	+
Supracommissural nucleus (Vs) **AUDITORY**, **VOCAL**	+	+	+	+	-	+
Postcommissural nucleus (Vp) **AUDITORY**	-	+	+	+	-	-
Dorsal nucleus (Vd)	-	+	+	-	-	+
Intermediate nucleus (Vi)	+	+	+	-	-	-
Dorsal telencephalon						
Central zone (Dc)	-	+	+	+	-	-
Central medial division of medial zone (Dm-cm)	+	+	+	+	-	-
Posterior division of medial zone (Dm-p) **AUDITORY**, **VOCAL**	+	+	+	+	-	-
Dorsal posterior zone (Dp)	+	-	+	+	-	-
Preoptic area						
Anterior parvocellular (PPa) **AUDITORY**, **VOCAL**	+	+	+	+	+	+
Posterior parvocellular (PPp) **AUDITORY**, **VOCAL**	-	+	+	-	-	+
Magnocellular (PM/PMg)	-	+	+	+	+	-
Ventral hypothalamus						
Anterior tuberal (AT) **AUDITORY**, **VOCAL**	+	+	+	+	-	+
Ventral tuberal (vT) **AUDITORY, VOCAL**	+	+	+	-	-	-
Periventricular (Hv/Hd)	+	+	+	+	-	+
Thalamus						
Central posterior nucleus (CP) **AUDITORY**	+	+	+	+	-	-
Dorsal posterior (DPo)	-	+	+	+	-	-
Nucleus preglomerulosus (PGl/m) **AUDITORY**	+	+	+	-	-	-
Periventricular nucleus of posterior tuberculum (TPp)	+	+	+	+	-	+
Posterior tuberal nucleus (TP)	+	+	+	-	-	+
Pineal	-	-	+	+	-	-

Table 3.2 (continued)

Anatomical location	Mel1b	AR	ARO	ERα	ERβ1	ERβ2
Brainstem						
Periacqueductal gray (PAG) **VOCAL**	-	+	+	-	+	+
Mesencephalic tectum (Te)	+	+	-	+	-	-
Reticular formation (RF)	+	+	+	-	-	-
Nucleus of medial longitudinal fasiculus (nMLF)	+	+	+	+	-	-
Periventricular cell layer of TS (Pe) **AUDITORY**	+	+	-	-	-	+
Griseum central (GC)	+	+	+	-	-	-
Medial octavolateralis nucleus (MED)	+	+	-	-	-	-
Vagal motor nucleus (Xm)	+	+	+	-	+	+
Descending octavolateralis nucleus (ri) **AUDITORY**	+	-	-	-	-	-
Vocal prepacemaker nucleus (VPP) **VOCAL**	+	+	-	-	-	-
Vocal pacemaker nucleus (VPN) **VOCAL**	+					
Vocal motor nucleus (VMN) **VOCAL**	-	+	+	+	+	+

showing androgen and estrogen receptor expression and association with vocal and/or auditory functions. The nomenclature follows that of Braford and Northcutt (1983) (Braford and Northcutt, 1983). There was no above-background level expression in the three sense control brains (data not shown).

Olfactory Bulb and Telencephalon

Robust labeling of mel1b was observed throughout the olfactory bulb (Fig. 3.1A,B), discrete regions in the dorsal (Figs. 3.1B, 3.2A) and ventral (Figs. 3.1C; 3.2A) telencephalon, and the anterior parvocellular preoptic area (PPa; Fig. 3.1C). Mel1b labeling in the rostral forebrain was found in several dorsal (D) telencephalic nuclei, including the medial, dorsal, and lateral divisions (Dm, Dd, Dl, respectively; Fig. 3.1B). More caudally, mel1b was found throughout Dl, the central medial division of Dm (Dm-cm), the posterior division of DM (Dm-p), and the posterior zone of the dorsal telencephalon (Dp) (Fig. 3.2A,B). This dense labeling in the dorsal telencephalon occurs both on the ventricular surface and more centrally. However, the cells on the very edge of the ventricular surface are not labeled, suggesting that mel1b is not expressed in previously identified aromatase-expressing glial cells (Forlano et al., 2001). Robust labeling in the ventral division (V) of the telencephalon included the central (Vc), supracommisural (Vs) and intermediate (Vi) nuclei (Figs. 3.1C; 3.2A), all of which are targets of the olfactory bulb in midshipman (A. Bass, unpub observ) and other teleosts [e.g. (Bass, 1981; Levine and Dethier, 1985)].

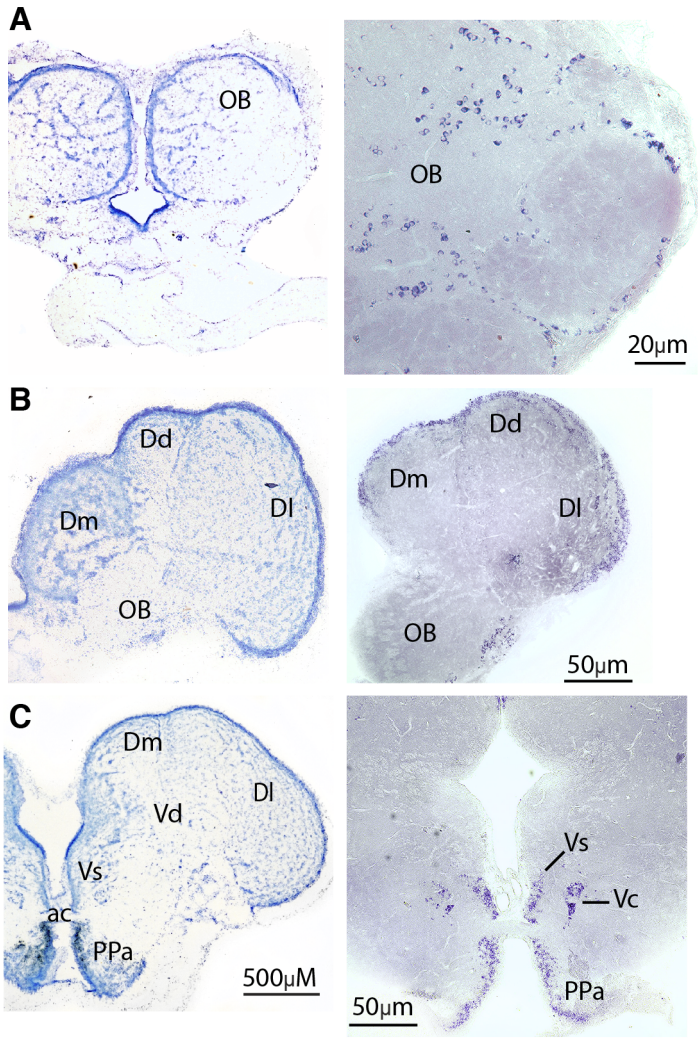

Figure 3.1
Mel1b mRNA distribution in the rostral forebrain. Olfactory bulb (OB), dorsal (D) and ventral (V) telencephalon, and the anterior parvocellular preoptic nucleus (PPa) expressed mel1b in discrete cell groups. Left panels are reference, cresyl violet stained sections. See Table 3.1 for complete list of abbreviations.

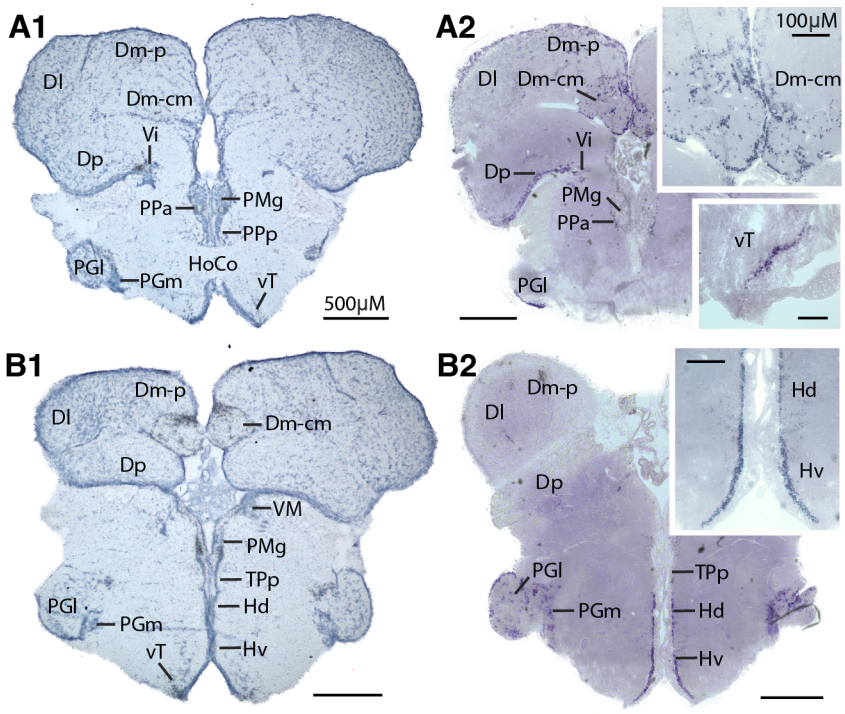

Figure 3.2
Mel1b mRNA distribution in the caudal telencephalon and rostral diencephalon. **A1-2:** Mel1b is distributed in discrete regions throughout the dorsal telencephalon, including in the central medial division of the medial zone of the dorsal telencephalon (Dm-cm; top insert in A2). Mel1b was also found in the ventral tuberal nucleus of the hypothalamus (vT; bottom insert in A2), the caudal extent of the anterior parvocellular preoptic nucleus (PPa) that forms a border surrounding the gigantocellular division of the magnocellular preoptic nucleus (PMg). **B1-2:** Mel1b was highly expressed in the dorsal (Hd) and ventral (Hv) periventricular hypothalamus (insert in B2), as well as the lateral (PGl) and medial (PGm) division of nucleus preglomerulosus. Diffuse labeling is observed in the periventricular nucleus of the posterior tuberculum (TPp). Left panels show cresyl violet stained reference sections. See Table 3.1 for complete list of abbreviations.

Diencephalon

Three diencephalic regions that receive auditory input from the midbrain (Bass et al., 2000) showed dense mel1b labeling: the central posterior thalamic nucleus in the dorsal thalamus (CP; Fig. 3.3A), the lateral preglomerular nucleus in the posterior tuberculum (PGl; Fig 3.2), and the anterior tuberal nucleus in the hypothalamus (AT; Fig. 3.3A). Mel1b is also expressed in two known targets of the olfactory bulb in midshipman (A. Bass, unpub obs) and other teleosts [e.g. (Bass, 1981; Levine and Dethier, 1985)], namely the periventricular nucleus of the posterior tuberculum (TPp), and the posterior tuberal nucleus (TP) (Fig. 3.3A1,B1). The ventral tuberal nucleus, a vocally active site in the far anterior hypothalamus that innervates the midbrain PAG (Goodson and Bass, 2000; Kittelberger, 2006; Kittelberger and Bass, 2013), also expressed mel1b (vT; Fig. 3.2A1,A2 lower insert).

Other diencephalic areas with Mel1b labeling, but no known specific sensory or vocal function, included the ventral and dorsal periventricular areas of the hypothalamus (Hv, Hd) (Figs. 3.2B; 3.3A), and the medial division of the nucleus preglomerulosus (PGm; Figs. 3.2B; 3.3A,B; 3.4A) and the nucleus glomerulosus (G; Fig. 3.3A,B) in the posterior tuberculum. No mel1b expression was found in the pineal (not shown), a major site of melatonin synthesis in vertebrates, including fish (Ekström and Meissl, 1997; Reiter, 1991).

Midbrain

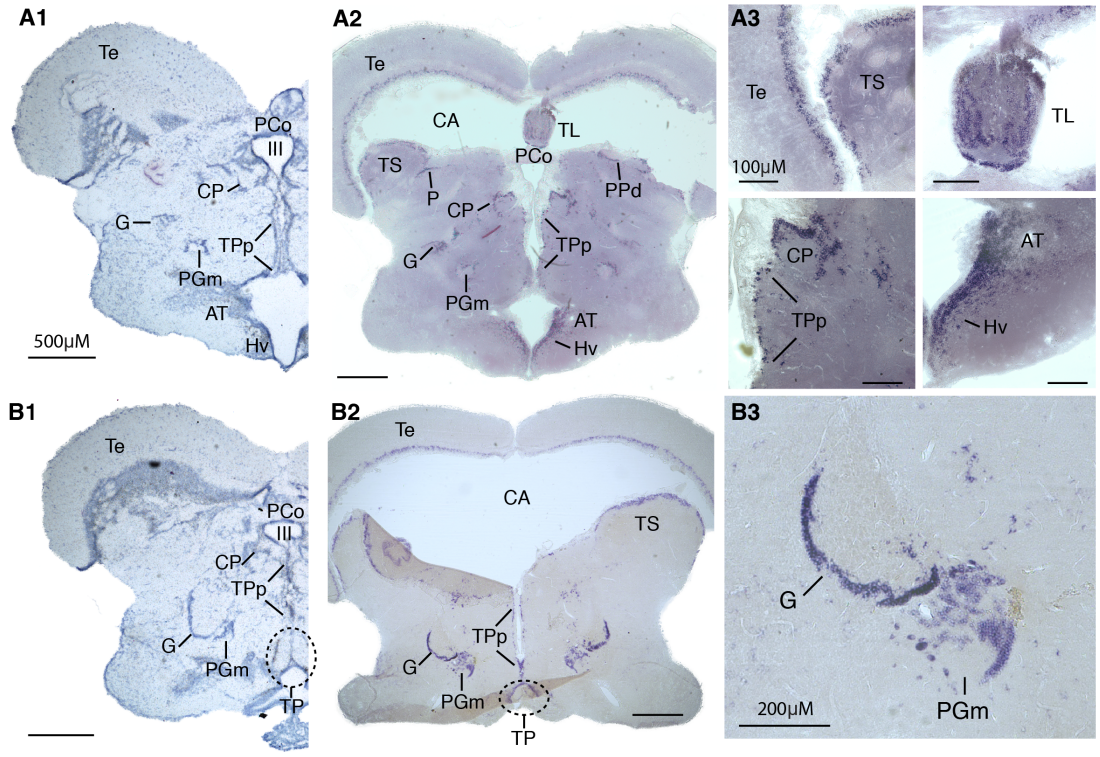

Figure 3.3
Mel1b mRNA distribution in the diencephalon and rostral midbrain. A1-3: Mel1b is highly expressed in visual areas such as the periventricular gray zone of the optic tectum (Te) and the torus longitudinalis (TL; A2 and A3 top right panel), and in auditory areas such as the periventricular cell layer of the torus semicircularis (TS), the central posterior nucleus of the thalamus (CP; A2 and bottom left panel in A3), and the periventricular nucleus of the posterior tuberculum (TPp; A2 and A3 bottom left panel). Hypothalamic regions expressing mel1b included the ventral periventricular hypothalamus (Hv; A2 and A3 bottom right panel) and the anterior tuberal nucleus (AT; A2 and A3 bottom right panel). **B1-3:** The posterior tuberal nucleus (TP), nucleus glomerulosus (G; B2-3), and medial division of G (PGm; B2-3) showed dense mel1b binding. Left panels show cresyl violet stained reference sections. See Table 3.1 for complete list of abbreviations.

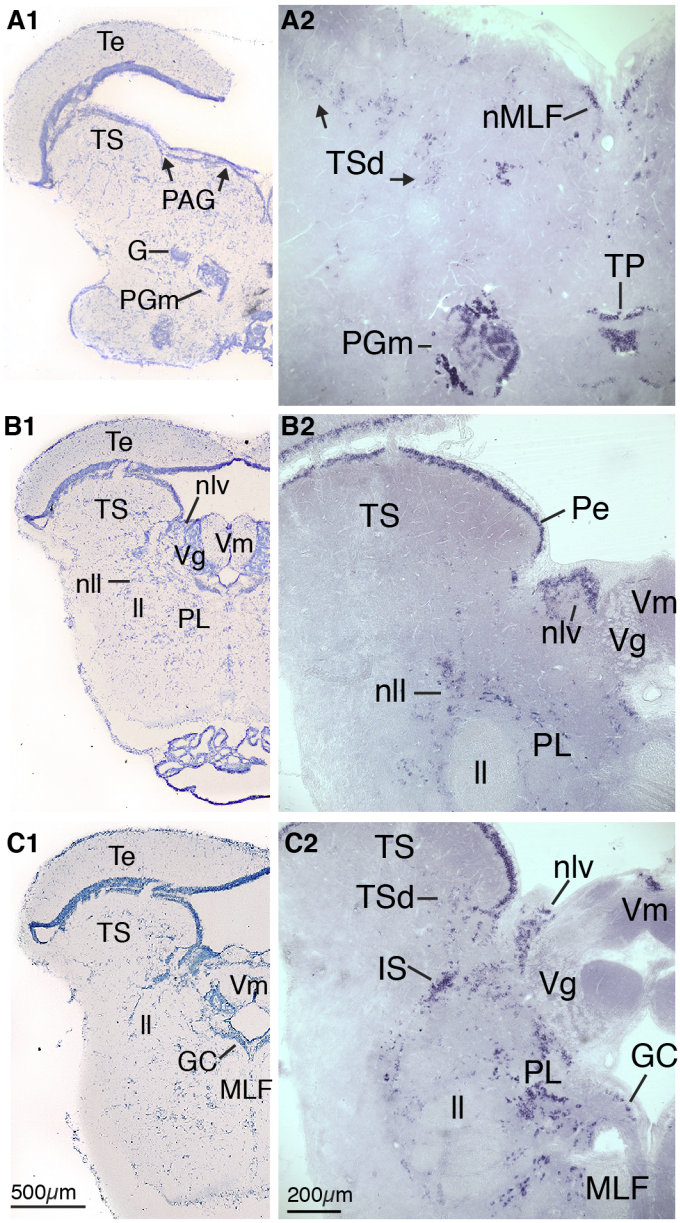

Figure 3.4
Mel1b mRNA distribution in the caudal midbrain. Mel1b is found in vocally active sites in the midbrain tegmentum, such as the deep layer of the torus semicircularis (TSd; A2), nucleus of the lateral lemniscus (nll; B2), and paralemniscal nucleus (PL; C2). Left panels show cresyl violet stained, reference sections. See Table 3.1 for complete list of abbreviations.

Two retinal-recipient areas in the midbrain of midshipman (A. Bass, unpub obs) and other teleosts [e.g. (Striedter, 1990)], the periventricular gray zone (PGZ) of the tectum (Te) and nucleus pretectalis periventricularis, showed consistent mel1b expression throughout their rostral-caudal extent (see Figs. 3.3; 3.4). Midbrain auditory areas showing dense mel1b label included the periventricular cell layer of the torus semicircularis (TS; Figs. 3.3A,B; 3.4B,C), the main auditory relay center (Bass et al., 2000; Bodnar and Bass, 1997), the pretoral nucleus (P; Fig. 3.3A2) that is reciprocally connected with the TS (Bass et al., 2000), and the deep layer of the TS that is also a vocally active site (TSd; Fig. 3.4A2) [(Feng and Bass, 2014); also see (Bass et al., 2000) for connectivity to TS].

More caudally in the midbrain, several vocally active sites in the medial and lateral tegmentum were densely labeled with mel1b, namely the TSd, nucleus of the lateral lemniscus (nll), and the paralemniscal nucleus (PL) (Fig. 3.4). These sites differ in their response to electrical stimuli, with longer duration calls with longer latencies evoked at lateral sites (Feng and Bass, 2014). In summary, the results suggest that both auditory and vocal centers in the midbrain and diencephalon are sensitive to melatonin action by expressing mel1b.

Isthmus and Hindbrain

Mel1b expression was found in diverse sensory and motor nuclei in the isthmus and hindbrain. This included several areas within the vocal circuitry previously identified by transneuronal biotin transport following labeling of a single vocal nerve with either biocytin or neurobiotin (Bass et al., 1994). At isthmal levels, a densely labeled cell

cluster below the caudal TS at the lateral border of the isthmal nucleus (IS; Figs. 3.4C2; 3.5A), exhibited terminal-like boutons after vocal nerve labeling (Bass et al., 1994). Additionally, the trigeminal isthmal periventricular nucleus (IP; Fig. 3.5A2), which contains biocytin-filled somata after vocal nerve labeling (Bass et al., 1994), expressed mel1b. Both IS and IP also receive input from the vocal PAG region (Kittelberger and Bass, 2013). One nucleus at isthmal levels that that showed dense expression of mel1b but has not been linked to either vocal or auditory function is the nucleus lateralis vavulae (nlv; Fig. 3.4B,C). This nucleus has reciprocal connections with the cerebellum, and receives a diversity of other inputs from the dorsal division of the telencephalon, the pretectum, and the inferior lobe of the hypothalamus in fish (Ito and Yoshimoto, 1990; Xue et al., 2005; Yang et al., 2004).

In the rostral hindbrain, dense mel1b label was found in the rostral and caudal divisions of nucleus medialis (MED; Fig. 3.5B,C) that receives direct input from lateral line afferents in midshipman and other teleosts (Weeg and Bass, 2000). Motor areas expressing mel1b included the reticular formation (RF) that is labeled throughout its rostral-caudal extent, including in the margins surrounding the medial longitudinal fasciculus (MLF; Fig. 3.5). At the caudal end of RF, mel1b is expressed in cells whose position correspond to the vocal prepacemaker nucleus (VPP; Fig. 3.5C) that receives input from the vocal PAG and codes for call duration (Bass et al., 1994; Chagnaud et al., 2011; Kittelberger and Bass, 2013).

Further caudally, mel1b is expressed throughout the vocal pacemaker nucleus (VPN; Fig. 3.5D), a ventral-lateral column adjacent to the vocal motor nucleus (VMN; Fig. 3.5D) and above the vocal tract (VT; Fig. 3.5D) that determines the pulse

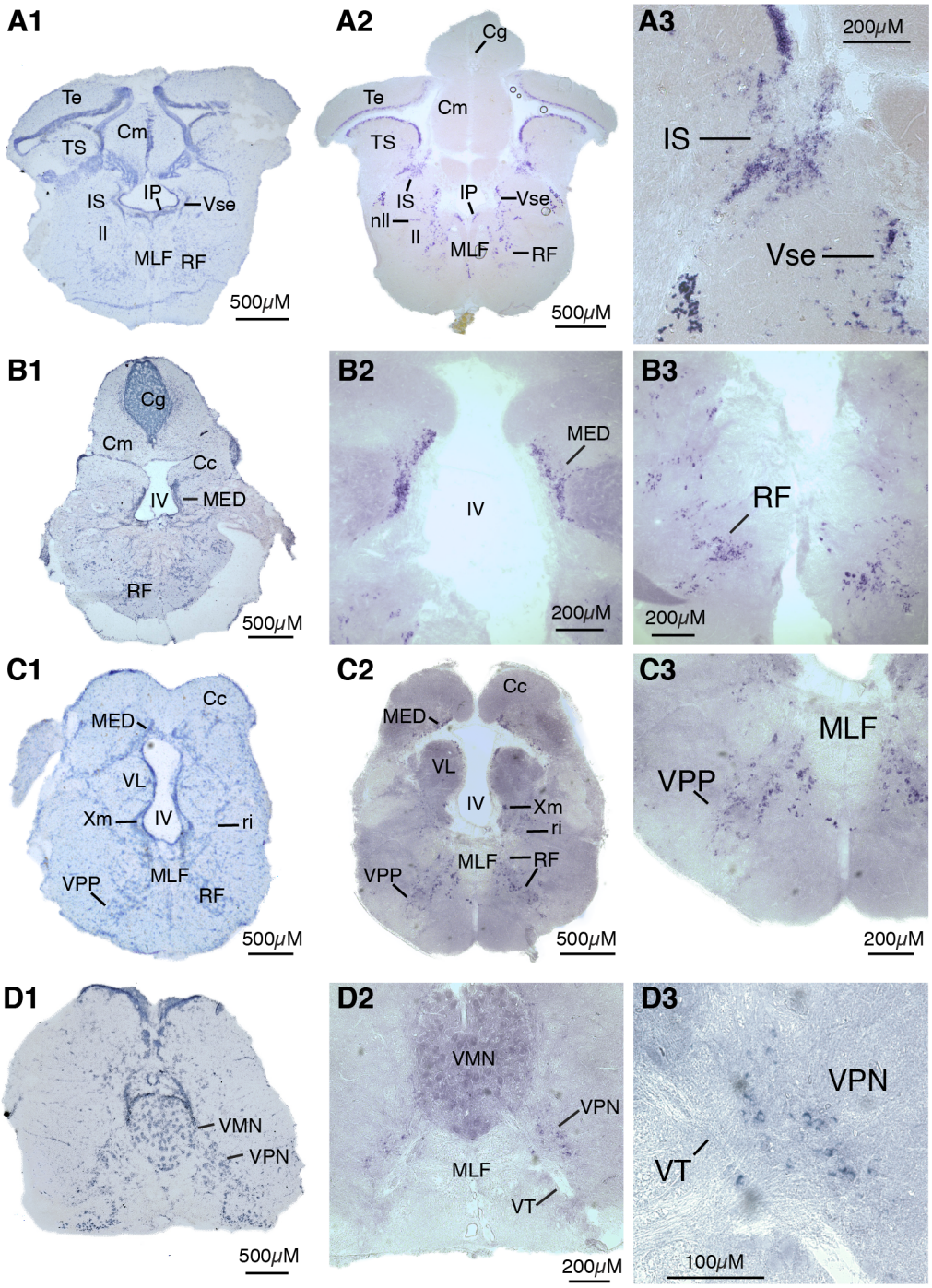

Figure 3.5
Mel1b expression in caudal midbrain and hindbrain. Mel1b is expressed in two nuclei of the hindbrain vocal pattern generator, the vocal prepacemaker nucleus (VPP; C2-3) and the vocal pacemaker nucleus (VPN; D2-3). Left panels show cresyl violet stained reference sections. See Table 3.1 for complete list of abbreviations.

repetition rate and fundamental frequency of vocalization (Bass and Baker, 1990; Chagnaud et al., 2011). Unlike the two pattern generating vocal premotor nuclei, VPP and VPN, the VMN that innervates the vocal muscle was devoid of mel1b label (Fig. 3.5D).

Discussion

These results showed robust mel1b expression in neuroendocrine rich regions and major nodes of the expansive central audio-vocal network in a highly vocal vertebrate, the plainfin midshipman fish. With few exceptions, all regions listed in Table 3.2 that express Mel1b, also express estrogen receptors, androgen receptors, or estrogen synthetase/aromatase (Fergus and Bass, 2013; Forlano et al., 2001; Forlano et al., 2005; Forlano et al., 2010). Many of these same regions are innervated by nonapeptide synthesizing neurons in the POA (Goodson et al., 2003). A recent review provides a more detailed overview of neuroendocrine centers in midshipman (Forlano et al., 2015).

Comparison with other teleost and/or midshipman studies

To our knowledge, only two other studies have localized specific melatonin receptor subtypes in the brains of teleost fish (Herrera-Pérez et al., 2010; Mazurais et al., 1999), while many have used 2-[^{125}I]-iodomelatonin (IMel) to probe general melatonin binding sites [see (Falcón et al., 2010) and references therein]. We mainly compare our results to a more recent study that performed mel1a/MT1 *in-situ* hybridization in the brain of the European sea bass (*Dicentrarchus labrax*) (Herrera-Pérez et al., 2010).

Unlike the widespread pattern of midshipman mel1b expression in the dorsal telencephalon (Figs. 3.1B; 3.2), the sea bass mel1a receptor was only expressed in two discrete cell clusters of Dd and Dm (Herrera-Pérez et al., 2010). The same is true for the ventral telencephalon where mel1b is in two nuclei in sea bass (Vs and Vv only), but four in midshipman (Vs, Vv, Vc, Vi; Figs. 3.1C; 3.2A; Table 3.2). Both sea bass mel1a and midshipman mel1b were expressed in the PPa, the auditory dorsal thalamus (CP), and the olfactory-recipient posterior tuberculum (TPp, apparently identified as lateral tuberal nucleus in sea bass) (Herrera-Pérez et al., 2010).

Visual areas (Striedter, 1990) such as the dorsal periventricular pretectal nucleus (PPd), the periventricular gray zone of the midbrain tectum (PGZ), nucleus glomerulosus (G) in the posterior tuberculum, and the midbrain's torus longitudinalis (TL) all showed positive label in both sea bass and midshipman. Furthermore, the midbrain's auditory-recipient torus semicircularis (TS), the eurydendroid cells lying between the molecular and granule cell layers of the corpus and valvula of the cerebellum (not illustrated here) (Bass, 1982; Ikenaga et al., 2006; Straka et al., 2006), and the reticular formation (RF), all shared staining for sea bass mel1a and midshipman mel1b. Herrera-Pérez et al. (2010) observed dense IMel binding but sparse distribution of mel1a in the TS, suggesting that mel1b receptors are responsible for the IMel binding, supported here by the dense label of mel1b in the midshipman TS. Sea bass mel1a was not found more caudally than the RF, while the vocal pre-pacemaker (VPP) and pacemaker (VPN) nuclei both expressed mel1b. Furthermore, no mention of the lateral line recipient nucleus medialis (MED), densely labeled in midshipman, was mentioned in the sea bass study. Thus, although major sensory and

neuroendocrine brain regions show similar mel1a and mel1b distribution in these two distantly related teleosts, some differences are observed in the telencephalon, and in the caudal hindbrain where the midshipman vocal pattern generator is located.

Contrary to previous PCR studies that showed low mel1b expression in the sea bass brain (Sauzet et al., 2008), we showed that mel1b is highly expressed in many areas in the midshipman brain. Furthermore, inconsistent with amplification of mel1b in sea bass pituitary (Sauzet et al., 2008), the midshipman pituitary was devoid of mel1b label. Compared to mel1b mRNA localization in rainbow trout, areas such as the PPa and PGZ of the midbrain tectum were consistent with midshipman mel1b distribution (Mazurais et al., 1999). However, unlike the midshipman mel1b, the rainbow trout mel1b was undetectable in the dorsal and ventral telencephalon (Mazurais et al., 1999).

Comparison with other vertebrates

Melatonin receptor expression has been observed in restricted regions and with species-specific patterns in the mammalian brain (Reppert et al., 1996). Mel1a/ MT1 receptor expression has been found in the hypothalamic suprachiasmatic nucleus (SCN), considered the "master" circadian clock in mammals, and in the anterior pituitary (Reppert et al., 1996; Reppert et al., 1994), while mel1b has been found in the retina, the hippocampus, and the cerebellum (Al-Ghoul et al., 1998; Reppert et al., 1996). Within the human cerebellum, mel1b was localized to Bergmann glial cells at the interface between the granule cell layer and the molecular layer (Al-Ghoul et al., 1998), where we also found mel1b in midshipman cerebellum. Within the Siberian

hamster brain, IMel and cRNA binding sites were found in four regions: the paraventricular nucleus of the thalamus (PT), SCN, the median eminence, and the arcuate nucleus (Reppert et al., 1994). The rat brain also shows restricted melatonin receptor expression in just the PT and SCN (Reppert et al., 1994).

A recent *in-situ* hybridization study in two songbirds, the zebra finch (*Taeniopygia guttata castanotis*) and the blackcap (*Sylvia atricapilla*), identified all three avian melatonin receptor subtypes (mel1a, mel1b, mel1c) in most sensory systems, although there was no expression of any receptor subtypes in the ascending auditory system (Fusani and Gahr, 2015). By contrast, midshipman mel1b is expressed in thalamic, midbrain and hindbrain auditory areas (TS, P, CP, ri), and in the lateral line system (MED) that also encodes acoustic stimuli with natural call properties (Weeg and Bass, 2002). Similar to the songbirds, midshipman mel1b is expressed in the olfactory bulb (Fusani and Gahr, 2015). Mel1b, but not mel1a, was found in critical nodes of the descending vocal motor pathway of songbirds: the HVC (letter based name), the premotor nucleus robustus arcopallialis (RA), and the midbrain vocal center nucleus intercollicularis (ICo) (Fusani and Gahr, 2015), which were consistent with a previous study (Jansen et al., 2005).

Within the neuroendocrine system, both midshipman and songbirds express mel1b in the preoptic area (POA) (Fusani and Gahr, 2015). The POA, a rich neuroendocrine region for steroid and peptide signaling and synthesis, exerts a strong influence on reproductive and social behavior in vertebrates via its projections to the pituitary and other downstream neural targets (Butler and Hodos, 2005; Goodson and Bass, 2000). However, in contrast to the lack of mel1b binding in the midshipman

SCN, mel1b is expressed in the SCN of both songbird species examined (Fusani and Gahr, 2015). Future studies examining expression patterns of other melatonin receptors in the midshipman brain are warranted.

Melatonin regulation of vocal behavior and underlying neurophysiology

Mel1b expression in song control nuclei likely mediates the melatonin-sensitive circadian vocal activity rhythm in songbirds (Wang et al., 2012). Furthermore, melatonin action via mel1b in specific song nuclei could be responsible for diel changes in fine temporal properties such as fundamental frequency and amplitude (Wood et al., 2013), as well as melatonin-dependent changes in gross temporal properties such as syllable, motif, and song duration (Derégnaucourt et al., 2012; Jansen et al., 2005). A mammalian mel1b antagonist decreased song duration the first day after intraperitoneal injection (Jansen et al., 2005). Melatonin, likely acting through mel1b, inhibited the firing rate of RA neurons in the zebra finch brain (Jansen et al., 2005). These studies support the hypothesis that melatonin action via mel1b regulates temporal characteristics of vocalizations in addition to their circadian timing.

As in songbird RA, melatonin seems in general to act in an inhibitory manner in the central nervous system (Dubocovich et al., 2010), including acute inhibition of firing rate in the SCN (Liu et al., 1997). However, melatonin has been shown to exert either inhibitory or dis-inhibitory effects depending on the receptor subtype expressed in a brain region (Wan et al., 1999). Specifically, melatonin acting via mel1b receptors decreased hyperpolarizing currents through type-A-γ-aminobutyric acid ($GABA_A$) receptors while mel1a receptors mediated the opposite effect (Wan et al., 1999). Given

the expression of mel1b in the midshipman POA, midbrain vocal-active sites, and hindbrain vocal premotor nuclei encoding the temporal properties of natural calls, a similar mechanism involving mel1b modulation of GABAergic inhibition could underlie melatonin's potentiation of vocal network excitability (Feng and Bass, 2014) and naturally occurring vocal behavior (Feng and Bass, in preparation).

In summary, mel1b is expressed at all levels of the brain within multiple sensory, motor, sensori-motor integration, and neuroendocrine centers. Melatonin can therefore act via mel1b within these brain regions to carry out diverse functions in midshipman, including the regulation of vocal-acoustic communication.

Materials and Methods

Animals and tissue collection

Midshipman fish were collected from the intertidal zone in Tomales Bay, California during the summer breeding season, held for 1-3 days in large outdoor aquaria with running seawater at the Bodega Marine Laboratory, then shipped overnight to Cornell University. At Cornell University, the fish were held under 15:9 h light:dark cycles that mimic the long-day photoperiod of the summer. Brains from six type I nest-guarding males, one female, and one type II sneak-spawning male were used to investigate mel1b distribution with anti-sense mRNA probes and three type I male brains were used with sense control probes.

Midshipman fish were deeply anesthetized in seawater containing 0.025% benzocaine (Sigma Chemical St. Louis, MO), and then perfused transcardially with teleost ringer followed by 4% paraformaldehyde in 0.1 M phosphate buffer (PB; pH

7.2). All fish were sacrificed during the dark phase of the light cycle. Brains were removed and postfixed in the same fixative for 1-2 h in 4°C and stored in PB. Brains were cryoprotected in 25% sucrose overnight, frozen in Cryo-M-bed (Hacker Instruments, Huntington, UK), and later sectioned in the transverse plane in 20μm onto Superfrost Plus slides (Fisher Scientific, Pittsburgh, PA). All procedures were approved by the Cornell Institutional Animal Care and Use Committee.

Mel1b RNA probe synthesis

First, we obtained a 613 bp predicted mel1b sequence (GenBank accession number KT878765) from an earlier, unpublished assembly of a midshipman brain transcriptome (Feng et al., 2015). NCBI blastp protein sequence alignment results indicated that this is a melatonin receptor 1b-b isoform, but we refer to the gene as mel1b throughout the current study. Top blastp results with 100% query coverage included sequences from 15 teleost species and showed high sequence identities (87-90%). NCBI blastn results showed nucleotide sequence identities of 83-85% for those sequences that had query coverage above 80%. Midshipman brain poly-A mRNA was isolated using TRIzol Reagent (Life Technologies, Carlsbad, CA). The following primers: forward: ATTTGCCCAGACCGTCAACACT, and reverse: TGACTCATTGTTGTTGTGCGGC amplified a region of 505 bp from the midshipman mel1b gene. The PCR product was ligated into pCRII vectors using the TA Cloning Kit (Life Technologies). Plasmid DNA was isolated from colonies were amplified using T7 and SP6 promoters, purified and submitted for sequencing at Cornell's Genomics Facility. Approximately 500 ηg of the PCR product was then

labeled with digoxygenin (Roche Life Science, Indianapolis, IN).

In-situ hybridization

Our in-situ hybridization protocol largely followed previously reported studies (Albersheim-Carter et al., 2015). Briefly, slides were held in RNase free slide mailers, warmed to room temperature (RT), dried at 50°C for 15 min, then fixed with 4% paraformaldehyde at RT for 20 min. After two washes in DEPC-PBS, slides were laid flat and treated with proteinase K in proteinase buffer for 7 min. Slides were washed in 0.1M triethanolamine-HCl (pH 8.0) with 0.25% acetic anhydride, blocked with hybridization buffer at 65°C for 12-16 h, then placed in hybridization buffer containing 1μg dig-labeled mel1b probes overnight. Slides were first washed in sodium citrate buffer at 62°C, blocked in alkaline phosphatase buffer with 0.1% Triton X-100, then incubated with dig antibody in the same buffer but containing 10% horse serum. Finally, for antibody visualization, slides were incubated in nitro blue tetrazolium chloride and 5-Bromo-4-chloro-3-indolyl phosphate (NBT-BCIP, Roche, Indianapolis, IN) until labeling is clear. Slides were then fixed in 4% Paraformaldehyde, washed in 0.1M PB, covered in mounting medium, coverslipped, and sealed with Vectamount. Photographs were taken by a Nikon Eclipse E800 digital camera.

Acknowledgments

We would like to thank Margaret Marchaterre for trouble shooting and performing the *in situ* hybridization protocol and Dr. Paul Gray for lending his expertise and advice.

This work was supported by NSF IOS 1120925 and 1457108.

References

Al-Ghoul, W. M., Herman, M. D. and Dubocovich, M. L. (1998). Melatonin receptor subtype expression in human cerebellum. *Neuroreport* **9**, 4063–4068.

Albersheim-Carter, J., Blubaum, A., Ballagh, I. H., Missaghi, K., Siuda, E. R., McMurray, G., Bass, A. H., Dubuc, R., Kelley, D. B., Schmidt, M. F., et al. (2015). Testing the evolutionary conservation of vocal motoneurons in vertebrates. *Respir Physiol Neurobiol*.

Bass, A. H. (1981). Olfactory bulb efferents in the channel catfish, Ictalurus punctatus. *Journal of Morphology* **169**, 91–111.

Bass, A. H. (1982). Evolution of the vestibulolateral lobe of the cerebellum in electroreceptive and nonelectroreceptive teleosts. *Journal of Morphology* **174**, 335–348.

Bass, A. H. and Baker, R. (1990). Sexual dimorphisms in the vocal control system of a teleost fish: Morphology of physiologically identified neurons. *Journal of Neurobiology* **21**, 1155–1168.

Bass, A. H., Bodnar, D. A. and Marchaterre, M. A. (2000). Midbrain acoustic circuitry in a vocalizing fish. *J. Comp. Neurol.* **419**, 505–531.

Bass, A. H., Marchaterre, M. A. and Baker, R. (1994). Vocal-acoustic pathways in a teleost fish. *Journal of Neuroscience* **14**, 4025–4039.

Bodnar, D. A. and Bass, A. H. (1997). Temporal coding of concurrent acoustic signals in auditory midbrain. *Journal of Neuroscience* **17**, 7553–7564.

Boutin, J. A., Audinot, V., Ferry, G. and Delagrange, P. (2005). Molecular tools to study melatonin pathways and actions. *Trends Pharmacol. Sci.* **26**, 412–419.

Braford, M. R., Jr and Northcutt, R. G. (1983). *Organization of the diencephalon and pretectum of the ray-finned fishes*. Fish neurobiology.

Brantley, R. K. and Bass, A. H. (1994). Alternative Male Spawning Tactics and Acoustic Signals in the Plainfin Midshipman Fish Porichthys notatus Girard (Teleostei, Batrachoididae). *Ethology* **96**, 213–232.

Butler, A. B. and Hodos, W. (2005). *Comparative vertebrate neuroanatomy: evolution and adaptation*.

Chagnaud, B. P. and Bass, A. H. (2013). Vocal Corollary Discharge Communicates Call Duration to Vertebrate Auditory System. *Journal of Neuroscience* **33**, 18775–18780.

Chagnaud, B. P., Baker, R. and Bass, A. H. (2011). Vocalization frequency and duration are coded in separate hindbrain nuclei. *Nature Communications* **2**, 346–11.

Derégnaucourt, S., Saar, S. and Gahr, M. (2012). Melatonin affects the temporal pattern of vocal signatures in birds. *J. Pineal Res.* **53**, 245–258.

Dubocovich, M. L., Delagrange, P., Krause, D. N., Sugden, D., Cardinali, D. P. and Olcese, J. (2010). International Union of Basic and Clinical Pharmacology. LXXV. Nomenclature, classification, and pharmacology of G protein-coupled melatonin receptors. *Pharmacol Rev* **62**, 343–380.

Ekström, P. and Meissl, H. (1997). The pineal organ of teleost fishes. *Reviews in Fish Biology and Fisheries* **7**, 199–284.

Falcón, J., Migaud, H., Muñoz-Cueto, J. A. and Carrillo, M. (2010). Current knowledge on the melatonin system in teleost fish. *General and Comparative Endocrinology* **165**, 469–482.

Feng, N. Y. and Bass, A. H. (2014). Melatonin action in a midbrain vocal-acoustic network. *Journal of Experimental Biology* **217**, 1046–1057.

Fergus, D. J. and Bass, A. H. (2013). Localization and divergent profiles of estrogen receptors and aromatase in the vocal and auditory networks of a fish with alternative mating tactics. *J. Comp. Neurol.* **521**, 2850–2869.

Forlano, P. M., Deitcher, D. L. and Bass, A. H. (2005). Distribution of estrogen receptor alpha mRNA in the brain and inner ear of a vocal fish with comparisons to sites of aromatase expression. *J. Comp. Neurol.* **483**, 91–113.

Forlano, P. M., Deitcher, D. L., Myers, D. A. and Bass, A. H. (2001). Anatomical distribution and cellular basis for high levels of aromatase activity in the brain of teleost fish: aromatase enzyme and mRNA expression identify glia as source. *J. Neurosci.* **21**, 8943–8955.

Forlano, P. M., Kim, S. D., Krzyminska, Z. M. and Sisneros, J. A. (2014). Catecholaminergic connectivity to the inner ear, central auditory, and vocal motor circuitry in the plainfin midshipman fish porichthys notatus. *J. Comp. Neurol.* **522**, 2887–2927.

Forlano, P. M., Marchaterre, M., Deitcher, D. L. and Bass, A. H. (2010). Distribution of androgen receptor mRNA expression in vocal, auditory, and neuroendocrine circuits in a teleost fish. *J. Comp. Neurol.* **518**, 493–512.

Forlano, P. M., Sisneros, J. A., Rohmann, K. N. and Bass, A. H. (2015). Neuroendocrine control of seasonal plasticity in the auditory and vocal systems of fish. *Frontiers in Neuroendocrinology* **37**, 129–145.

Fusani, L. and Gahr, M. (2015). Differential expression of melatonin receptor subtypes MelIa, MelIb and MelIc in relation to melatonin binding in the male songbird brain. *Brain Behav Evol* **85**, 4–14.

Goodson, J. L. and Bass, A. H. (2000). Forebrain peptides modulate sexually polymorphic vocal circuitry. *Nature* **403**, 769–772.

Goodson, J. L., Evans, A. K. and Bass, A. H. (2003). Putative isotocin distributions in sonic fish: relation to vasotocin and vocal-acoustic circuitry. *J. Comp. Neurol.* **462**, 1–14.

Herrera-Pérez, P., Del Carmen Rendón, M., Besseau, L., Sauzet, S., Falcón, J. and Muñoz-Cueto, J. A. (2010). Melatonin receptors in the brain of the European sea bass: An in situ hybridization and autoradiographic study. *The Journal of comparative neurology* **518**, 3495–3511.

Hoegg, S., Brinkmann, H., Taylor, J. S. and Meyer, A. (2004). Phylogenetic timing of the fish-specific genome duplication correlates with the diversification of teleost fish. *J. Mol. Evol.* **59**, 190–203.

Ibara, R. M., Penny, L. T., Ebeling, A. W., van Dykhuizen, G. and Cailliet, G. (1983). The mating call of the plainfin midshipman fish, Porichthys notatus. In *Predators and prey in fishes*, pp. 205–212. Dordrecht: Springer Netherlands.

Ikegami, T., Azuma, K., Nakamura, M., Suzuki, N., Hattori, A. and Ando, H. (2009a). Diurnal expressions of four subtypes of melatonin receptor genes in the optic tectum and retina of goldfish. *Comp. Biochem. Physiol., Part A Mol. Integr. Physiol.* **152**, 219–224.

Ikegami, T., Motohashi, E., Doi, H., Hattori, A. and Ando, H. (2009b). Synchronized diurnal and circadian expressions of four subtypes of melatonin receptor genes in the diencephalon of a puffer fish with lunar-related spawning cycles. *Neuroscience Letters* **462**, 58–63.

Ikenaga, T., Yoshida, M. and Uematsu, K. (2006). Cerebellar efferent neurons in teleost fish. *Cerebellum* **5**, 268–274.

Ito, H. and Yoshimoto, M. (1990). Cytoarchitecture and fiber connections of the nucleus lateralis valvulae in the carp (Cyprinus carpio). *J. Comp. Neurol.* **298**, 385–399.

Jansen, R., Metzdorf, R., van der Roest, M., Fusani, L., Maat, ter, A. and Gahr, M. (2005). Melatonin affects the temporal organization of the song of the zebra

finch. *FASEB J.* **19**, 848–850.

Kittelberger, J. M. (2006). Midbrain Periaqueductal Gray and Vocal Patterning in a Teleost Fish. *Journal of Neurophysiology* **96**, 71–85.

Kittelberger, J. M. and Bass, A. H. (2013). Vocal-motor and auditory connectivity of the midbrain periaqueductal gray in a teleost fish. *J. Comp. Neurol.* **521**, 791–812.

Lee, J. S. F. (2006). Dimorphic male midshipman fish: reduced sexual selection or sexual selection for reduced characters? *Behavioral Ecology* **17**, 670–675.

Levine, R. L. and Dethier, S. (1985). The connections between the olfactory bulb and the brain in the goldfish. *The Journal of comparative neurology* **237**, 427–444.

Li, D. Y., Smith, D. G., Hardeland, R., Yang, M. Y., Xu, H. L., Zhang, L., Yin, H. D. and Zhu, Q. (2013). Melatonin receptor genes in vertebrates. *Int J Mol Sci* **14**, 11208–11223.

Liu, C., Weaver, D. R., Jin, X., Shearman, L. P. and Pieschl, R. L. (1997). Molecular dissection of two distinct actions of melatonin on the suprachiasmatic circadian clock. *Neuron* **19**, 91–102.

Mazurais, D., Brierley, I., Anglade, I., Drew, J., Randall, C., Bromage, N., Michel, D., Kah, O. and Williams, L. M. (1999). Central melatonin receptors in the rainbow trout: comparative distribution of ligand binding and gene expression. *J. Comp. Neurol.* **409**, 313–324.

McIver, E. L., Marchaterre, M. A., Rice, A. N. and Bass, A. H. (2014). Novel underwater soundscape: acoustic repertoire of plainfin midshipman fish. *J. Exp. Biol.* **217**, 2377–2389.

Moore-Ede, M. C., Sulzman, F. M. and Fuller, C. A. (1982). *The clocks that time us*. Cambridge: Harvard University Press.

Reiter, R. J. (1991). Pineal gland interface between the photoperiodic environment and the endocrine system. *Trends Endocrinol. Metab.* **2**, 13–19.

Reiter, R. J. (1993). The melatonin rhythm: both a clock and a calendar. *Experientia* **49**, 654–664.

Reiter, R. J., Tan, D. X. and Galano, A. (2014). Melatonin: exceeding expectations. *Physiology (Bethesda)* **29**, 325–333.

Reppert, S. M., Weaver, D. R. and EBISAWA, T. (1994). Cloning and Characterization of a Mammalian Melatonin Receptor That Mediates Reproductive and Circadian Responses. *Neuron* **13**, 1177–1185.

Reppert, S. M., Weaver, D. R. and Godson, C. (1996). Melatonin receptors step into the light: Cloning and classification of subtypes. *Trends Pharmacol. Sci.* **17**, 100–102.

Reppert, S. M., Weaver, D. R., Cassone, V. M., Godson, C. and Kolakowski, L. F. (1995). Melatonin receptors are for the birds: molecular analysis of two receptor subtypes differentially expressed in chick brain. *Neuron* **15**, 1003–1015.

Rohmann, K. N., Fergus, D. J. and Bass, A. H. (2013). Plasticity in Ion Channel Expression Underlies Variation in Hearing during Reproductive Cycles. *Current Biology* **23**, 678–683.

Sauzet, S., Besseau, L., Herrera-Pérez, P., Covès, D., Chatain, B., Peyric, E., Boeuf, G., Muñoz-Cueto, J. A. and Falcón, J. (2008). Cloning and retinal expression of melatonin receptors in the European sea bass, Dicentrarchus labrax. *General and Comparative Endocrinology* **157**, 186–195.

Straka, H., Beck, J. C., Pastor, A. M. and Baker, R. (2006). Morphology and physiology of the cerebellar vestibulolateral lobe pathways linked to oculomotor function in the goldfish. *Journal of Neurophysiology* **96**, 1963–1980.

Striedter, G. F. (1990). The Diencephalon of the Channel Catfish, Ictalurus punctatus. II. Retinal, tectal cerebellar and telencephalic connections. *Brain Behav Evol* **36**, 355–377.

Taniguchi, M., Murakami, N., Nakamura, H., Nasu, T., Shinohara, S. and Etoh, T. (1993). Melatonin release from pineal cells of diurnal and nocturnal birds. *Brain Research* **620**, 297–300.

Wan, Q., Man, H. Y., Liu, F., Braunton, J., Niznik, H. B., Pang, S. F., Brown, G. M. and Wang, Y. T. (1999). Differential modulation of GABAA receptor function by Mel1a and Mel1b receptors. *Nature Neuroscience* **2**, 401–403.

Wang, G., Harpole, C. E., Trivedi, A. K. and Cassone, V. M. (2012). Circadian Regulation of Bird Song, Call, and Locomotor Behavior by Pineal Melatonin in the Zebra Finch. *Journal of Biological Rhythms* **27**, 145–155.

Weeg, M. S. and Bass, A. H. (2000). Central lateral line pathways in a vocalizing fish. *J. Comp. Neurol.* **418**, 41–64.

Weeg, M. S. and Bass, A. H. (2002). Frequency response properties of lateral line superficial neuromasts in a vocal fish, with evidence for acoustic sensitivity. *Journal of Neurophysiology* **88**, 1252–1262.

Wikelski, M., Tarlow, E. M., Eising, C. M., Groothuis, T. G. G. and Gwinner, E. (2005). Do night-active birds lack daily melatonin rhythms? A case study comparing a diurnal and a nocturnal-foraging gull species. *J Ornithol* **147**, 107–

111.

Wood, W. E., Osseward, P. J., Roseberry, T. K. and Perkel, D. J. (2013). A daily oscillation in the fundamental frequency and amplitude of harmonic syllables of zebra finch song. *PLoS ONE* **8**, e82327.

Xue, H.-G., Yang, C.-Y., Yamamoto, N., Ito, H. and Ozawa, H. (2005). An indirect trigeminocerebellar pathway through the nucleus lateralis valvulae in a perciform teleost, Oreochromis niloticus. *Neuroscience Letters* **390**, 104–108.

Yang, C.-Y., Yoshimoto, M., Xue, H.-G., Yamamoto, N., Imura, K., Sawai, N., Ishikawa, Y. and Ito, H. (2004). Fiber connections of the lateral valvular nucleus in a percomorph teleost, tilapia (Oreochromis niloticus). *J. Comp. Neurol.* **474**, 209–226.

CHAPTER 4

NEURAL TRANSCRIPTOME REVEALS MOLECULAR MECHANISMS FOR TEMPORAL CONTROL OF VOCALIZATION ACROSS MULTIPLE TIMESCALES

Abstract

Vocalization is a prominent social behavior among vertebrates, including in the midshipman fish, an established model for elucidating the neural basis of acoustic communication. Courtship vocalizations produced by territorial males are essential for reproductive success, vary over daily and seasonal cycles, and last up to hours per call. Vocalizations rely upon extreme synchrony and millisecond precision in the firing of a homogeneous population of motoneurons, the vocal motor nucleus (**VMN**). Although studies have identified neural mechanisms driving rapid, precise, and stable neuronal firing over long periods of calling, little is known about underlying genetic/molecular mechanisms. We used RNA sequencing-based transcriptome analyses to compare patterns of gene expression in VMN to the surrounding hindbrain across three daily and seasonal time points of high and low sound production to identify candidate genes that underlie VMN's intrinsic and network neuronal properties. Results from gene ontology enrichment, enzyme pathway mapping, and gene category-wide expression levels highlighted the importance of cellular respiration in VMN function, consistent with the high energetic demands of sustained vocal behavior. Functionally important candidate genes upregulated in the VMN, including at time points corresponding to high natural vocal activity, encode ion channels and neurotransmitter receptors,

* Previously published as Feng NY, Fergus DJ, Bass AH. 2015. *BMC Genomics* 16:408

hormone receptors and biosynthetic enzymes, neuromodulators, aerobic respiration enzymes, and antioxidants. Quantitative PCR and RNA-seq expression levels for 28 genes were significantly correlated. Many candidate gene products regulate mechanisms of neuronal excitability, including those previously identified in VMN motoneurons, as well as novel ones that remain to be investigated. Supporting evidence from previous studies in midshipman strongly validate the value of transcriptomic analyses for linking genes to neural characters that drive behavior. Transcriptome analyses highlighted a suite of molecular mechanisms that regulate vocalization over behaviorally relevant timescales, spanning milliseconds to hours and seasons. To our knowledge, this is the first comprehensive characterization of gene expression in a dedicated vocal motor nucleus. Candidate genes identified here may belong to a conserved genetic toolkit for vocal motoneurons facing similar energetic and neurophysiological demands.

Introduction

Vocal-acoustic communication is a prominent feature of vertebrate social behavior. Despite having evolved diverse peripheral sonic organs, brainstem vocal networks that control vocalization are remarkably conserved across vertebrate taxa (Bass et al., 2008; Kingsbury et al., 2011). In tetrapods and several clades of fishes, sound production relies upon temporally stable modulations of acoustic waveforms over millisecond timescales (Bass and Chagnaud, 2012; Elemans et al., 2011; Elemans et al., 2008; Elemans et al., 2004). Although vocal networks in several vertebrate lineages achieve high degrees of synchrony and precision [e.g., (Amador et al., 2013;

Chagnaud et al., 2012; Goldberg et al., 2013; Yamaguchi et al., 2003)], it is unknown whether these properties depend on a suite of conserved genetic/molecular mechanisms.

Recent microarray and genome analyses in a songbird, the zebra finch (*Taeniopygia guttata*), have advanced our understanding of the relationship between genes and vocal behavior by identifying transcription factors and gene networks activated in forebrain song nuclei (Lovell et al., 2013; Lovell et al., 2008; Whitney et al., 2014), including during singing (Hilliard et al., 2012; Warren et al., 2010b; Whitney et al., 2014). Similar large-scale gene expression studies in other species that aim to link gene expression to behavior typically use whole brains or regions containing multiple neuron types [e.g. (Fraser et al., 2014; Hilliard et al., 2012; Lovell et al., 2008; Lovell et al., 2013; Rittschof et al., 2014; Schunter et al., 2014; Warren et al., 2010a; Whitney et al., 2014)]. While these studies provide significant insight into the genetic regulation of behavioral states, cellular and network level interpretations of results are confounded by the complexity of the underlying neural structure or behavior.

For the vast majority of vocal vertebrates that currently lack either genomic data or species-specific microarrays, no large-scale expression study has examined genes whose products directly support the function of a single neuronal population devoted to sound production. Here, we identify candidate molecular mechanisms contributing to the neural coding of vocal behavior in the plainfin midshipman fish (*Porichthys notatus*), an established model for the neural basis of acoustic communication. In order to link gene expression to neurophysiological events that

directly translate to behavior, we focused RNA sequencing (RNA-seq) transcriptome analyses on a single hindbrain nucleus that is dedicated to the temporal patterning of a simple vocal behavior.

Midshipman belong to an order of highly vocal teleost fish known as toadfishes (Batrachodiformes) (Greenfield et al., 2008) that produce different call types depending on social context (Brantley and Bass, 1994; Rice and Bass, 2009). Nest-guarding males, which are used in this study, produce several call types, including a long duration advertisement "hum". The hum is a stable, high frequency (100 Hz at ~16°C) call that is energetically demanding and essential for mate attraction (McKibben and Bass, 1998). Hums are produced continuously for minutes to hours, including in captivity (e.g., see 1.85 h hum in Fig. 4.1A), throughout the night during the summer breeding season (Brantley and Bass, 1994; Ibara et al., 1983; McIver et al., 2014; Rubow and Bass, 2009).

In midshipman, well-delineated forebrain, midbrain, and hindbrain nuclei comprise a vocal network (Bass et al., 1994; Goodson and Bass, 2002; Kittelberger and Bass, 2013) (Fig. 4.1B). The collective output of this network determines the natural vocalization's fine (e.g. fundamental frequency) and gross (e.g. duration) temporal structure (Chagnaud et al., 2011). This motor command is relayed to a single pair of dedicated vocal muscles by way of the hindbrain vocal motor nucleus (VMN), which forms a hindbrain vocal central pattern generator with separate premotor pacemaker and prepacemaker nuclei (CPG) (Fig. 4.1B) (Bass, 2014; Bass and Baker, 1990; Chagnaud et al., 2012; Chagnaud et al., 2011; Remage-Healey and Bass, 2007; Remage-Healey and Bass, 2004; Remage-Healey and Bass, 2006b; Remage-Healey

and Bass, 2009). Although forebrain and midbrain vocal nuclei gate and modulate hindbrain vocal CPG output and are highly sensitive to hormone action (Feng and Bass, 2014; Goodson and Bass, 2000a; Goodson and Bass, 2000b; Remage-Healey and Bass, 2004), the surgically isolated hindbrain vocal CPG region is both necessary and sufficient for generating the vocal command signal, and remains sensitive to hormonal modulation (Remage-Healey and Bass, 2004).

VMN's intrinsic and network neuronal properties drive synchronous and stable population-level firing that faithfully amplifies premotor temporal input (Chagnaud et al., 2012). Each VMN spike leads to a single sound pulse, resulting in a one-to-one translation between VMN output and the temporal properties of natural vocalization, such as call duration and fundamental frequency (compare Fig. 4.1A and B). Terrestrial vertebrates such as songbirds, bats, primates, rely on vocal networks that integrate input from breathing circuits (Hage and Jürgens, 2006; Hage et al., 2013; Riede and Goller, 2010; Rübsamen and Betz, 1986; Sturdy et al., 2003) to drive multiple vocal and respiratory muscles. In contrast, the simpler vocal systems of fishes do not rely on airflow and engage a single pair of sonic muscles, providing a straightforward link between gene expression, neural networks, and behavior (Chagnaud et al., 2012; Yamaguchi et al., 2003).

In addition to the direct translation between neurophysiological activity and behavior, the midshipman VMN provides several advantages for revealing molecular mechanisms underlying vocal patterning. First, the paired midline VMN together (Fig. 4.1C) form a highly interconnected, homogenous population of ~4000 vocal motoneurons (Bass and Andersen, 1991; Chagnaud et al., 2012), inclusive of

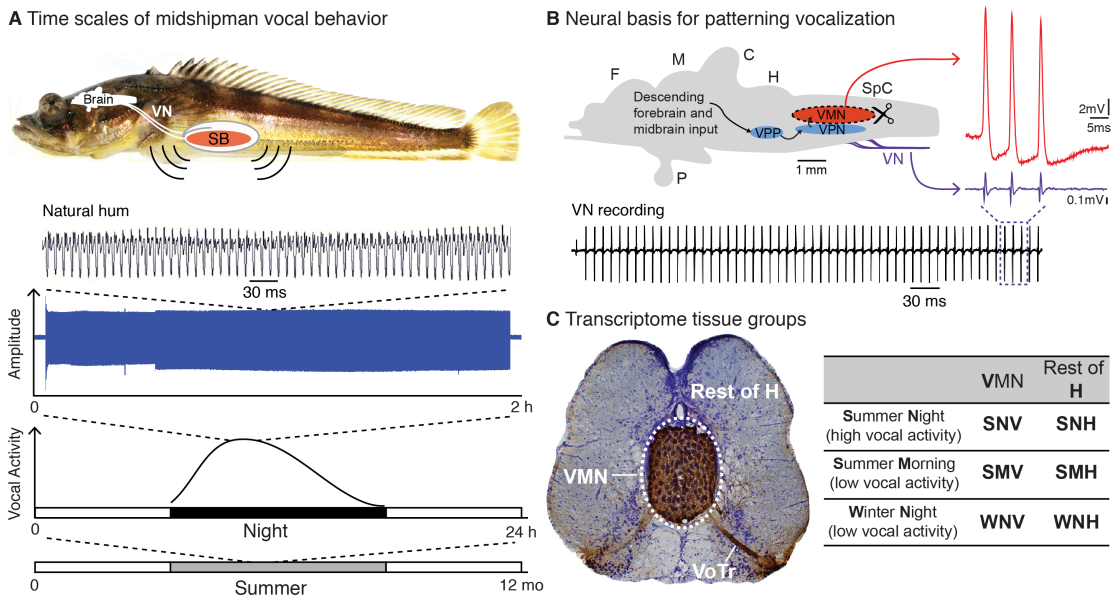

	VMN	Rest of H
Summer Night (high vocal activity)	SNV	SNH
Summer Morning (low vocal activity)	SMV	SMH
Winter Night (low vocal activity)	WNV	WNH

Figure 4.1

Midshipman is a neuroethological model for studying neural control of vocalization. A) Midshipman vocal behavior varies across a range of time scales. Picture of a midshipman fish (top) with schematic side view of the brain, vocal nerve (VN), and sonic swimbladder (SB), the sound-producing organ with vocal muscles (red) attached to the sidewalls. Continuous hums can last from mins to >1 h, as shown in the 1.85 h hum recorded from a captive male (blue trace), and are produced repetitively throughout the night during the summer breeding season (bottom). Close-up of natural hum is adapted from (Rubow and Bass, 2009). **B)** Schematic saggital view of the midshipman brain showing the hindbrain vocal pattern generator that consists of the vocal pre-pacemaker nucleus (VPP), vocal pacemaker nucleus (VPN), and vocal motor nucleus (VMN) (left). Forebrain and midbrain vocal centers drive the hindbrain pattern generator, which provides a precise and synchronous code that controls sonic muscle contraction in a one-to-one manner (compare the series of sound pulses in the natural hum in A to the vocal nerve potentials directly to the right in the bottom trace in B). Extreme temporal precision of motoneuron firing is shown by corresponding traces from an intracellular VMN recording (red) and VN recording [purple; adapted from (Chagnaud et al., 2012)]. Trace of a long duration VN recording (bottom) adapted from (Feng and Bass, 2014). **C)** Tissue groups used for transcriptome analysis and their notations. Left: a transverse section at the level of VMN showing bilateral, transneuronal biocytin labeling in VMN and the vocal tract (VoTr) (Bass et al., 1994); each VMN innervates the ipsilateral vocal SB muscle. In this study, we surgically separated the midline pair of VMN from the surrounding hindbrain tissue (Rest of H). Right: abbreviations of sample groups according to the tissue and time of collection, used throughout this paper.

surrounding glial cells and presynaptic inputs that support VMN network function, which can be excised *in-toto* for focal molecular analysis of a single brain nucleus (Fergus and Bass, 2013). Second, a set of intrinsic (low baseline excitability, rapid membrane repolarization) and network (dense excitatory and inhibitory inputs; electrotonic coupling) neuronal properties of the VMN are well characterized (Chagnaud et al., 2012). These properties guide the identification of candidate genes encoding specific molecular counterparts that likely contribute to VMN's extreme population-level synchrony on a millisecond timescale (Fig. 4.1B). Third, midshipman vocal behavior follows predictable daily and seasonal cycles (Brantley and Bass, 1994; Feng and Bass, 2014; McIver et al., 2014; Rubow and Bass, 2009). This allows us to utilize temporal variation to identify genes driving changes in vocal network excitability at different daily and seasonal time points (Rubow and Bass, 2009) (Fig. 4.1C). Fourth, a large body of work that documents hormonal modulation of the vocal system at multiple levels of analyses (neuroanatomy, neurophysiology, qPCR quantification, behavior) informs the functional significance of gene expression patterns [see (Bass and Remage-Healey, 2008; Forlano et al., 2015)].

We aimed to identify molecular pathways specific to VMN function by comparing patterns of gene expression in the VMN to the surrounding hindbrain (**H**) across daily and seasonal time points of high and low sound production (Fig. 4.1A,C). As outlined in Figure 4.2, we focused first on between-tissue differences in gene expression to identify candidate gene pathways important for VMN function, then on within-tissue comparisons to identify candidate gene pathways with biologically relevant expression patterns across the day and season.

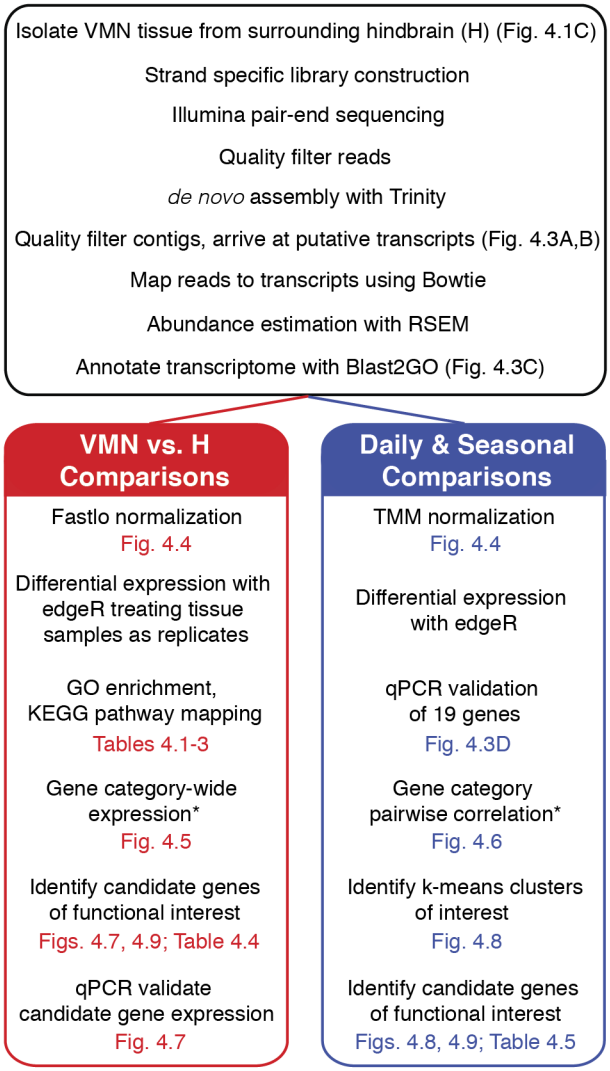

Figure 4.2
Schematic of analytic approaches with associated figure and table numbers. We took a two-pronged approach in analyzing the vast array of data generated from RNA-seq. First, for VMN vs. H comparisons, we used a cyclic loess method, fastlo, to eliminate a non-linear tissue-dependent skew between datasets (left, red). We then treated time point samples as replicates for each tissue for differential expression with edgeR. Second, we followed the Trinity-supported downstream analyses of clustering differentially expressed transcripts and focused these analyses on clusters with biologically relevant expression patterns across the day and season (right, blue). Additionally, we analyzed expression and correlation patterns of transcripts belonging to six broad gene functional categories. *Genes were grouped in broad categories regardless of whether they were differentially expressed.

By harnessing the extensive knowledge of the midshipman vocal network, the VMN transcriptome elucidated a set of molecular pathways underlying neuronal excitability in a motor nucleus that instructs vocal patterning across multiple timescales, from milliseconds to hours and seasons. Our results directly inform future studies using molecular, anatomical, and neurophysiological methods to validate the function and cellular localization of candidate genes in the VMN. We propose that the candidate genes and molecular pathways identified here may belong to a shared genetic toolkit for vocal motoneurons in many species that face similar energetic and neurophysiological demands. Thus, our results will inform future comparative studies to achieve a broader understanding of the molecular machinery required for vocalization.

Results and discussion

In order to globally characterize molecular pathways governing vocal motor patterning, we compared the transcriptome of surgically isolated VMN to H tissue at three time points corresponding to high (reproductive summer night) and low (reproductive summer morning and non-reproductive winter night) vocal activity (Fig. 4.1C). In order to minimize activity-induced gene-expression, we used males who had not been humming prior to sacrifice. See Methods, and Figs. 4.1 and 4.2 for explanations of sample groups and analysis pipelines.

Transcriptome assembly, annotation, and qPCR validation

Sequencing using the Illumina HiSeq2000 system yielded approximately 200 million 100 bp reads across all brain groups used here and ear sample groups used for a companion study (Fergus et al., 2015). Over 90% of the raw reads survived quality filtering and trimming, resulting in 21.4 ± 2.8 million (mean ± S.D.) paired-end reads per brain sample. Our initial assembly produced 293,702 contigs, with a mean length of 1006.86±1259.72 bp. After discarding contigs with open reading frames (ORFs) of less than 50 amino acids and lowly supported transcripts (isoforms) with less than 1% mapped reads for the gene (component), the final transcriptome contained 83,967 assembled transcripts, with a mean length of 1713.57±1585.21 bp (range 201-18,637; N50=2647), representing 40,656 gene components across brain and ear sample groups. The transcript length distribution and number of transcripts per gene are shown in Fig. 4.3A and 4.3B. The mean GC content for this filtered transcriptome was 48.22%. Of the 83,967 transcripts, 46,629 (55.5%) contained complete ORFs, comparable to a recent zebra finch transcriptome (Balakrishnan et al., 2014). Additionally, CEGMA (Core Eukaryotic Genes Mapping Approach) analysis of conserved eukaryotic genes (CEGs), determined that our filtered transcriptome contained 453 full-length CEGs of the complete set of 458 CEGs (99%), and 238 of the more-conserved set of 248 CEGs (96%) (Parra et al., 2007; Parra et al., 2009). Blast2GO annotation resulted in 74,000 (88.1%) of our assembled transcripts with significant annotation hits, comparable to or above reported rates [see (Gotz et al., 2008; Huth and Place, 2013; Schunter et al., 2014)]. Seventeen of the top 26 blast hit species were teleost fish, with the top nine all being teleosts (Fig. 4.3C). There were

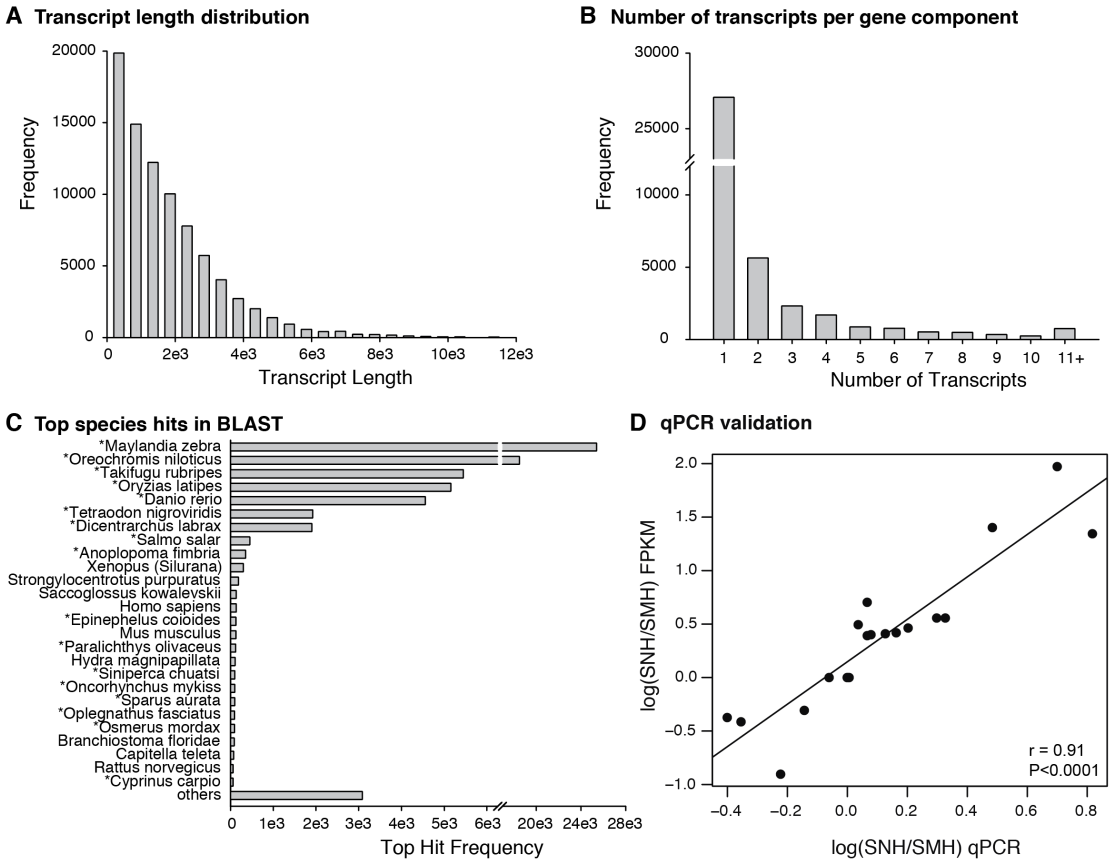

Figure 4.3

Transcriptome assembly quality assessment. A) Transcript length distribution. **B)** Number of transcripts per gene component as determined by Trinity. **C)** Top species hits from BLAST against NCBI's nr database, first nine species are teleost fish sequences out of a total of 17 teleost species within the list, indicated by *. **D)** Quantitative PCR (qPCR) was used to verify transcriptome-derived FPKM values of 19 genes in SNH and SMH tissue groups. Pearson's correlation analysis showed that qPCR and transcriptome measured ratios of SNH/SMH are significantly correlated with each other.

77,285 transcripts, representing 35,983 gene components, expressed in brain samples (>0 counts in at least one brain sample).

Using qPCR, we validated the relative abundances of 19 transcripts from two of the same, pooled H samples that were submitted for Illumina sequencing: reproductive summer morning (SMH) and reproductive summer night (SNH). Our results showed a tight and highly significant correlation between the log-normalized SNH/SMH ratios by qPCR and FPKM (fragments per kilobase of transcript per million reads mapped) (Pearson's $r=0.91$, $P<0.0001$; Fig. 4.3D). Additionally, expression levels of nine candidate genes also showed significant correlation between RNA-seq and qPCR values (see section below). Together, these results validated our transcriptome-predicted abundances and demonstrated the high quality of our *de novo* assembled transcriptome.

VMN versus H tissue comparisons

Overview: In order to identify molecular pathways and candidate genes important for VMN function, we first focused on between-tissue comparisons. The cyclic loess "fastlo" normalization method (Ballman et al., 2004), as opposed to trimmed mean of M values (TMM) normalization (Robinson and Oshlack, 2010), successfully removed the nonlinear tissue-dependent skew (Fig. 4.4A-C), while preserving biologically relevant sample group similarities as seen in the clustering of samples by tissue and season in the multidimensional scaling plot (Fig. 4.4D). By conservatively treating the three sample groups collected at different times as biological replicates from which to estimate transcript-wise dispersion values in edgeR's differential expression analysis

Figure 4.4
Evaluating TMM and fastlo normalization of tissue comparisons. A) Plots of log2(VMN/H) ratios (y axis) versus mean expression across all sample groups (x axis). N = 76,878 genes. Alignment along 0 horizontal is expected. Fitted loess lines are shown in blue. **B)** Histograms of VMN/H mean ratios. Even with peak at 0 indicates good normalization. **C)** Box plots of each sample group. Medians are expected to align along 0 with even distribution about the median across sample groups. RLE: Relative log ratio. **D)** Multidimensional scaling plots showing similarities between VMN (red) and H (black) sample groups. Samples show biologically relevant grouping by tissue and by season. BCV: biological coefficient of variation.

Figure 4.4 (continued)

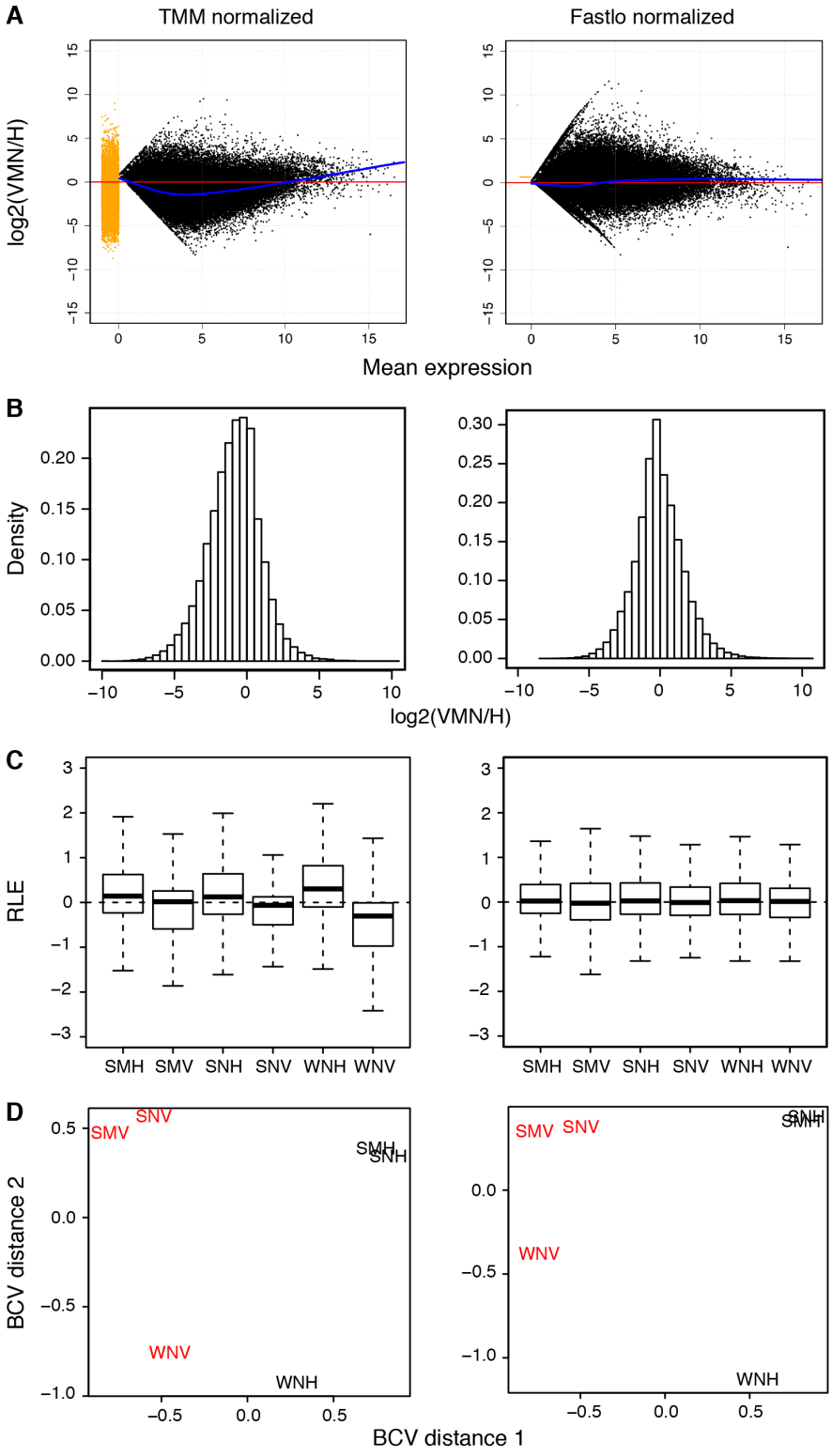

(Robinson et al., 2010), we identified 1,717 transcripts significantly upregulated in H and 2,948 transcripts upregulated in VMN, which were the focus of downstream analyses.

GO term enrichment (Tables 4.1, 4.2): We performed Fisher's exact test on GO terms to identify gene functions that are enriched in VMN or H. By comparing the subset of genes upregulated in VMN to the entire transcriptome, we found 279 over-represented GO terms [see (Feng et al., 2015) for complete list]. The enrichment results overwhelmingly highlighted the importance of ATP production in VMN, with 29% of the enriched GO terms relating to aerobic metabolism. This high metabolic activity in the VMN is exemplified by the 10 most significantly enriched GO terms (Table 4.1). Although few VMN enriched GO terms were related to neural transmission functions, the GO terms "neurotransmitter biosynthetic process" and "choline O-acetyltransferase activity" were enriched, consistent with VMN motoneurons being cholinergic (Brantley and Bass, 1988). Furthermore, we found several enriched GO terms related to steroid hormone signaling, including "gonadotropin secretion", "endocrine hormone secretion", and "sterol biosynthetic process", indicating that the VMN is hormonally active. Finally, GO terms related to post-transcriptional processes were also enriched for VMN, including "translation" (Biological process, Table 4.1), "ribosome" (Cellular component, Table 4.1), "gene expression", and "RNA processing", indicating that VMN is translationally active.

In contrast, 75% of the 130 GO terms enriched in transcripts upregulated in H were related to synaptic function and neurotransmission [see (Feng et al., 2015) for

Table 4.1
Enriched GO terms of genes upregulated in VMN compared to H. Significantly over represented gene ontology (GO) terms found in transcripts upregulated in VMN compared to the surrounding hindbrain. Top 10 GO terms from each GO category (cellular component, biological process, and molecular function) are listed in order of decreasing significance by false discovery rate (FDR).

Table 4.1 (continued)

GO Term	Name	FDR
Biological process		
GO:0006412	Translation	2.90E-18
GO:0006119	Oxidative phosphorylation	3.60E-18
GO:0022900	Electron transport chain	8.20E-18
GO:0042775	Mitochondrial ATP synthesis coupled electron transport	1.60E-17
GO:0042773	ATP synthesis coupled electron transport	1.60E-17
GO:0022904	Respiratory electron transport chain	2.30E-17
GO:0045333	Cellular respiration	2.30E-17
GO:0044283	Small molecule biosynthetic process	3.10E-15
GO:0055114	Oxidation-reduction process	5.10E-15
GO:0044711	Single-organism biosynthetic process	7.40E-15
Molecular function		
GO:0003735	Structural constituent of ribosome	2.30E-17
GO:0016491	Oxidoreductase activity	1.90E-15
GO:0003954	NADH dehydrogenase activity	6.20E-10
GO:0050136	NADH dehydrogenase (quinone) activity	6.20E-10
GO:0008137	NADH dehydrogenase (ubiquinone) activity	6.20E-10
GO:0015078	Hydrogen ion transmembrane transporter activity	1.70E-07
GO:0016655	Oxidoreductase activity, acting on NAD(P)H, quinone or similar compound as acceptor	3.50E-07
GO:0015002	Heme-copper terminal oxidase activity	3.80E-07
GO:0016676	Oxidoreductase activity, acting on a heme group of donors, oxygen as acceptor	3.80E-07
GO:0016675	Oxidoreductase activity, acting on a heme group of donors	3.80E-07
Cellular component		
GO:0005739	Mitochondrion	8.80E-53
GO:0044429	Mitochondrial part	1.20E-22
GO:0044444	Cytoplasmic part	1.70E-21
GO:0005840	Ribosome	2.10E-21
GO:0005743	Mitochondrial inner membrane	4.40E-20
GO:0019866	Organelle inner membrane	6.10E-19
GO:0070469	Respiratory chain	1.50E-16
GO:0005740	Mitochondrial envelope	1.50E-16
GO:0030529	Ribonucleoprotein complex	2.50E-16
GO:0005737	Cytoplasm	3.00E-16

Table 4.2
Enriched GO terms of genes upregulated in H compared to VMN. Significantly over represented gene ontology (GO) terms found in sequences upregulated in the surrounding hindbrain compared to the VMN. Top 10 GO terms from each GO category (cellular component, biological process, and molecular function) are listed in order of decreasing significance by false discovery rate (FDR).

Table 4.2 (continued)

GO term	Name	FDR
Biological process		
GO:0007154	Cell communication	7.30e-15
GO:0044700	Single organism signaling	1.60e-14
GO:0023052	Signaling	1.60e-14
GO:0019226	Transmission of nerve impulse	6.50e-14
GO:0007267	Cell-cell signaling	3.50e-13
GO:0035637	Multicellular organismal signaling	6.90e-13
GO:0007268	Synaptic transmission	1.20e-12
GO:0044699	Single-organism process	1.20e-11
GO:0044763	Single-organism cellular process	7.10e-11
GO:0050877	Neurological system process	3.60e-10
Molecular function		
GO:0005515	Protein binding	3.40e-17
GO:0015291	Secondary active transmembrane transporter activity	1.80e-09
GO:0015293	Symporter activity	4.00e-08
GO:0022804	Active transmembrane transporter activity	6.90e-08
GO:0015075	Ion transmembrane transporter activity	2.70e-07
GO:0015294	Solute:cation symporter activity	4.00e-07
GO:0015081	Sodium ion transmembrane transporter activity	1.20e-06
GO:0022857	Transmembrane transporter activity	1.40e-06
GO:0022891	Substrate-specific transmembrane transporter activity	1.70e-06
GO:0008324	Cation transmembrane transporter activity	4.40e-06
Cellular component		
GO:0031224	Intrinsic to membrane	8.00e-10
GO:0016021	Integral to membrane	5.20e-09
GO:0044425	Membrane part	6.70e-09
GO:0016020	Membrane	2.40e-07
GO:0005886	Plasma membrane	1.70e-06
GO:0030054	Cell junction	8.30e-06
GO:0071944	Cell periphery	1.00e-05
GO:0045202	Synapse	1.60e-04
GO:0097060	Synaptic membrane	3.10e-04
GO:0044456	Synapse part	3.30e-04

complete list]. The top 10 *Biological Process* GO terms were all related to cell signaling and synaptic transmission, the top 10 *Molecular Function* terms were related to membrane transporter activity, and the top 10 *Cellular component* GO terms were related to the synapse or membrane (Table 4.2). The observation that H contains a higher diversity of neurotransmission genes is consistent with H containing diverse motor and non-motor nuclei as well as abundant white matter [see (Bass et al., 1994)] compared to the high homogeneity of motoneurons in VMN. In contrast to VMN, we found no enriched terms related to steroid hormones in H, although "neuropeptide signaling pathway" was enriched.

KEGG (Kyoto Encyclopedia of Genes and Genomes) pathways (Table 4.3): In order to compare the relative representation of biochemical signaling pathways in VMN vs. H, we mapped differentially expressed transcripts to KEGG pathways (Kanehisa et al., 2014) [see (Feng et al., 2015) for complete list]. Transcripts upregulated in VMN mapped predominantly to pathways directly related to ATP production, including "oxidative phosphorylation", "pyruvate metabolism", "citrate cycle (TCA cycle)", and "glycolysis/gluconeogenesis", which is consistent with GO term enrichment results that also indicated high levels of metabolic activity in VMN. Pathways unique to transcripts upregulated in VMN also included those involved in antioxidant defense against oxidative stress, such as "glutathione metabolism" (Wu et al., 2004a), indicating that VMN is capable of combating reactive oxygen species generated by aerobic metabolism. Additionally, we found steroid hormone related pathways ("steroid hormone biosynthesis", "steroid biosynthesis", "steroid degradation"; Table

4.3) that support GO term enrichment results highlighting VMN as a hormonally active nucleus. Transcripts in the "carbon fixation pathways in prokaryotes" found in VMN were confirmed by BLAST to have high identity to transcripts of other fish and likely represent metabolic genes conserved from bacteria through vertebrates. In contrast, transcripts upregulated in H mapped predominantly to phospholipid metabolism and signaling pathways (Table 4.3). Phospholipids are important components of cell membranes and precursors to important secondary messengers such as diacyl glycerol and inositol 1,4,5-triphosphate (Delage et al., 2013).

Together, KEGG pathway and GO term enrichment results showed that VMN is metabolically, hormonally, and post-transcriptionally active. In contrast, transcription in the surrounding hindbrain is devoted to synaptic transmission and membrane processes. It has been estimated that acoustic courtship in ectotherms requires an eight-fold increase from resting metabolic rate (Gillooly and Ophir, 2010; Ophir et al., 2010). Results highlighting the importance of cellular respiration in VMN are consistent with its ability to sustain high frequency firing that drives advertisement hums up to hours (Fig. 4.1A) repetitively throughout a single night of courtship-related activity (Brantley and Bass, 1994; Ibara et al., 1983; McIver et al., 2014). While studies have extensively characterized the high aerobic demands of "superfast" muscles in midshipman and closely related toadfish, among the fastest contracting skeletal muscles in vertebrates (Rome, 2006; Walsh et al., 1995), our results indicate a concomitantly high metabolic demand in the motoneurons that drive these muscles.

Table 4.3
KEGG pathways mapped to transcripts differentially upregulated in VMN vs. H.
Top 10 KEGG (Kyoto Encyclopedia of Genes and Genomes) pathways with the highest number of mapped transcripts that were upregulated in VMN or H. Additionally, we show that more transcripts upregulated in VMN are mapped to glutathione metabolism, steroid and steroid hormone biosynthesis pathways.

VMN		**H**	
Pathway	**# seqs**	**Pathway**	**# seqs**
Purine metabolism	60	Phosphatidylinositol signaling system	19
Pyrimidine metabolism	29	Glycerophospholipid metabolism	15
Oxidative phosphorylation	28	Purine metabolism	12
Aminoacyl-tRNA biosynthesis	25	Lysine degradation	12
Carbon fixation pathways in prokaryotes	16	Glycerolipid metabolism	11
Pyruvate metabolism	16	T cell receptor signaling pathway	9
Valine, leucine and isoleucine degradation	14	Inositol phosphate metabolism	7
Citrate cycle (TCA cycle)	13	Alanine, aspartate and glutamate metabolism	4
Porphyrin and chlorophyll metabolism	13	Arginine and proline metabolism	3
Glycolysis / Gluconeogenesis	13	Fatty acid biosynthesis	3
Glutathione metabolism	11	Glutathione metabolism	0
Steroid hormone biosynthesis	7	Steroid hormone biosynthesis	0
Steroid biosynthesis	5	Steroid biosynthesis	0
Steroid degradation	3	Steroid degradation	0

Gene category analyses (Figs. 4.5, 4.6): Guided by the above results and previous studies of VMN characteristics, we wanted to compare expression levels of transcripts belonging to different functional categories with significant implications for cellular and network level excitability. Thus, regardless of differential expression, we selectively analyzed transcripts belonging to the following functional categories: neurotransmission (ion channels and neurotransmitter receptors), neuroendocrine (genes related to steroid and thyroid hormone function), neuropeptides, neuromodulators, cellular respiration, and antioxidants (Figs. 4.5 and 4.6) [see Additional file 1, Table S4 in (Feng et al., 2015) for complete list of transcripts in each category].

While the overall pool of expressed transcripts was smaller in VMN than in H (Chi squared test, $P<0.0001$) (Fig. 4.5A), transcript abundances were comparable between tissues in most gene categories (Fig. 4.5B). Two exceptions were cellular respiration, which had significantly higher expression in the VMN (ANOVA, $F=30.84$, $P<0.0001$), and neurotransmission, which had significantly higher expression in the H (ANOVA, $F=12.07$, $P=0.0005$) (Fig 4.5B,C), substantiating our interpretations of GO term enrichment results as discussed above (Tables 4.1-2).

Pairwise Spearman correlation analyses revealed that overall, cellular respiration had the highest correlation between sample groups (Fig. 4.6). Because the Spearman coefficient is derived from calculating the Pearson correlation of transcript abundance ranks between two samples, these results demonstrate that although cellular respiration expression levels were higher in VMN (Fig. 4.5), the relative abundances of transcripts to one another is conserved across sample groups (Fig. 4.6). In contrast,

Figure 4.5
Tissue comparison of functional category expression. A) Raw counts from the brain transcriptome were dichotomized into expressed (1, gray) or not expressed (0, black) based on the summed tissue values. Compared to VMN, H has significantly more expressed genes. Chi sq: Chi squared test. **B)** Normalized abundances for each unique transcript expressed were summed from VMN or H sample groups, box-cox transformed, and a generalized linear model compared expression levels by tissue, gene category, and their interaction. Cellular respiration transcripts had significantly higher expression in the VMN while neurotransmission transcripts were higher in H. **** P<0.0001, *** P=0.0005. **C**) Mean VMN vs. H expression levels (fastlo-normalized) of transcripts within each of the six gene categories (black triangles) are plotted on top of all transcripts (gray dots). N: number of transcripts in each category. Cell res: cellular respiration; Antiox: antioxidants; Neurotrans: neurotransmission; Neuroendo: neuroendocrinology; Neuropep: neuropeptide; Neuromod: neuromodulators.

Figure 4.5 (continued)

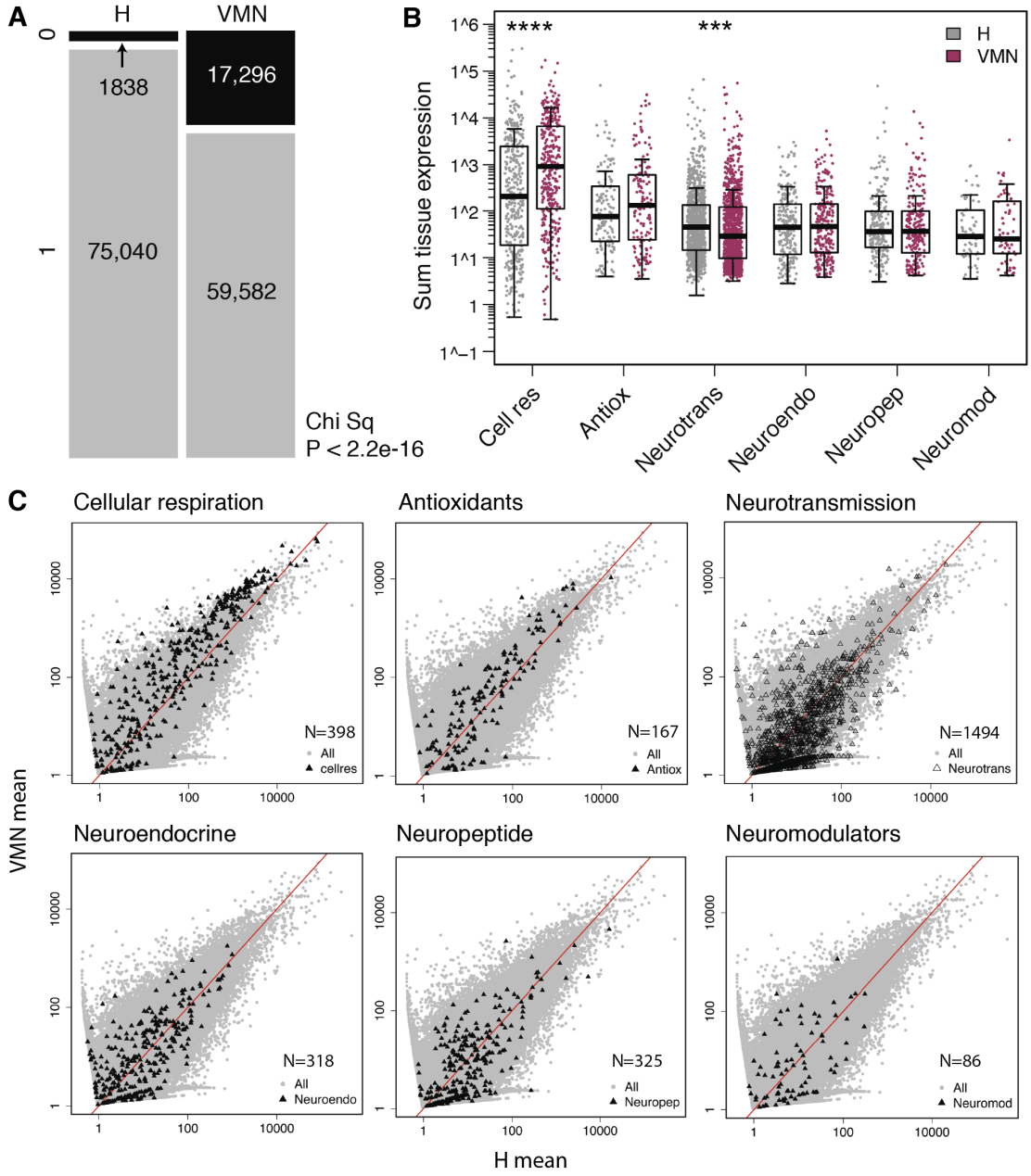

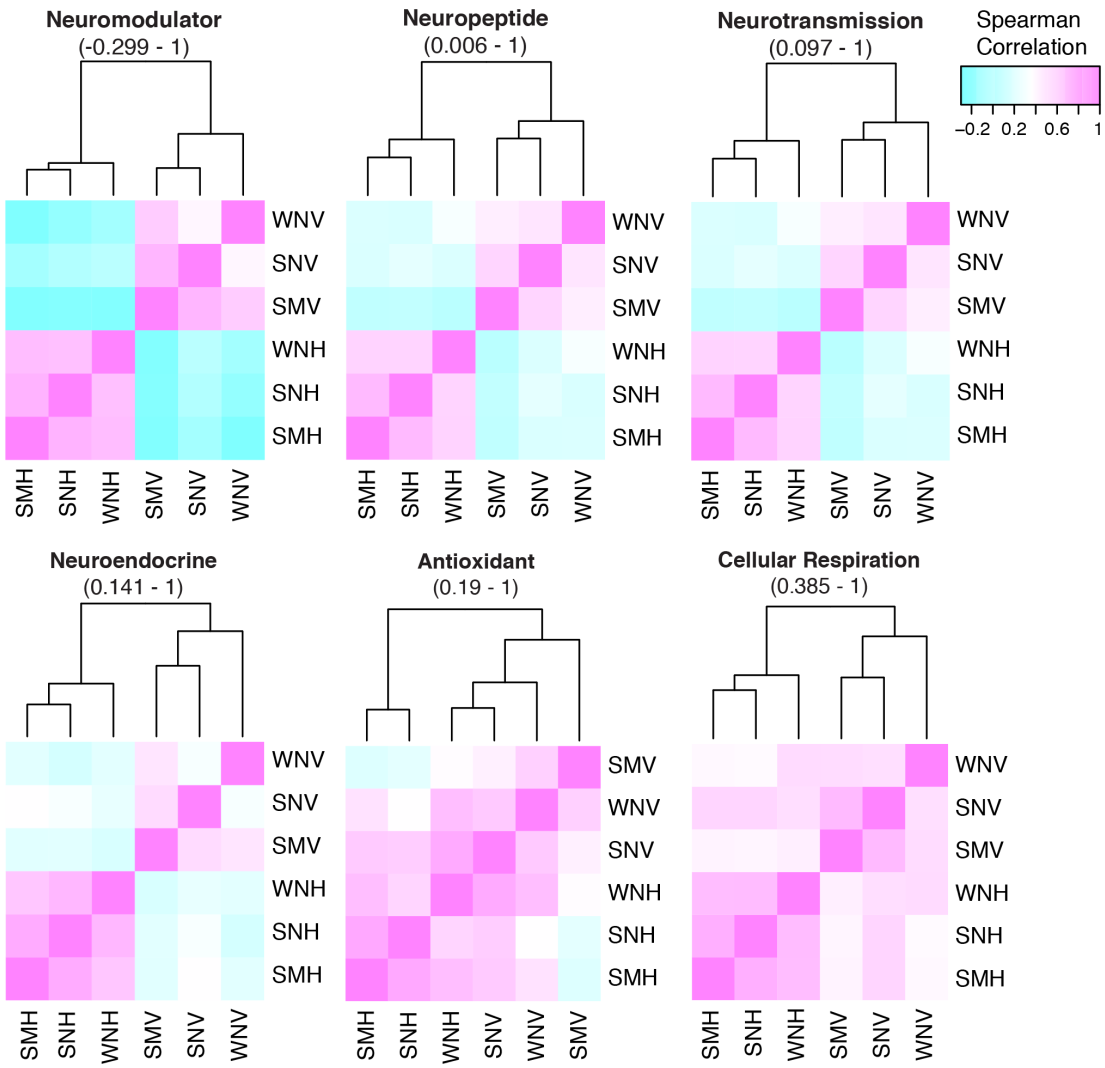

Figure 4.6
Spearman correlation heatmaps of functional gene categories. Heatmaps are generated from Spearman correlation coefficients (rho) for each pair of samples based on TMM-normalized FPKM values. Values in parenthesis are the ranges of rho.

the other functional categories, especially neuromodulators, showed lower correlation between VMN and H (Fig. 4.6).

Candidate genes (Fig. 4.7; Table 4.4): Supporting the hypothesis that VMN expresses a unique molecular toolkit dedicated to vocal motor coding, the majority of functionally important transcripts upregulated in VMN (Table 4.4) were unique from those upregulated in H [see Additional file 1, Table S5 in (Feng et al., 2015)]. Among the transcripts significantly upregulated in the VMN relative to H (Fig. 4.7A), we identified those with neurotransmission functions, including ligand- and voltage-gated ion channels as well as metabotropic neurotransmitter receptors (Table 4.4). We also identified transcripts with neuroendocrine functions, including steroid signaling and biosynthesis, neuropeptides and peptide hormones, and other neuromodulators (Table 4.4). Neurotransmission and neuroendocrine functions were the focus because of relevance to neural excitability and previous midshipman studies focusing on these mechanisms.

Candidate Neurotransmission Genes: VMN's synchronous and temporally precise activity is dependent on both synaptic interactions of the network as well as intrinsic properties of individual motoneurons (Chagnaud et al., 2012). There were 57 transcripts with 34 unique neurotransmission gene annotations upregulated in the VMN (Table 4.4). These candidate genes included those supporting two of VMN's major network components: electrical synapses formed by gap junctions and GABAergic inhibition (Chagnaud et al., 2012), both of which are also prominent mechanisms promoting network-level synchrony in other systems

Table 4.4
Functionally important candidate genes upregulated in VMN. Gene descriptions with neurotransmission, neuroendocrine, and antioxidant functions from transcripts upregulated in VMN compared to surrounding hindbrain. Genes that are mentioned in the text or shown in figures have gene symbols in parentheses.

Table 4.4 (continued)

Neurotransmission
Anoctamin-5-like isoform x4
ATP-sensitive inward rectifier potassium channel 8-like
Calcium-activated potassium channel subunit alpha-1-like (*kcnma1*) isoform 3
Gamma-aminobutyric acid receptor subunit alpha-3-like (*gabra3*)
Gamma-aminobutyric acid receptor subunit alpha-5-like (*gabra5*)
Gamma-aminobutyric acid receptor subunit pi-like (*gabrp*)
Gamma-aminobutyric acid type b receptor subunit 1-like
Gap junction beta-6 (*cx30*)
Glutamate ionotropic kainate 3-like
Glutamate ionotropic kainate 5-like
Glutamate receptor delta-1 subunit-like
Glycine receptor subunit beta
Glycine receptor subunit beta-like
Kv channel-interacting protein 4-like
Muscarinic acetylcholine receptor m2 (*chrm2*)
Neuronal acetylcholine receptor subunit alpha-2-like (*chrna2*)
Neuronal acetylcholine receptor subunit alpha-3-like
Neuronal acetylcholine receptor subunit alpha-9-ii-like
Neuronal acetylcholine receptor subunit beta-2-like
Neuronal acetylcholine receptor subunit non-alpha-3-like (*chrnb3*)
Potassium sodium hyperpolarization-activated cyclic nucleotide-gated channel 2-like
Potassium voltage-gated channel subfamily b member 2 (*kcnb2*/Kv2.2)
Potassium voltage-gated channel subfamily c member 3-like (*kcnc3*/Kv3.3) isoform x1
Potassium voltage-gated channel subfamily e member 1-like
Potassium voltage-gated channel subfamily h member 5
Potassium voltage-gated channel subfamily kqt member 2-like (*kcnq2*/Kv7.2)
Potassium voltage-gated channel subfamily s member 1-like (*kcns1*/Kv9.1)
Potassium voltage-gated channel subfamily s member 3-like
Sodium channel protein type 5 subunit alpha
Sodium channel subunit beta-4-like
Transient receptor potential cation channel subfamily m member 2-like
Two pore calcium channel protein 1-like
Voltage-dependent l-type calcium channel subunit alpha-1f-like
Voltage-dependent r-type calcium channel subunit alpha-1e
Voltage-gated potassium channel subunit beta-1 isoform 1 (*kcnab1*)
Voltage-gated potassium channel subunit beta-2-like isoform 1

Table 4.4 (continued)
Steroid pathway
3-keto-steroid reductase-like (*hsd17b7*)
Androgen receptor alpha (*ar-a*)
Androgen-induced gene 1 protein
Dihydroxyvitamin d 24- mitochondrial-like isoform 1
Estrogen receptor beta 2 (*esr2*)
Estrogen-related receptor alpha
Hydroxysteroid 11-beta-dehydrogenase 1-like (*hsd11b1l*)
Lanosterol 14-alpha demethylase-like
Ovarian aromatase (*cyp19a1a*)
Sterol regulatory element-binding protein 1
Sterol regulatory element-binding protein 2
Neuropeptides/peptide hormones
Atrial natriuretic peptide-converting enzyme-like
Calcitonin gene-related peptide precursor
Cholecystokinin type a receptor
Growth hormone receptor
Inhibin beta b chain-like
Insulin gene enhancer protein isl-1
Insulin-like growth factor binding protein 1
Insulin-like growth factor i
Neuropeptide b precursor
Peptide yy-like
Pituitary adenylate cyclase-activating polypeptide type i receptor-like
Vasoactive intestinal polypeptide receptor 1-like
Thyroid hormone
Thyroid hormone receptor alpha
Thyroid hormone receptor-associated protein 3-like
Thyroid receptor-interacting protein 6-like
Other neuromodulators
Adenosine receptor a1-like
D-like dopamine receptor-like (*drd2*)
Melatonin receptor type 1a-like
Prostaglandin e synthase 2-like
Prostaglandin f2-alpha receptor-like
Antioxidants
Cu/Zn superoxide dismutase (*sod1*)
Glutaredoxin 3
Glutaredoxin-related protein 5

Table 4.4 (continued)
Glutathione peroxidase 4b (*gpx4b*)
Glutathione s-transferase (*gst*)
Peroxiredoxin 6
Thioredoxin domain-containing protein 17
Thioredoxin-dependent peroxide mitochondrial precursor
Thioredoxin-like protein 1
Thioredoxin-like protein 4a

Figure 4.7
Candidate functional genes from tissue comparisons for qPCR. A) MA plot showing log2 VMN/H mean ratios by average expression level for each transcript. Mean values were calculated from the three sample groups for each tissue. Transcripts with positive log ratios are higher in VMN, while transcripts with negative log ratios are higher in H. The numbers of significantly upregulated transcripts for each tissue are shown in parentheses. Red dots indicate significantly differentially expressed transcripts in VMN or H. Blue lines indicate log2 values of +/- 2, representing fold-change of 4. **B)** Nine candidate genes that were chosen for qPCR verification are plotted on top of a scatter plot of VMN mean vs. H mean values for all transcripts, calculated from the three sample groups for each tissue. Number of differentially expressed isoforms per gene is indicated in parentheses. Dark gray dots are significantly differentially expressed transcripts in VMN or H. The line of unity is in red. **C)** Correlation of SMV/SMH ratios derived from qPCR data or fastlo-normalized RNAseq data. For RNAseq data, ratios were calculated from the average expression of all isoforms within a gene component. Linear regression line is in black. **D)** qPCR validation of SMV and SMH expression for the candidate genes showed significant upregulation of candidate genes in SMV.

Figure 4.7 (continued)

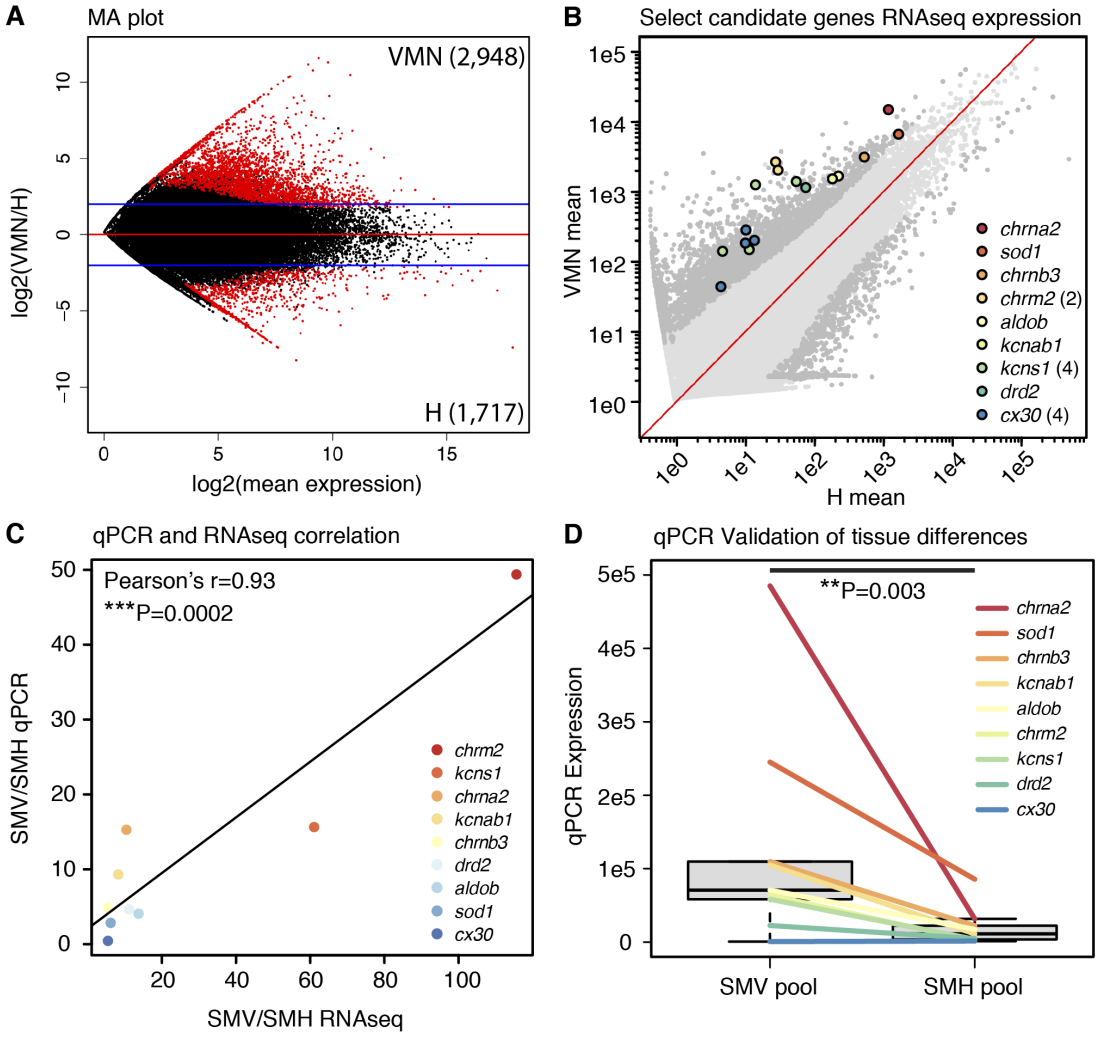

(Bartos et al., 2007; Pereda, 2014). The presence of elevated gap junction subunit expression in VMN (Table 4.4) affirmed previous evidence of electrotonic coupling in VMN, demonstrated by electron microscopy (Bass and Marchaterre, 1989), transneuronal dye diffusion (Bass et al., 1994; Chagnaud et al., 2012), and intracellular neurophysiology (Chagnaud et al., 2012). The multiple GABA receptor subunits upregulated in VMN (Table 4.4) likely provide the prominent network-dependent afterhyperpolarization observed in VMN motoneurons, supported by the pharmacological blocking of $GABA_A$ receptors that severely reduced the duration and amplitude of VMN output (Chagnaud et al., 2012).

VMN's intrinsic neuronal properties are likely mediated by several voltage-gated potassium channel (KCN/Kv) subunits that have known functions in controlling neuronal excitability [Table 4.4; we report potassium channel gene names by both the KCN and Kv nomenclature systems (Gutman et al., 2003; Judge and Bever, 2006)]. First, VMN showed increased expression of *potassium voltage-gated channel subfamily c member 3-like* (*kcnc3*/Kv3.3) subunits (Table 4.4), which contributes significantly to action potential repolarization and recovery of sodium channels from inactivation [e.g. (Ding et al., 2011)], permitting high-frequency repetitive firing that is a key feature of VMN motoneurons (Chagnaud et al., 2012). Second, it has been shown that while nonfunctional alone, KCNS1/Kv9.1 subunits decrease KCNB1/Kv2.1 currents when coassembled in heteromeric channels, which was modeled to increase the firing fidelity of a simulated neuron to a 100 Hz stimulus (Richardson and Kaczmarek, 2000). The potential interaction of our candidate *potassium voltage-gated channel subfamily s member 1-like* (*kcns1*/Kv9.1) and

potassium voltage-gated channel subfamily b member 2 (*kcnb2*/Kv2.*2*) subunits (Table 4.4) may therefore regulate VMN firing frequency that directly determines the pulse repetition rate and fundamental frequency of natural vocalizations (Bass and Baker, 1990). KCNS1/Kv9.1 subunits also decrease the conductance of KCNC/Kv3 subunits, mentioned above, when they form heteromeric channels (Stocker et al., 1999). Third, channels composed of *potassium voltage-gated channel subfamily kqt member 2-like* (*kcnq2*/Kv7.2) subunits, also elevated in VMN (Table 4.4), dampen neural excitability by being partially activated at resting membrane potentials (Brown, 1988). We propose *kcnq2*/Kv7.2 underlies the low baseline excitability of VMN neurons, which contributes to their ability to fire with high fidelity to presynaptic input (Chagnaud et al., 2012) from the vocal pacemaker nucleus that sets call frequency (Chagnaud et al., 2011). In the fully aquatic frog *Xenopus laevis*, male laryngeal motoneurons that drive vocalizations also have a strong low-threshold potassium current (Yamaguchi et al., 2003), leading to the hypothesis that low intrinsic excitability conferred by high *kcnq2*/Kv7.2 expression may be a shared feature of vertebrate vocal motoneurons.

Although we identified transcripts of candidate neurotransmission genes predicted *a priori* to be important for VMN function, we also found candidates previously not well studied in this system. One example is evidence of cholinergic input to VMN, supported by choline acetyltransferase staining of somata in the vocal premotor pacemaker region of midshipman [(Brantley and Bass, 1988), A. Bass, unpub observ], that has potentially significant contributions to VMN function. The alpha and beta subunits of neuronal nicotinic receptors found in our candidate list

(Table 4.4) could mediate fast, postsynaptic action of acetylcholine (Grove et al., 2011), or modulation of presynaptic neurotransmitter release, including GABA (McMahon et al., 1994), shown to play a prominent role in regulating VMN output (see above). Furthermore, evidence from other motor systems indicates cholinergic control of motoneuron excitability and firing frequency (Bellingham and Berger, 1996; Miles et al., 2007; Zagoraiou et al., 2009), including actions mediated via postsynaptic muscarinic receptors and KCNB1/Kv2.1 potassium channels (Bellingham and Berger, 1996; Hellström et al., 2003; Miles et al., 2007; Muennich and Fyffe, 2004), transcripts of which were elevated in VMN: *muscarinic acetylcholine receptor m2* (*chrm2*) and *kcnb2*/Kv2.2 (Table 4.4). Another target of muscarinic modulation is the KCNQ/Kv7 family of voltage gated potassium channels that decrease baseline neural excitability, of which *kcnq2*/Kv7.2 is found among our candidates (discussed above; Table 4.4) (Brown, 1988).

Importantly, many of the candidate ion channels we note above are ideal targets for pharmacological validation using selective blockers [e.g. see (Brown and Passmore, 2009) for *kcnq2*/Kv7.2 blockers; (Ding et al., 2011) for *kcnc*/Kv3 blockers; (Judge and Bever, 2006) for other potassium channel blockers; (Caulfield and Birdsall, 1998) for muscarinic and (Luetje et al., 1993; McIntosh et al., 2002) for neuronal nicotinic acetylcholine receptor blockers; (Chambers et al., 2003) for *gabra5* blocker]. It is also worth highlighting that both *kcns1*/Kv9.1 and *kcnq2*/Kv7.2 mRNA levels were elevated in four major telencephalic song control nuclei in the zebra finch (Lovell et al., 2013), with *kcns1*/Kv9.1 showing additional label in the tracheosyringeal division of the hypoglossal motor nucleus (nXIIts) (see the ZEBrA

database, Oregon Health & Science University, Portland, OR 97239; http://www.zebrafinchatlas.org), the brainstem region representing VMN's analogue, if not homologue [see (Bass and Chagnaud, 2012)].

Candidate Neuroendocrine and Neuromodulator Genes: Both behavioral and neurophysiological studies have shown that steroids exert rapid and robust effects on vocal behavior and the output of the vocal CPG via classical steroid receptors in midshipman and a closely related toadfish species [e.g. (Remage-Healey and Bass, 2004; Remage-Healey and Bass, 2006a)]. Consistent with these studies, steroid receptors *androgen receptor alpha* (*ar-a*) and *estrogen receptor beta 2* (*esr2*) were both upregulated in the VMN (Table 4.4). The estradiol synthetic enzyme *ovarian aromatase* (*cyp19a1a*) was upregulated in the VMN (Table 4.4), consistent with previous studies showing dense aromatase protein and mRNA expression in a dorsal layer of glial cells that surrounds and projects throughout the VMN (Forlano et al., 2001). The steroidogenic enzyme *3-keto-steroid reductase-like* (*hsd17b7*), responsible for the interconversion between estrone and estradiol (Labrie et al., 2000), was also elevated in the VMN (Table 4.4). Additionally, we found higher VMN expression of *hydroxysteroid 11-beta-dehydrogenase 1-like* (*hsd11b1l*), a crucial enzyme that converts 11-beta-hydroxytestosterone to 11-ketotestosterone, and cortisol to the inactive metabolite cortisone (Kusakabe et al., 2003) (Table 4.4). 11-ketotestosterone and cortisol are the major circulating androgen and glucocorticoid, respectively, in type I male midshipman that are the source of tissues used here [see (Genova et al., 2012)], and cause a rapid increase in vocal CPG output duration within five minutes of systemic injection (Remage-Healey and Bass, 2004; Remage-Healey and Bass,

2006b). Thus, many of the candidate neuroendocrine transcripts upregulated in VMN have direct relevance to VMN function as corroborated by prior studies.

Additionally, we found previously under-studied neuroendocrine or neuromodulatory signaling pathways in VMN, including growth hormone, thyroid hormone, prostaglandin and dopamine, the latter of which is consistent with dense catecholaminergic input to VMN (Forlano et al., 2014) (Table 4.4). One intriguing example is *Prostaglandin f2-alpha receptor-like*, because Prostaglandin f2-alpha is a potent sex pheromone that induces spawning behavior in fish (Stacey, 2003), though little is known about its effects on vocal behavior.

Together, the steroid signaling candidate genes indicate that VMN exhibits high androgen and estrogen sensitivity by expressing steroid receptors and steroidogenic enzymes, consistent with prior studies showing their anatomical localization to VMN and influence on vocal CPG output [e.g. (Fergus and Bass, 2013; Forlano et al., 2005)]. VMN function is also likely modulated by candidate gene products belonging to novel neuroendocrine and neuromodulatory pathways identified here.

Based on the enrichment of cellular respiration genes being upregulated in VMN, expected to generate harmful reactive oxygen species (Davies, 2000), we hypothesized that the VMN combats oxidative stress by expressing high levels of antioxidant enzymes and proteins. Supporting this hypothesis, we found the increased expression of several antioxidant genes in the VMN compared to H (Table 4.4). Notably, these included the well-studied *Cu/Zn superoxide dismutase (sod1)* enzyme (Fig. 4.7B,C; Table 4.4), which catalyzes the conversion of two superoxide radicals

into hydrogen peroxide (Davies, 2000). The importance of *sod1* in motoneuronal function is demonstrated by human *sod1* mutations that lead to the motoneuron degenerative disease amyotrophic lateral sclerosis (ALS) (Cozzolino et al., 2012; Lin and Beal, 2006). The suite of antioxidants upregulated in VMN also included enzymes that produce or utilize glutathione for reducing reactive oxygen species, such as *glutathione s-transferase* (*gst*), which synthesizes glutathione (Wu et al., 2004b), and *glutathione peroxidase 4b* (*gpx4b*), which detoxifies hydrogen peroxide (Davies, 2000) (Table 4.4). These results support our hypothesis that the VMN must combat oxidative stress incurred by high rates of cellular respiration resulting from prolonged activity (Brantley and Bass, 1994; Ibara et al., 1983; McIver et al., 2014). Because the fish used in this study were not actively engaged in vocal activity at the time of sacrifice (see Methods), these results highlight a constitutive feature of the VMN. Based on the implication of antioxidant enzymes and proteins in motoneuron and neural degenerative diseases (Lin and Beal, 2006), we believe the VMN is a motor nucleus capable of withstanding extreme oxidative stress and therefore a useful model for studying the relationship between antioxidants and neural function.

Candidate gene qPCR validation (Fig. 4.7): We chose nine candidate genes upregulated in VMN to validate expression levels with qPCR (Fig. 4.7C). We used the same, pooled SMV and SMH RNA for generating our RNA-seq libraries to validate our findings of upregulated transcripts in the VMN. There was a high correlation of expression levels of all nine candidate genes measured by the two methods (SMV: Pearson's $r=0.97$, $P<0.0001$; SMH: Pearson's $r=0.89$, $P=0.0002$) (Appendix Fig. S1).

Similarly, SMV/SMH fold changes calculated from qPCR correlated significantly with RNA-Seq derived fold changes (Pearson's r=0.93, P=0.0002) (Fig. 4.7C). Finally, in concordance with RNA-seq results, qPCR expression levels of candidate genes were significantly higher in SMV when compared to SMH (t=4.22, P=0.003) (Fig. 4.7D). The only gene not showing the expected pattern, *cx30*, had 20 assembled isoforms and had the lowest expression among the tested candidates (Fig. 4.7D). Altogether, qPCR results largely supported RNA-seq results.

Seasonal and daily variation in the VMN

Overview: We aimed to identify functionally important candidate genes whose expression levels change on a daily or seasonal basis. Hierarchical clustering of differentially expressed transcripts revealed that sample groups were most divergent across tissues (H vs. VMN samples) and reproductive state (reproductive summer vs. non-reproductive winter) (Appendix Fig. S2A), consistent with the above results (Fig. 4.4D). Furthermore, the Spearman correlation matrix showed higher within-tissue differences in the VMN than in the H (Appendix Fig. S2B). Significantly differentially expressed transcripts were separated into 109 K-means clusters, from which we identified clusters showing seasonal and daily expression patterns (Fig. 4.8A) with upregulated expression in: all summer reproductive samples ("All-Summer": SMV, SNV, SMH and SNH), summer VMN samples ("VMN-Summer": SMV and SNV), or SNV ("Peak-SNV").

Figure 4.8
K-means clusters showing seasonal and daily patterns of gene expression. A) Representative k means clusters showing upregulation in all summer sample groups, VMN summer groups, and peak expression in summer night VMN (SNV; see Fig. 4.1C for other abbreviations). Total transcript numbers for each K-means cluster expression pattern are shown next to the cluster type names used in the text. **B)** FPKM expression levels are plotted for our candidate ion channels exhibiting peak expression in SNV. *chrnb2*: neuronal acetylcholine receptor subunit beta-2; *gabrp*: gamma-aminobutyric acid receptor subunit pi; *cx30*: connexin 30/gap junction beta-6; *kcnma1* (or Kca1.1): calcium-activated potassium channel subunit alpha-1

Figure 4.8 (continued)

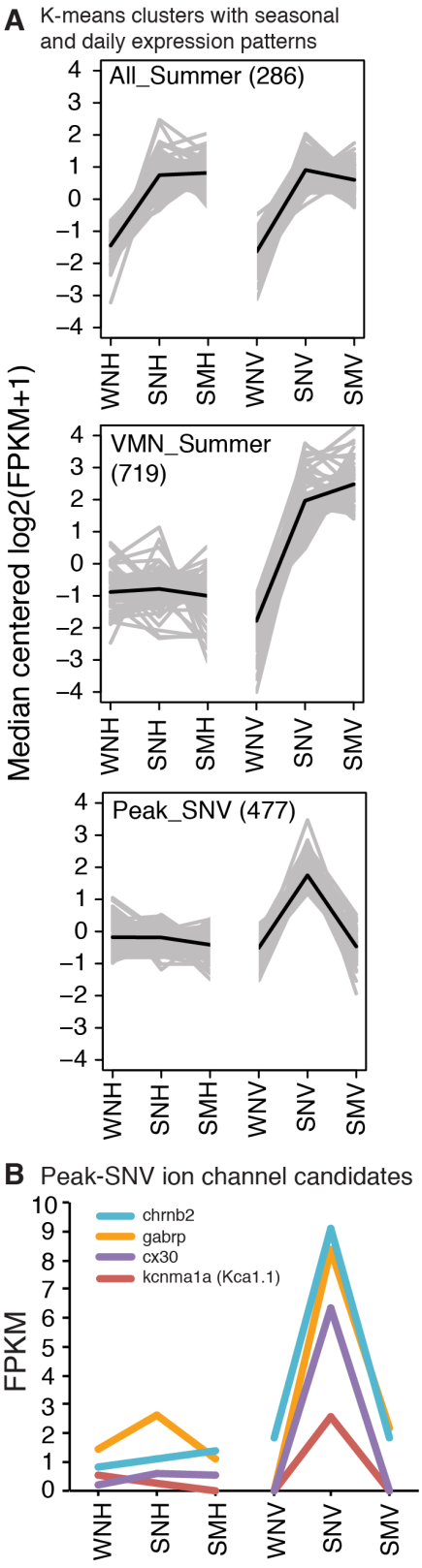

Candidate genes (Fig. 4.8; Table 4.5): We found evidence for daily and seasonal regulation of candidate genes for specific ion channel subtypes as well as steroidogenic enzymes and receptors belonging to major hormone signaling pathways previously implicated in regulating seasonal and daily cycles of vocal motor excitability and behavior in midshipman.

Seasonal comparisons (Fig. 4.8; Table 4.5): We first focused on finding candidate genes in All-Summer and VMN-Summer clusters (Fig. 4.8A) that would contribute to known VMN neurophysiological properties (Fig. 4.9). Neurotransmission related transcripts in All-Summer clusters included the *gap junction alpha 1* (*cx43*) that was unique to All-Summer when compared to All-Winter clusters (Table 4.5). Among the ion channel subunit genes upregulated in VMN-Summer clusters were *cx30*, excitatory ionotropic glutamate receptors, inhibitory glycine receptors, voltage-gated potassium channel subunits, and a *transient receptor potential cation channel subfamily M member 7* (*trpm7*) (Table 4.5). Interestingly, *trpm7*, which encodes a protein with both channel and kinase functions and is involved in regulating intracellular Ca^{2+} and Mg^{2+} levels, has been implicated in Guamanian ALS and Parkinson's dementia (Hermosura et al., 2005).

All-Summer clusters also contained a *potassium voltage-gated channel subfamily c member 4-like* (*kcnc4*/Kv3.4) transcript (Table 4.5). Like the functional attributes of the *kcnc3*/Kv3.3 subunit discussed in the tissue comparisons section, potassium channels composed of KCNC4/Kv3.4 subunits could contribute to VMN's ability to fire repetitively at high frequencies (Table 4.5, Fig. 4.9). As also mentioned

Table 4.5
Functionally important candidate genes showing seasonal regulation

Cluster pattern	Blast2GO description
Neurotransmission	
Peak-SNV	Anoctamin-10-like isoform x1
Peak-SNV	Anoctamin-10-like isoform x4
Peak-SNV	ATP-sensitive inward rectifier potassium channel 8-like
Peak-SNV	Calcium-activated potassium channel subunit alpha-1-like (*kcnma1*/Kca1.1) isoform x1
Peak-SNV	Calcium-activated potassium channel subunit alpha-1-like (*kcnma1*/Kca1.1) isoform x4
Peak-SNV	GABA receptor subunit pi-like (*gabrp*)
All-Summer	Gap junction alpha 1 (*cx43*)
VMN-Summer, Peak-SNV	Gap junction beta 6 (*cx30*)
VMN-Summer	Glutamate ionotropic kainate 4
All-Summer	Glycine receptor subunit beta
VMN-Summer	Glycine receptor subunit beta-like
VMN-Summer, Peak-SNV	Neuronal acetylcholine receptor subunit alpha-3-like
Peak-SNV	Neuronal acetylcholine receptor subunit beta-2-like (*chrnb2*)
All-Summer	Potassium voltage-gated channel subfamily c member 4-like (*kcnc4*/Kv3.4)
VMN-Summer	Potassium voltage-gated channel subfamily h member 5-like
VMN-Summer	Potassium voltage-gated channel subfamily kqt member 2-like (*kcnq2*/Kv7.2)
All-Summer	Sodium channel protein type 8 subunit alpha-like
VMN-Summer	Sodium channel subunit beta-4-like
VMN-Summer	Transient receptor potential cation channel subfamily m member 7-like (*trpm7*)
VMN-Summer	Two pore calcium channel protein 1-like
Steroid receptors and metabolic enzymes	
VMN-Summer	3-keto-steroid reductase-like
All-Summer	Androgen receptor alpha (*ar-a*)
VMN-Summer	Androgen-induced gene 1
All-Summer	Cholesterol 25-hydroxylase-like protein member 1-like
Peak-SNV	Estrogen receptor alpha (*esr1*)
VMN-Summer	Glucocorticoid receptor (*nr3c1*)
VMN-Summer	Hydroxysteroid dehydrogenase-like protein 2
VMN-Summer	Neutral cholesterol ester hydrolase 1-like

Table 4.5 (continued)	
VMN-Summer	Oxysterol-binding protein 10 isoform 1
VMN-Summer	Oxysterol-binding protein 8-like
Peak-SNV	Oxysterol-binding protein 9-like isoform 3
Peak-SNV	Sterol 26- mitochondrial-like
Peptide hormones and receptors	
VMN-Summer, All-VMN	Calcitonin gene-related peptide precursor
Peak-SNV	Growth hormone receptor
All-Summer	Growth hormone-regulated tbc protein 1-a-like
VMN-Summer	Insulin gene enhancer protein isl-2a-like
All-Summer	Insulin receptor-like
VMN-Summer	Insulin-like growth factor-binding protein 1-like
VMN-Summer	Opioid growth factor receptor-like
VMN-Summer	Parathyroid hormone/parathyroid hormone-related peptide receptor-like
Melatonin	
All-Summer	Acetylserotonin o-methyltransferase-like

Figure 4.9

Summary of proposed candidate genes as molecular basis of known VMN properties. A) Known VMN neurophysiological properties. Extreme temporal precision of motoneuron firing is demonstrated by superimposed traces from an intracellular recording (bottom, red) and corresponding VN recording (top, purple) [adapted from (Chagnaud et al., 2012)]. Numbers 1-5 correspond to intrinsic neuronal and network VMN properties listed in C. **B)** Schematic of known VMN neuroanatomical properties. Most of the motoneuron somata appear gray with subsets of red and black somata to highlight properties that are representative of the entire VMN. Glial expression of aromatase (Forlano et al., 2001) and androgen receptor beta (Forlano et al., 2010) is depicted in blue and orange. One of the black somata in the left VMN also depicts each motoneuron's dendritic arbor that branches throughout each of the midline pair of motor nuclei and a single unbranched axon that exits via the ipsilateral vocal nerve (VN) [see (Chagnaud et al., 2012)]. The subsection of dense GABAergic innervation by cells lying outside of the VMN is also representative of the entire VMN. Abbreviations: AR: androgen receptor; ER: estrogen receptor; GABA: gamma-aminobutyric acid. **C)** For the suite of VMN properties, we identified corresponding transcripts that were significantly upregulated in the VMN compared to the surrounding hindbrain, and provide substantiating evidence from previous midshipman studies. Abbreviations: *ar-a*: androgen receptor alpha; *esr*: estrogen receptor; *cyp19a1a*: aromatase; *nrc3c1*: glucocorticoid receptor; *cx*: connexin (gap junction); AP: action potential; *kcn*: voltage-gated potassium channels; AHP; afterhyperpolarization; *gabra*/GABAaR: $GABA_A$ receptor; ICC: immunocytochemistry; *chrm2*: muscarinic acetylcholine receptor m2. *indicates kcn subunits known to regulate the function of subunits listed in the row above.

Figure 4.9 (continued)

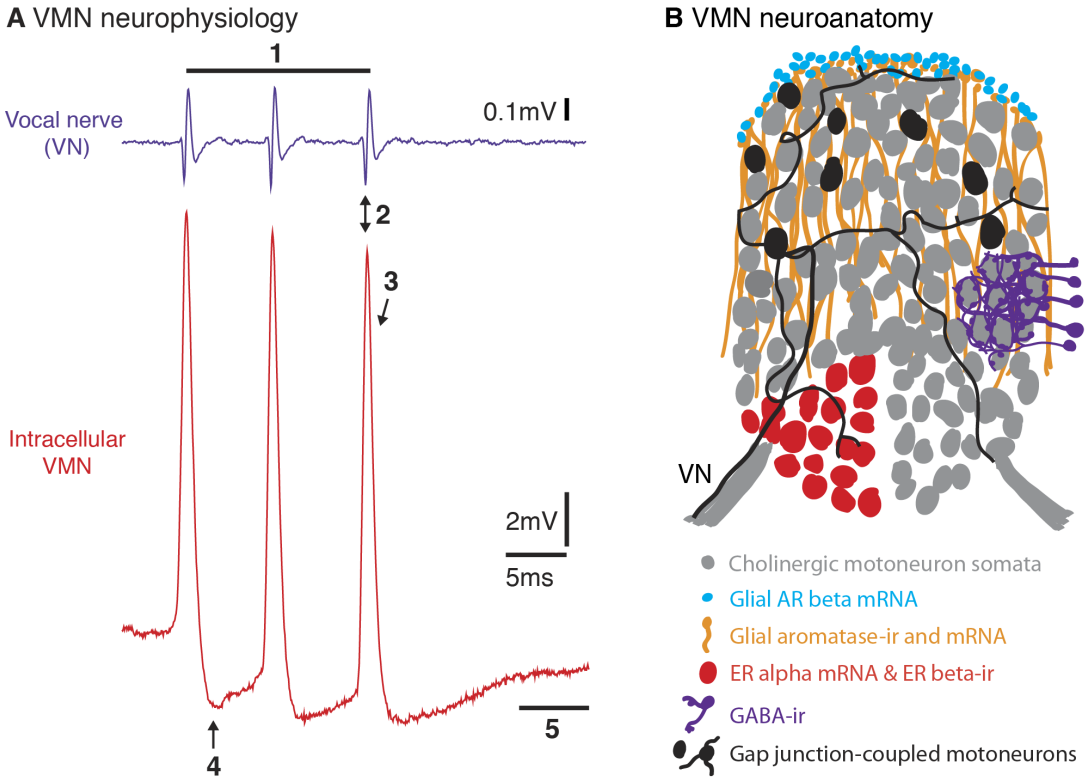

C Proposed candidate genes for VMN function

	VMN neurophysiology	Candidate genes	Corroborating evidence from VMN neurophysiology & anatomy
1	Steroid hormone action modulates duration of VMN output	*ar-a, esr1, esr2, cyp19a1a, nr3c1*	In-vivo neuropharmacology Field behavior Anatomical localization Quantitative PCR
2	Synchronous population firing leads to vocal nerve spikes	*cx30, cx43*	Electron microscopy Transneuronal dye diffusion Electrophysiological collision
3	Fast AP repolarization promotes repetitive firing	*kcnb2, kcnc3, kcnc4 kcns1**	*See Discussion for support from other systems*
4	Prominent AHP resulting from inhibitory VMN network input promotes synchrony and repetitive firing	*gabra3, gabra5*	GABAaR neuropharmacology ICC staining of GABA in VMN
5	Low intrinsic excitability (no spontaneous firing) ensures firing fidelity to excitatory input	*kcnq2 chrm2**	*See Discussion for support from other systems*

earlier, KCNC4/Kv3.4 currents are modulated by KCNS/Kv9 subunits, transcripts of which are highly expressed in VMN (Table 4.4), when coassembled in heteromeric channels (Richardson and Kaczmarek, 2000; Stocker et al., 1999). Strikingly, in motoneurons of an ALS mouse model carrying the human *sod1* mutation, *kcnc4*/Kv3.4 was significantly downregulated relative to expression in wild type mice (Bandyopadhyay et al., 2013), supporting its important role in motoneuronal function.

Steroid signaling transcripts, such as *ar-a* (a different isoform than the one significantly upregulated in VMN in tissue comparisons), were found in All-Summer clusters (Table 4.5), indicating a summer-dependent increase in androgen sensitivity within both VMN and surrounding H. VMN's androgen sensitivity is a shared trait with other vocal vertebrates. It has been well documented that songbird syringeal motoneurons within the nXIIts concentrate high levels of androgens (Arnold et al., 1976). Both midshipman VMN and songbird nXIIts are sexually dimorphic in size, with males having larger motoneuronal somata and neuropil volume than females (Bass and Marchaterre, 1989; Bass et al., 1996; DeVoogd et al., 1991). Furthermore, the songbird nXIIts responds to androgen treatment by increasing the size of motoneuronal somata, synaptic density, and the number of synaptic vesicles (Clower et al., 1989; DeVoogd et al., 1991), which could increase their ability to drive vocalizations during the breeding season. Similarly, juvenile male midshipman treated with androgens exhibit increased size of VMN somata (Bass and Forlano, 2008). We also found a *glucocorticoid receptor* (*nr3c1*) in VMN-Summer clusters, indicating a summer-dependent increase in glucocorticoid sensitivity specifically in the VMN (Table 4.5). The presence of both androgen and glucocorticoid receptors is consistent

with androgen- and cortisol-induced lengthening of hindbrain vocal CPG output (Remage-Healey and Bass, 2004; Remage-Healey and Bass, 2006b).

The neurotransmission and neuroendocrine mechanisms highlighted by our candidate genes could influence each other to bring about seasonal changes in VMN function and midshipman vocal behavior. For example, ultrastructure studies in songbirds and rodents have shown that estrogen and androgens can increase gap junction expression (Gahr and Garcia-Segura, 1996; Matsumoto et al., 1988; Perez et al., 1990). Testosterone treatment in female songbirds induced an increase in the number of soma-somatic gap junctions in HVC, a telencephalic song control nucleus, correlated with an increased repetition rate and decreased variability in frequency modulation of male-like song (Gahr and Garcia-Segura, 1996). Steroid-dependent seasonal regulation of gap junction abundance in vocal control nuclei influencing vocal behavior could also apply to midshipman fish.

Daily comparisons (Fig. 4.8B, Table 4.5): We found nine neurotransmission transcripts within Peak-SNV clusters (Table 4.5) that were all unique from those found in Peak-SNH clusters. These included an isoform of c*x30*, *$GABA_A$ receptor subunit pi-like* (*gabrp*), and two *calcium-activated potassium channel subunit alpha-1* (*kcnma1*/Kca1.1) isoforms (Table 4.5, Fig. 4.8B). While *cx30* and *gabrp* were both found in transcripts upregulated in the VMN compared to H (Table 4.4), they are different Trinity-predicted isoforms. Similar to between-tissue comparisons that highlighted the importance of cholinergic action in VMN, we found acetylcholine receptors, including *neuronal acetylcholine receptor beta-2-like* (*chrnb2*) in Peak-

SNV clusters (Table 4.5, Fig. 4.8B). Steroid signaling transcripts in Peak-SNV clusters included an *estrogen receptor alpha* (*esr1*) isoform (Table 4.5), shown by in-situ to be expressed in vocal motoneurons (Forlano et al., 2005). We propose that seasonal and/or daily variation in the expression levels of neurotransmission and steroid hormone related transcripts support modulation of known VMN firing properties that, in turn, translates directly into changes in vocal behavior at times of high vocal activity.

Conclusions

The vocal motor system of midshipman fish exemplifies a simple vertebrate model with which we can identify genetic components supporting neural network function leading to a single behavior, in this case vocalization that serves a social communication function in multiple vertebrate lineages. This VMN transcriptome project provides a global view of molecular pathways responsible for neuronal function and hormone modulation in the vocal motoneurons of midshipman and vertebrate in general. We identified a suite of candidate genes whose functions underlie previously identified VMN firing properties, as well as novel candidates whose functions regulate aspects of neuronal excitability that remain to be studied in VMN (summarized in Fig. 4.9).

The interpretive power of our results benefits directly from a large body of corroborating evidence in the midshipman model system, from synaptic ultrastructure to intracellular neurophysiology, anatomical localization of steroid signaling pathways, and hormonal modulation of VMN output and vocal behavior (Fig. 4.9).

The new results presented here guide future molecular, anatomical, and pharmacological investigations for determining how specific metabolic, hormonal, and neurotransmission pathways sculpt neurophysiological events that pattern vocal behavior.

Our findings have broad relevance to other vertebrate taxa given the highly conserved nature of vocal mechanisms, shared demands for temporal precision in sound production, and the equally widespread occurrence of seasonal and daily variation in vocal behaviors [see discussions in (Bass and Chagnaud, 2012; Feng and Bass, 2014)]. We propose that candidate genes and pathways identified here shape neurophysiological characters of motoneuronal populations driving the sound producing superfast muscles in toadfish (Rome, 2006), birds (Elemans et al., 2004; Elemans et al., 2008), bats (Elemans et al., 2011), and rattlesnakes (Rome et al., 1996). The hypothesis that fish use the same fundamental molecular machinery as other vertebrates for controlling acoustic communication is challenging but testable. Furthermore, contrasting our results to other motor systems will yield insight into the molecular machinery utilized by neuromuscular systems varying in speed, synchrony, and precision. Finally, molecular insights into motoneuronal function will also be relevant for motoneuron dysfunction, such as diseases characterized by the loss of resilience to oxidative stress.

Materials and methods

Tissue collection

Midshipman fish have two male reproductive morphs: type I males that build and

guard nests, acoustically court females and are the focus of this study, and type II males that sneak spawn (Brantley and Bass, 1994; McIver et al., 2014). We collected tissue samples from type I males at different time points in the summer reproductive and winter non-reproductive seasons (see Fig. 4.1D). None of the fish used were actively vocalizing when sacrificed, although we cannot completely discount recently produced isolated grunting or growling behavior (see below). All procedures were approved by the Institutional Animal Care and Use Committee at Cornell University.

Reproductive fish: In May 2011, type I males were hand collected from rocky intertidal zones in northern California. Fish were then held for 1-2 days at the University of California Bodega Marine Laboratory in large outdoor tanks with artificial shelters and flow-through seawater. We are confident that the fish used in this study were not engaged in extended vocal behaviors such as humming for several reasons. First, although the fish could have been producing isolated agonistic grunts or growls in this setting, we did not observe the inflated swim bladders associated with humming (AHB unpub obs). Second, males from California do not take up residence and engage in any defense or courtship vocal behaviors until three weeks in captivity (NYF and AHB upub obs); fish used in this study were only held in large communal tanks for 1-2 days. Future transcriptome experiments using tissues from fish that were recorded and confirmed to be actively humming will provide insight into genes upregulated during vocal behavior.

The ambient light:dark cycle was approximately 14.25 h light: 9.75 h dark, with sunrise at approximately 6:00 am and sunset at 8:15 pm. The “summer night (SN)” males (n=6) were sacrificed at the middle of the dark phase (middark), between

12:00 am and 2:00 am; and the "summer morning (SM)" males (n=6) were sacrificed after sunrise, between 7:00 am and 9:40 am. Fish were deeply anesthetized under 0.025% benzocaine (Sigma-Aldrich, St. Louis, MO) and exsanguinated from the heart. The brain was removed after craniotomy, transected at the midbrain-hindbrain boundary, and stored in tubes containing RNAlater solution (Life Technologies, Carlsbad, CA) overnight in 4°C followed by -20°C. The samples were shipped overnight to Cornell University (Ithaca, NY) on dry ice and stored in -20°C until use.

Non-reproductive fish: Midshipman migrate offshore to deeper waters in the winter non-reproductive season (Sisneros et al., 2004). In January 2011, type I males were obtained by otter trawl (R/V John H. Marin, Moss Landing Marine Laboratories) in Monterey Bay, offshore from Moss Landing, CA at depths of 115-150 meters. These fish, referred to as "winter night (WN) ", were kept under running seawater in large indoor tanks with ambient lighting through skylights, and sacrificed within 24 h of collection at middark (n=5; 11:30 pm to 1:00 am) following the same tissue collection procedures as used for reproductive fish.

cDNA library preparation and sequencing

The paired VMN located at the midline contain approximately 4000 homogeneous motoneurons, presynaptic input, and surrounding glial cells that can be isolated *in toto* (Figs. 4.1C & 4.9) (Bass and Andersen, 1991; Chagnaud et al., 2012; Fergus and Bass, 2013). Immediately before RNA extraction, we used fine forceps and minutien pins to isolate the paired VMN from the surrounding hindbrain (H) as previously described (Fergus and Bass, 2013). Separation of VMN from the rest of H, which included

premotor populations and other motor populations, was verified in sectioned material. Total RNA was extracted from VMN and H tissues using the Trizol reagent (Life Technologies) following the manufacturer's protocol. RNA concentrations were quantified using a Qubit fluorometer (Life Technologies), and equal masses of RNA were pooled by tissue and collection time. Reproductive summer night (SN) and summer morning (SM) VMN and H groups (SNV, SNH, SMV, SMH) were each pooled from 6 individuals, non-reproductive winter night (WN) VMN (WNV) was pooled from 4 individuals, and winter night H (WNH) was pooled from 5 individuals (Fig. 4.1D). Each pool contained 2μg of total RNA. We treated the pooled RNA samples with DNase I (Ambion) to eliminate potential genomic DNA contamination.

Figure 4.2 provides an overview of this study's key procedures and analyses with reference to relevant figures and tables. We closely followed the protocol of Zhong et al. (2011) for strand-specific cDNA library construction (Zhong et al., 2011), which included poly(A) RNA isolation and chemical fragmentation, first-strand cDNA synthesis, second-strand cDNA synthesis with dUTP, end-repair, dA-tailing, Y-shape barcoded adapter ligation, DNA purification and size selection. The second-strand DNA was digested with uracil DNA glycosylase to leave first-strand cDNA with differential adapters on the 5' and 3' ends. We then enriched our cDNA library using 14 cycles of PCR, and verified the size by agarose gel. Examining 40 ηg of each cDNA library with an Agilent Bioanalyzer in Cornell's Biotechnology Resource Center showed size peaks between 251 bp and 257 bp. Finally, 20 ηg of cDNA from each sample group were combined with 20 ηg from each of 4 other groups of cDNA from saccular epithelia of the inner ear into a single pool of 2000 ηg pooled cDNA

library; the auditory tissues contributed to a companion study (Fergus et al., 2015). The completed cDNA library was submitted for paired-end sequencing by Illumina HiSeq2000 at the Biotechnology Resource Center's Genomics Facility.

Transcriptome assembly and annotation

Read pairs were discarded if either read did not pass Illumina's quality control. Adaptor sequences and low quality nucleotides were removed from the ends using Trimmomatic tools and reads less than 10 bases after trimming were dropped (Bolger et al., 2014). Over 90% of raw reads passed quality filtering and trimming, leaving 20.2 ± 2.4 million (mean ± S.D.) reads per group. Forward and reverse reads from all sample groups, including those from the saccular epithelia, were concatenated and transferred to the Blacklight system at the Pittsburgh Supercomputing Center where the full transcriptome was assembled with the Trinity software package (version r2013-02-15) (Haas et al., 2013), one of the most robust *de novo* assembly methods (Li et al., 2014). In order to limit occurrences of fusion transcripts we used the "jaccard_clip" option and set the "min_kmer_cov" to 2.

We used Trinity's TransDecoder utility to discard assembled transcripts with open reading frames (ORF) of less than 50 amino acids (Haas et al., 2013). To assess the completeness of our transcriptome, we submitted our filtered transcriptome to the CEGMA software (Parra et al., 2009). CEGMA looks for the presence of 248 highly-conserved core eukaryotic genes (CEGs) and a larger set of 458 CEGs (Parra et al., 2009). We used Blast2GO to annotate our assembled transcriptome based on the NCBI non-redundant protein database (Gotz et al., 2008). All transcripts were

submitted to blastx using an E-value cutoff of 1e-10 via Blas2GO; those without blastx hits were then subjected to blastn a 1e-10 E-value cutoff. Mapping and annotation steps were performed with default settings (i.e., E-value cutoff=1e-6). InterProScan and GO-Enzyme Codes were run on all transcripts.

With Trinity-supported companion programs (i.e. bowtie and RSEM) we mapped the individual reads back onto the assembled transcriptome and estimated the abundance of transcripts from each tissue group (Haas et al., 2013). Lowly supported transcripts, accounting for less than 1% of total reads of a gene (IsoPct), were discarded. The length distribution statistics of surviving transcripts were obtained through PRINSEQ (Schmieder and Edwards, 2011). As an additional assessment of assembly quality, we submitted the final set of surviving transcripts to TransDecoder and counted the number of transcripts with complete ORFs (containing start and stop codons). The assembled transcriptome and sample group reads were submitted to the NCBI Transcriptome Shotgun Assembly and Sequence Read Archive databases under BioProject accession PRJNA269550.

Because four ear tissue groups were included in the transcriptome assembly, our analyses of the vocal system excluded transcripts with read count sums of zero across all six brain sample groups (see Fig. 4.1D). We focused on transcripts (isoforms) rather than predicted genes [also called “gene components” by Trinity, (Haas et al., 2013)] because the single sequence available for each transcript allows straight-forward annotations and the potential to identify differential regulation of alternate isoforms of a single gene.

VMN vs. H tissue comparisons

Tissue-based normalization

TMM normalization (Fig 4.4), used by default Trinity analysis pipeline (Haas et al., 2013), as well as several methods evaluated in (Glusman et al., 2013), was insufficient in correcting the nonlinear skew observed in VMN vs H comparisons, likely due to systematic sequencing biases caused by differential tissue RNA population composition [see (Glusman et al., 2013; Robinson and Oshlack, 2010) for discussion]. However, a cyclic loess method called fastlo (Ballman et al., 2004), originally designed for microarray data, worked well to correct our nonlinear skew (Fig. 4.4). To allow proper fastlo normalization, we added 1 to all raw counts prior to normalizing.

Differential expression using edgeR

For the comparison between tissues, we treated the three time points sampled as biological replicates, estimated transcript-wise dispersion values, followed by differential expression analysis with edgeR's exact test (Robinson and Smyth, 2007). Differentially expressed transcripts (FDR < 0.05, largely corresponding to fold change > 4; see blue lines in Fig. 4.7A) showing upregulation in VMN or H were then subjected to downstream, GO term enrichment and KEGG pathway mapping analyses. Furthermore, we selected nine candidate genes of functional interest upregulated in VMN samples for validation by sequencing and qPCR (see below).

Gene category-based analyses

To gain a sense of the relative contribution of gene functional categories to VMN function (Fig. 4.5), we extracted fastlo-normalized expression levels for transcripts (regardless of whether they were differentially expressed) that were classified under: 1) "**neurotransmission**": ion channels and neurotransmitter receptors; 2) "**neuroendocrine**": steroid hormone signaling genes such as receptors and biosynthetic enzymes, and thyroid hormone related genes; 3) "**neuropeptide**": neuropeptides and their receptors, as well as peptide hormones and their receptors; 4) "**neuromodulator**": neurochemicals other than steroids and neuropeptides that are known within this system, namely genes related to catecholamine, serotonin, and melatonin biosynthesis and signaling; 5) "**cellular respiration**": cellular respiration-related genes; and 6) "**antioxidant**": antioxidant enzymes and proteins [see Additional file 1, Table S4 in (Feng et al., 2015) for transcript IDs and descriptions in each gene category].

We compared the tissue expression levels of gene categories to assess the relative importance of each gene category for VMN vs. H (Fig. 4.5). We first examined whether H expressed more genes by dichotomizing the data into 1 if the total tissue expression was > 0 and 0 if the total was 0 (not expressed), followed by a chi square test (Fig. 4.5A). To compare total expression levels for each gene category, we summed expression levels across the three VMN or H sample groups for expressed genes (tissue sum > 0) (Fig. 4.5B). We then Box-Cox transformed this dataset in order to statistically compare H vs. VMN tissue expression with a generalized linear model (main effects = tissue, gene category, and tissue*gene category interaction) followed by post-doc Tukey HSD using JMP9.0 (SAS Institute Inc., Cary, NC, USA) (Fig.

4.5B). The non-parametric Wilcoxon rank sum test for tissue comparisons followed by Bonferroni correction produced the same results. Finally, to evaluate correlation patterns across sample groups for each gene category, we performed Spearman's correlation for pair-wise comparisons between all six-tissue groups in R (Team, 2014) (Fig. 4.6).

Daily and seasonal variation in gene expression

For daily and seasonal gene expression comparisons, we used Trinity's downstream analysis pipeline with default parameters (Haas et al., 2013). Transcripts that were differentially expressed in at least one pairwise sample comparison were identified using the Trinity-supported edgeR Bioconductor package (Robinson et al., 2010), We ran the TMM normalized FPKM matrix through Trinity-supported differential expression analyses to generate hierarchically clustered heatmaps of transcripts with at least four-fold differential expression and false discovery rate (FDR) corrected P values of <0.001 (23,855 out of 77,285 transcripts) (Appendix Fig. S2A). Spearman correlation matrices for pairwise sample group comparisons were also generated (Appendix Fig. S2B). We generated 109 K-means clusters based on the rule of thumb for determining cluster number (Mardia et al., 1979) with 23,855 differentially expressed genes from which we could extract sequence ID, annotation, and expression levels. We combined clusters exhibiting similar expression patterns of day-night and seasonal variation across sample groups. Candidate genes with functions directly related to neural transmission (e.g. ion channels) and neuromodulation (e.g. steroid

hormones) were identified and considered for potential actions in sculpting VMN firing properties.

Quantitative PCR (qPCR) validation of gene expression

We used qPCR on a subset of transcripts to confirm the accuracy of our assembled transcriptome and RSEM predicted differential transcript abundance among our sample groups. First, to validate within-tissue gene expression ratios we selected 19 transcripts chosen based on the following criteria: 1) each transcript was the only transcript in its gene component; 2) the SNH/SMH FPKM ratios of all the transcripts fell within a broad range (0.05-100); 3) the primers we chose based on the assembled transcript sequences produced only the predicted PCR product [Additional file 1, Table S6 in (Feng et al., 2015) contains gene descriptions and primer sequences]. These criteria allowed for straightforward qPCR analyses from H samples, which provided more cDNA for analysis than VMN samples. Specificity of the qPCR primers was verified by sequencing at the Cornell Genomics Core facility. We selected the reference gene based on its very low coefficient of variance (0.10) in FPKM values across all sample groups and being the only transcript for its gene component. The reference gene (Blast2Go annotation "btb poz domain-containing protein kctd6") was confirmed by qPCR to show no apparent or significant expression differences between SNH and SMN (P=0.26). Each qPCR was performed in triplicate on the same, pooled cDNA sample produced for RNA-seq as well as no template controls. Each reaction contained 5µl of 2x Power SYBR Green PCR Master Mix (Life Technologies, Carlsbad, CA), 1µl each of forward and reverse primers (50 ηM

final concentration for the reference gene and 100 nM for target genes), 1µl dH2O, and 2µl of the appropriate pooled cDNA. The qPCR reaction was run on an ABI Viia7 system at the Cornell Genomics Core facility. We used the standard curve method to extrapolate copy numbers, which were normalized against our reference gene. Pearson's correlations were calculated for qPCR and RNA-seq predicted SNH/SMH expression ratios (Fig. 4.3D).

Next, to validate VMN vs. H tissue comparisons with qPCR, we chose nine functionally important candidate genes that were upregulated in the VMN [see Additional file 1, Table S6 in (Feng et al., 2015)], regardless of how many isoforms were predicted by Trinity. We used the same, pooled SMV and SMH samples that were submitted for RNAseq. SMV and SMH samples were chosen due to cDNA availability. The qPCR procedures and reference gene were the same as above for SNH/SMH comparisons. Pearson's correlations were calculated for qPCR vs. fastlo-normalized SMV/SMH ratios, which were averaged across all isoforms for each Trinity predicted gene component (Fig. 4.7C), as well as for qPCR vs fastlo-normalized values separately analysed for SMV and SMH (Appendix Fig. S1). Student's paired t test was performed in R to compare qPCR measured SMV and SMH expression levels using log-transformed data (Fig. 4.7D).

Availability of supporting data

The assembled transcriptome and reads from each sample supporting the results of this article are available in the NCBI Transcriptome Shotgun Assembly and Sequence Read Archive databases under BioProject accession number [PRJNA269550].

Acknowledgments

We sincerely thank Silin Zhong and the Jim Giovannoni lab (USDA-ARS, Cornell University) for help with cDNA library construction. Cornell University BioHPC Lab resources and the Bioinformatics Facility, especially Dr. Qi Sun, provided us with the expertise, guidance, and computing resources to complete our project. We are grateful to Lynn M. Johnson at Cornell Statistical Consulting Unit, James Booth and Martin Wells at Cornell Department of Statistics for their generous help with data analysis and tissue normalization. We would also like to thank Brian Haas from the Broad Institute for his help with using Trinity, Cameron Finucane for programming support, as well as Richard Harrison, Alon Keinan and especially Ben Matthews for comments on early drafts of the manuscript. This work used the Extreme Science and Engineering Discovery Environment (XSEDE), which is supported by National Science Foundation grant number OCI-1053575. Research support, in part, came from NSF IOS 1120925 (AHB) and Cornell University's Center for Vertebrate Genomics (NYF).

References

Amador, A., Perl, Y. S., Mindlin, G. B. and Margoliash, D. (2013). Elemental gesture dynamics are encoded by song premotor cortical neurons. *Nature* **495**, 59–64.

Arnold, A. P., Nottebohm, F. and Pfaff, D. W. (1976). Hormone concentrating cells in vocal control and other areas of the brain of the zebra finch (Poephila guttata). *J. Comp. Neurol.* **165**, 487–511.

Balakrishnan, C. N., Mukai, M., Gonser, R. A., Wingfield, J. C., London, S. E., Tuttle, E. M. and Clayton, D. F. (2014). Brain transcriptome sequencing and assembly of three songbird model systems for the study of social behavior. *PeerJ* **2**, e396.

Ballman, K. V., Grill, D. E., Oberg, A. L. and Therneau, T. M. (2004). Faster cyclic loess: normalizing RNA arrays via linear models. *Bioinformatics* **20**, 2778–2786.

Bandyopadhyay, U., Cotney, J., Nagy, M., Oh, S., Leng, J., Mahajan, M., Mane, S., Fenton, W. A., Noonan, J. P. and Horwich, A. L. (2013). RNA-Seq Profiling of Spinal Cord Motor Neurons from a Presymptomatic SOD1 ALS Mouse. *PLoS ONE* **8**, e53575.

Bartos, M., Vida, I. and Jonas, P. (2007). Synaptic mechanisms of synchronized gamma oscillations in inhibitory interneuron networks. *Nature Reviews Neuroscience* **8**, 45–56.

Bass, A. and Andersen, K. (1991). Inter- and Intrasexual Dimorphisms in the Vocal Control System of a Teleost Fish: Motor Axon Number and Size. *Brain Behav Evol* **37**, 204–214.

Bass, A. H. (2014). ScienceDirectCentral pattern generator for vocalization: is there a vertebrate morphotype? *Current Opinion in Neurobiology* **28**, 94–100.

Bass, A. H. and Baker, R. (1990). Sexual dimorphisms in the vocal control system of a teleost fish: Morphology of physiologically identified neurons. *Journal of Neurobiology* **21**, 1155–1168.

Bass, A. H. and Chagnaud, B. P. (2012). Shared developmental and evolutionary origins for neural basis of vocal-acoustic and pectoral-gestural signaling. *Proc. Natl. Acad. Sci. U.S.A.* **109 Suppl 1**, 10677–10684.

Bass, A. H. and Forlano, P. M. (2008). *Neuroendocrine mechanisms of alternative reproductive tactics: the chemical language of reproductive and social plasticity*. (eds. Oliveira, R. F., Taborsky, M., and Brockmann, H. J. Cambridge: Cambridge University Press.

Bass, A. H. and Marchaterre, M. A. (1989). Sound-generating (sonic) motor system in a teleost fish (Porichthys notatus): Sexual polymorphisms and general synaptology of sonic motor nucleus. *J. Comp. Neurol.* **286**, 154–169.

Bass, A. H. and Remage-Healey, L. (2008). Central pattern generators for social vocalization: Androgen-dependent neurophysiological mechanisms. *Hormones and Behavior* **53**, 659–672.

Bass, A. H., Gilland, E. H. and Baker, R. (2008). Evolutionary Origins for Social Vocalization in a Vertebrate Hindbrain-Spinal Compartment. *Science* **321**, 417–421.

Bass, A. H., Horvath, B. J. and Brothers, E. B. (1996). Nonsequential developmental trajectories lead to dimorphic vocal circuitry for males with

alternative reproductive tactics. *Journal of Neurobiology* **30**, 493–504.

Bass, A. H., Marchaterre, M. A. and Baker, R. (1994). Vocal-acoustic pathways in a teleost fish. *Journal of Neuroscience* **14**, 4025–4039.

Bellingham, M. C. and Berger, A. J. (1996). Presynaptic depression of excitatory synaptic inputs to rat hypoglossal motoneurons by muscarinic M2 receptors. *Journal of Neurophysiology* **76**, 3758–3770.

Bolger, A. M., Lohse, M. and Usadel, B. (2014). Trimmomatic: a flexible trimmer for Illumina sequence data. *Bioinformatics* **30**, btu170–2120.

Brantley, R. K. and Bass, A. H. (1988). Cholinergic neurons in the brain of a teleost fish (Porichthys notatus) located with a monoclonal antibody to choline acetyltransferase. *J. Comp. Neurol.* **275**, 87–105.

Brantley, R. K. and Bass, A. H. (1994). Alternative Male Spawning Tactics and Acoustic Signals in the Plainfin Midshipman Fish Porichthys notatus Girard (Teleostei, Batrachoididae). *Ethology* **96**, 213–232.

Brown, D. (1988). M-currents: an update. *Trends in Neurosciences* **11**, 294–299.

Brown, D. A. and Passmore, G. M. (2009). Neural KCNQ (Kv7) channels. *Br. J. Pharmacol.* **156**, 1185–1195.

Caulfield, M. P. and Birdsall, N. J. (1998). International Union of Pharmacology. XVII. Classification of muscarinic acetylcholine receptors. *Pharmacol Rev* **50**, 279–290.

Chagnaud, B. P., Baker, R. and Bass, A. H. (2011). Vocalization frequency and duration are coded in separate hindbrain nuclei. *Nature Communications* **2**, 346–11.

Chagnaud, B. P., Zee, M. C., Baker, R. and Bass, A. H. (2012). Innovations in motoneuron synchrony drive rapid temporal modulations in vertebrate acoustic signaling. *Journal of Neurophysiology* **107**, 3528–3542.

Chambers, M. S., Atack, J. R., Broughton, H. B., Collinson, N., Cook, S., Dawson, G. R., Hobbs, S. C., Marshall, G., Maubach, K. A., Pillai, G. V., et al. (2003). Identification of a Novel, Selective GABA Aα5 Receptor Inverse Agonist Which Enhances Cognition. *J. Med. Chem.* **46**, 2227–2240.

Clower, R. P., Nixdorf, B. E. and DeVoogd, T. J. (1989). Synaptic plasticity in the hypoglossal nucleus of female canaries: structural correlates of season, hemisphere, and testosterone treatment. *Behav. Neural Biol.* **52**, 63–77.

Cozzolino, M., Pesaresi, M. G., Gerbino, V., Grosskreutz, J. and Carrì, M. T.

(2012). Amyotrophic Lateral Sclerosis: New Insights into Underlying Molecular Mechanisms and Opportunities for Therapeutic Intervention. *Antioxidants & Redox Signaling* **17**, 1277–1330.

Davies, K. J. (2000). Oxidative stress, antioxidant defenses, and damage removal, repair, and replacement systems. *IUBMB Life* **50**, 279–289.

Delage, E., Puyaubert, J., Zachowski, A. and Ruelland, E. (2013). Signal transduction pathways involving phosphatidylinositol 4-phosphate and phosphatidylinositol 4,5-bisphosphate: Convergences and divergences among eukaryotic kingdoms. *Progress in Lipid Research* **52**, 1–14.

DeVoogd, T. J., Pyskaty, D. J. and Nottebohm, F. (1991). Lateral asymmetries and testosterone-induced changes in the gross morphology of the hypoglossal nucleus in adult canaries. *J. Comp. Neurol.* **307**, 65–76.

Ding, S., Matta, S. G. and Zhou, F.-M. (2011). Kv3-like potassium channels are required for sustained high-frequency firing in basal ganglia output neurons. *Journal of Neurophysiology* **105**, 554–570.

Elemans, C. P. H., Mead, A. F., Jakobsen, L. and Ratcliffe, J. M. (2011). Superfast Muscles Set Maximum Call Rate in Echolocating Bats. *Science* **333**, 1885–1888.

Elemans, C. P. H., Mead, A. F., Rome, L. C. and Goller, F. (2008). Superfast vocal muscles control song production in songbirds. *PLoS ONE* **3**, e2581.

Elemans, C., Spierts, I., Müller, U. K. and van Leeuwen, J. L. (2004). Bird song: superfast muscles control dove's trill. *Nature* **431**, 146–146.

Feng, N. Y. and Bass, A. H. (2014). Melatonin action in a midbrain vocal-acoustic network. *Journal of Experimental Biology* **217**, 1046–1057.

Feng, N. Y., Fergus, D. J. and Bass, A. H. (2015). Neural transcriptome reveals molecular mechanisms for temporal control of vocalization across multiple timescales. *BMC Genomics* **16**, 417.

Fergus, D. J. and Bass, A. H. (2013). Localization and divergent profiles of estrogen receptors and aromatase in the vocal and auditory networks of a fish with alternative mating tactics. *J. Comp. Neurol.* **521**, 2850–2869.

Fergus, D. J., Feng, N. Y. and Bass, A. H. (2015). Gene expression underlying enhanced, steroid-dependent auditory sensitivity of hair cell epithelium in a vocal fish. *BMC Genomics* **16**, 782.

Forlano, P. M., Deitcher, D. L. and Bass, A. H. (2005). Distribution of estrogen receptor alpha mRNA in the brain and inner ear of a vocal fish with comparisons to sites of aromatase expression. *J. Comp. Neurol.* **483**, 91–113.

Forlano, P. M., Deitcher, D. L., Myers, D. A. and Bass, A. H. (2001). Anatomical distribution and cellular basis for high levels of aromatase activity in the brain of teleost fish: aromatase enzyme and mRNA expression identify glia as source. *J. Neurosci.* **21**, 8943–8955.

Forlano, P. M., Kim, S. D., Krzyminska, Z. M. and Sisneros, J. A. (2014). Catecholaminergic connectivity to the inner ear, central auditory, and vocal motor circuitry in the plainfin midshipman fish porichthys notatus. *J. Comp. Neurol.* **522**, 2887–2927.

Forlano, P. M., Marchaterre, M., Deitcher, D. L. and Bass, A. H. (2010). Distribution of androgen receptor mRNA expression in vocal, auditory, and neuroendocrine circuits in a teleost fish. *J. Comp. Neurol.* **518**, 493–512.

Forlano, P. M., Sisneros, J. A., Rohmann, K. N. and Bass, A. H. (2015). Neuroendocrine control of seasonal plasticity in the auditory and vocal systems of fish. *Frontiers in Neuroendocrinology* **37**, 129–145.

Fraser, B. A., Janowitz, I., Thairu, M., Travis, J. and Hughes, K. A. (2014). Phenotypic and genomic plasticity of alternative male reproductive tactics in sailfin mollies. *Proceedings of the Royal Society B: Biological Sciences* **281**, 20132310–20132310.

Gahr, M. and Garcia-Segura, L. M. (1996). Testosterone-dependent increase of gap-junctions in HVC neurons of adult female canaries. *Brain Research* **712**, 69–73.

Genova, R. M., Marchaterre, M. A., Knapp, R., Fergus, D. and Bass, A. H. (2012). Glucocorticoid and androgen signaling pathways diverge between advertisement calling and non-calling fish. *Hormones and Behavior* **62**, 426–432.

Gillooly, J. F. and Ophir, A. G. (2010). The energetic basis of acoustic communication. *Proceedings of the Royal Society B: Biological Sciences* **277**, 1325–1331.

Glusman, G., Caballero, J., Robinson, M., Kutlu, B. and Hood, L. (2013). Optimal Scaling of Digital Transcriptomes. *PLoS ONE* **8**, e77885.

Goldberg, J. H., Farries, M. A. and Fee, M. S. (2013). Basal ganglia output to the thalamus: still a paradox. *Trends in Neurosciences* **36**, 695–705.

Goodson, J. L. and Bass, A. H. (2000a). Forebrain peptides modulate sexually polymorphic vocal circuitry. *Nature* **403**, 769–772.

Goodson, J. L. and Bass, A. H. (2000b). Rhythmic midbrain-evoked vocalization is inhibited by vasoactive intestinal polypeptide in the teleost Porichthys notatus. *Brain Research* **865**, 107–111.

Goodson, J. L. and Bass, A. H. (2002). Vocal–acoustic circuitry and descending vocal pathways in teleost fish: Convergence with terrestrial vertebrates reveals conserved traits. *J. Comp. Neurol.* **448**, 298–322.

Gotz, S., Garcia-Gomez, J. M., Terol, J., Williams, T. D., Nagaraj, S. H., Nueda, M. J., Robles, M., Talon, M., Dopazo, J. and Conesa, A. (2008). High-throughput functional annotation and data mining with the Blast2GO suite. *Nucleic Acids Research* **36**, 3420–3435.

Greenfield, D. W., Winterbottom, R. and Collette, B. B. (2008). Review of the Toadfish Genera (Teleostei: Batrachoididae). *proceedings of the california academy of sciences* **59**, 665–710.

Grove, C. L., Szabo, T. M., McIntosh, J. M., Do, S. C., Waldeck, R. F. and Faber, D. S. (2011). Fast synaptic transmission in the goldfish CNS mediated by multiple nicotinic receptors. *The Journal of Physiology* **589**, 575–595.

Gutman, G. A., Chandy, K. G., Adelman, J. P., Aiyar, J., Bayliss, D. A., Clapham, D. E., Covarriubias, M., Desir, G. V., Furuichi, K., Ganetzky, B., et al. (2003). International Union of Pharmacology. XLI. Compendium of voltage-gated ion channels: potassium channels. *Pharmacol Rev* **55**, 583–586.

Haas, B. J., Papanicolaou, A., Yassour, M., Grabherr, M., Blood, P. D., Bowden, J., Couger, M. B., Eccles, D., Li, B., Lieber, M., et al. (2013). De novo transcript sequence reconstruction from RNA-seq using the Trinity platform for reference generation and analysis. *Nature Protocols* **8**, 1494–1512.

Hage, S. R. and Jürgens, U. (2006). On the role of the pontine brainstem in vocal pattern generation: a telemetric single-unit recording study in the squirrel monkey. *J. Neurosci.* **26**, 7105–7115.

Hage, S. R., Gavrilov, N., Salomon, F. and Stein, A. M. (2013). Temporal vocal features suggest different call-pattern generating mechanisms in mice and bats. *BMC Neuroscience* **14**, 99.

Hellström, J., Oliveira, A. L. R., Meister, B. and Cullheim, S. (2003). Large cholinergic nerve terminals on subsets of motoneurons and their relation to muscarinic receptor type 2. *J. Comp. Neurol.* **460**, 476–486.

Hermosura, M. C., Nayakanti, H., Dorovkov, M. V., Calderon, F. R., Ryazanov, A. G., Haymer, D. S. and Garruto, R. M. (2005). A TRPM7 variant shows altered sensitivity to magnesium that may contribute to the pathogenesis of two Guamanian neurodegenerative disorders. *Proc Natl Acad Sci USA* **102**, 11510–11515.

Hilliard, A. T., Miller, J. E., Fraley, E. R., Horvath, S. and White, S. A. (2012). Molecular microcircuitry underlies functional specification in a basal ganglia

circuit dedicated to vocal learning. *Neuron* **73**, 537–552.

Huth, T. J. and Place, S. P. (2013). De novo assembly and characterization of tissue specific transcriptomes in the emerald notothen, Trematomus bernacchii. *BMC Genomics* **14**, 805.

Ibara, R. M., Penny, L. T., Ebeling, A. W., van Dykhuizen, G. and Cailliet, G. (1983). The mating call of the plainfin midshipman fish, Porichthys notatus. In *Predators and prey in fishes*, pp. 205–212. Dordrecht: Springer Netherlands.

Judge, S. I. V. and Bever, C. T. (2006). Potassium channel blockers in multiple sclerosis: neuronal Kv channels and effects of symptomatic treatment. *Pharmacology & Therapeutics* **111**, 224–259.

Kanehisa, M., Goto, S., Sato, Y., Kawashima, M., Furumichi, M. and Tanabe, M. (2014). Data, information, knowledge and principle: back to metabolism in KEGG. *Nucleic Acids Research* **42**, D199–205.

Kingsbury, M. A., Kelly, A. M., Schrock, S. E. and Goodson, J. L. (2011). Mammal-like organization of the avian midbrain central gray and a reappraisal of the intercollicular nucleus. *PLoS ONE* **6**, e20720.

Kittelberger, J. M. and Bass, A. H. (2013). Vocal-motor and auditory connectivity of the midbrain periaqueductal gray in a teleost fish. *J. Comp. Neurol.* **521**, 791–812.

Kusakabe, M., Nakamura, I. and Young, G. (2003). 11beta-hydroxysteroid dehydrogenase complementary deoxyribonucleic acid in rainbow trout: cloning, sites of expression, and seasonal changes in gonads. *Endocrinology* **144**, 2534–2545.

Labrie, F., Luu-The, V., Lin, S. X., Simard, J., Labrie, C., El-Alfy, M., Pelletier, G. and Bélanger, A. (2000). Intracrinology: role of the family of 17 beta-hydroxysteroid dehydrogenases in human physiology and disease. *J. Mol. Endocrinol.* **25**, 1–16.

Li, B., Fillmore, N., Bai, Y., Collins, M., Thomson, J. A., Stewart, R. and Dewey, C. N. (2014). Evaluation of de novo transcriptome assemblies from RNA-Seq data. *Genome Biol* **15**, 553.

Lin, M. T. and Beal, M. F. (2006). Mitochondrial dysfunction and oxidative stress in neurodegenerative diseases. *Nature* **443**, 787–795.

Lovell, P. V., Carleton, J. B. and Mello, C. V. (2013). Genomics analysis of potassium channel genes in songbirds reveals molecular specializations of brain circuits for the maintenance and production of learned vocalizations. *BMC Genomics* **14**, 470.

Lovell, P. V., Clayton, D. F., Replogle, K. L. and Mello, C. V. (2008). Birdsong "transcriptomics": neurochemical specializations of the oscine song system. *PLoS ONE* **3**, e3440.

Luetje, C. W., Piattoni, M. and Patrick, J. (1993). Mapping of Ligand-Binding Sites of Neuronal Nicotinic Acetylcholine-Receptors Using Chimeric Alpha-Subunits. *Mol. Pharmacol.* **44**, 657–666.

Mardia, K. V., Kent, J. T. and Bibby, J. M. (1979). *Multivariate analysis*. London ; New York : Academic Press.

Matsumoto, A., Arnold, A. P., Zampighi, G. A. and Micevych, P. E. (1988). Androgenic regulation of gap junctions between motoneurons in the rat spinal cord. *Journal of Neuroscience* **8**, 4177–4183.

McIntosh, J. M., Dowell, C., Watkins, M., Garrett, J. E., Yoshikami, D. and Olivera, B. M. (2002). Alpha-conotoxin GIC from Conus geographus, a novel peptide antagonist of nicotinic acetylcholine receptors. *Journal of Biological Chemistry* **277**, 33610–33615.

McIver, E. L., Marchaterre, M. A., Rice, A. N. and Bass, A. H. (2014). Novel underwater soundscape: acoustic repertoire of plainfin midshipman fish. *J. Exp. Biol.* **217**, 2377–2389.

McKibben, J. R. and Bass, A. H. (1998). Behavioral assessment of acoustic parameters relevant to signal recognition and preference in a vocal fish. *J. Acoust. Soc. Am.* **104**, 3520–3533.

McMahon, L. L., Yoon, K. W. and Chiappinelli, V. A. (1994). Electrophysiological evidence for presynaptic nicotinic receptors in the avian ventral lateral geniculate nucleus. *Journal of Neurophysiology* **71**, 826–829.

Miles, G. B., Hartley, R., Todd, A. J. and Brownstone, R. M. (2007). Spinal cholinergic interneurons regulate the excitability of motoneurons during locomotion. *Proc Natl Acad Sci USA* **104**, 2448–2453.

Muennich, E. A. L. and Fyffe, R. E. W. (2004). Focal aggregation of voltage-gated, Kv2.1 subunit-containing, potassium channels at synaptic sites in rat spinal motoneurones. *The Journal of Physiology* **554**, 673–685.

Ophir, A. G., Schrader, S. B. and Gillooly, J. F. (2010). Energetic cost of calling: general constraints and species-specific differences. *Journal of Evolutionary Biology* **23**, 1564–1569.

Parra, G., Bradnam, K. and Korf, I. (2007). CEGMA: a pipeline to accurately annotate core genes in eukaryotic genomes. *Bioinformatics* **23**, 1061–1067.

Parra, G., Bradnam, K., Ning, Z., Keane, T. and Korf, I. (2009). Assessing the gene space in draft genomes. *Nucleic Acids Research* **37**, 289–297.

Pereda, A. E. (2014). Electrical synapses and their functional interactions with chemical synapses. *Nature Reviews Neuroscience* **15**, 250–263.

Perez, J., Tranque, P. A., Naftolin, F. and Garcia-Segura, L. M. (1990). Gap junctions in the hypothalamic arcuate neurons of ovariectomized and estradiol-treated rats. *Neuroscience Letters* **108**, 17–21.

Remage-Healey, L. and Bass, A. H. (2007). Plasticity in Brain Sexuality Is Revealed by the Rapid Actions of Steroid Hormones. *Journal of Neuroscience* **27**, 1114–1122.

Remage-Healey, L. and Bass, A. H. (2004). Rapid, hierarchical modulation of vocal patterning by steroid hormones. *J. Neurosci.* **24**, 5892–5900.

Remage-Healey, L. and Bass, A. H. (2006a). From social behavior to neural circuitry: Steroid hormones rapidly modulate advertisement calling via a vocal pattern generator. *Hormones and Behavior* **50**, 432–441.

Remage-Healey, L. and Bass, A. H. (2006b). A rapid neuromodulatory role for steroid hormones in the control of reproductive behavior. *Brain Research* **1126**, 27–35.

Remage-Healey, L. and Bass, A. H. (2009). Estradiol interacts with an opioidergic network to achieve rapid modulation of a vocal pattern generator. *J Comp Physiol A* **196**, 137–146.

Rice, A. N. and Bass, A. H. (2009). Novel vocal repertoire and paired swimbladders of the three-spined toadfish, Batrachomoeus trispinosus: insights into the diversity of the Batrachoididae. *Journal of Experimental Biology* **212**, 1377–1391.

Richardson, F. C. and Kaczmarek, L. K. (2000). Modification of delayed rectifier potassium currents by the Kv9.1 potassium channel subunit. *Hearing Research* **147**, 21–30.

Riede, T. and Goller, F. (2010). Peripheral mechanisms for vocal production in birds - differences and similarities to human speech and singing. *Brain Lang* **115**, 69–80.

Rittschof, C. C., Bukhari, S. A., Sloofman, L. G., Troy, J. M., Caetano-Anollés, D., Cash-Ahmed, A., Kent, M., Lu, X., Sanogo, Y. O., Weisner, P. A., et al. (2014). Neuromolecular responses to social challenge: common mechanisms across mouse, stickleback fish, and honey bee. *Proc. Natl. Acad. Sci. U.S.A.* **111**, 17929–17934.

Robinson, M. D. and Oshlack, A. (2010). A scaling normalization method for differential expression analysis of RNA-seq data. *Genome Biol* **11**, R25.

Robinson, M. D. and Smyth, G. K. (2007). Moderated statistical tests for assessing differences in tag abundance. *Bioinformatics* **23**, 2881–2887.

Robinson, M. D., McCarthy, D. J. and Smyth, G. K. (2010). edgeR: a Bioconductor package for differential expression analysis of digital gene expression data. *Bioinformatics* **26**, 139–140.

Rome, L. C. (2006). Design and function of superfast muscles: new insights into the physiology of skeletal muscle. *Annu. Rev. Physiol.* **68**, 193–221.

Rome, L. C., Syme, D. A., Hollingworth, S., Lindstedt, S. L. and Baylor, S. M. (1996). The Whistle and the Rattle: The Design of Sound Producing Muscles. *Proc. Natl. Acad. Sci. U.S.A.* **93**, 8095–8100.

Rubow, T. K. and Bass, A. H. (2009). Reproductive and diurnal rhythms regulate vocal motor plasticity in a teleost fish. *Journal of Experimental Biology* **212**, 3252–3262.

Rübsamen, R. and Betz, M. (1986). Control of echolocation pulses by neurons of the nucleus ambiguus in the rufous horseshoe bat, Rhinolophus rouxi. I. Single unit recordings in the ventral motor nucleus of the laryngeal nerves in spontaneously vocalizing bats. *J Comp Physiol A* **159**, 675–687.

Schmieder, R. and Edwards, R. (2011). Quality control and preprocessing of metagenomic datasets. *Bioinformatics* **27**, 863–864.

Schunter, C., Vollmer, S. V., Macpherson, E. and Pascual, M. (2014). Transcriptome analyses and differential gene expression in a non-model fish species with alternative mating tactics. *BMC Genomics* **15**, 1–13.

Sisneros, J. A., Forlano, P. M., Knapp, R. and Bass, A. H. (2004). Seasonal variation of steroid hormone levels in an intertidal-nesting fish, the vocal plainfin midshipman. *General and Comparative Endocrinology* **136**, 101–116.

Stacey, N. (2003). Hormones, pheromones and reproductive behavior. *Fish Physiology and Biochemistry* **28**, 229–235.

Stocker, M., Hellwig, M. and Kerschensteiner, D. (1999). Subunit assembly and domain analysis of electrically silent K+ channel alpha-subunits of the rat Kv9 subfamily. *Journal of Neurochemistry* **72**, 1725–1734.

Sturdy, C. B., Wild, J. M. and Mooney, R. (2003). Respiratory and telencephalic modulation of vocal motor neurons in the zebra finch. *J. Neurosci.* **23**, 1072–1086.

Team, R. C. (2014). *R: A Language and Environment for Statistical Computing. R Foundation for Statistical Computing, Vienna, Austria. Retrieved April 10, 2014*.

Walsh, P. J., Mommsen, T. P. and Bass, A. H. (1995). Biochemical and molecular aspects of singing in batrachoidid fishes. In *Biochemistry and Molecular Biology of Fishes.* (eds. Hochachka, P. W. and Mommsen, T. P., pp. 279–289.

Warren, W. C., Clayton, D. F., Ellegren, H., Arnold, A. P., Hillier, L. W., Künstner, A., Searle, S., White, S., Vilella, A. J., Fairley, S., et al. (2010a). The genome of a songbird. *Nature* **464**, 757–762.

Warren, W. C., Clayton, D. F., Ellegren, H., Arnold, A. P., Hillier, L. W., Künstner, A., Searle, S., White, S., Vilella, A. J., Fairley, S., et al. (2010b). The genome of a songbird. *Nature* **464**, 757–762.

Whitney, O., Pfenning, A. R., Howard, J. T., Blatti, C. A., Liu, F., Ward, J. M., Wang, R., Audet, J. N., Kellis, M., Mukherjee, S., et al. (2014). Core and region-enriched networks of behaviorally regulated genes and the singing genome. *Science* **346**, 1256780–1256780.

Wu, G., Fang, Y.-Z., Yang, S., Lupton, J. R. and Turner, N. D. (2004a). Glutathione metabolism and its implications for health. *J. Nutr.* **134**, 489–492.

Wu, G., Fang, Y.-Z., Yang, S., Lupton, J. R. and Turner, N. D. (2004b). Glutathione metabolism and its implications for health. *J. Nutr.* **134**, 489–492.

Yamaguchi, A., Kaczmarek, L. K. and Kelley, D. B. (2003). Functional specialization of male and female vocal motoneurons. *J. Neurosci.* **23**, 11568–11576.

Zagoraiou, L., Akay, T., Martin, J. F., Brownstone, R. M., Jessell, T. M. and Miles, G. B. (2009). A Cluster of Cholinergic Premotor Interneurons Modulates Mouse Locomotor Activity. *Neuron* **64**, 645–662.

Zhong, S., Joung, J.-G., Zheng, Y., Chen, Y.-R., Liu, B., Shao, Y., Xiang, J. Z., Fei, Z. and Giovannoni, J. J. (2011). High-throughput illumina strand-specific RNA sequencing library preparation. *Cold Spring Harb Protoc* **2011**, 940–949.

Appendix

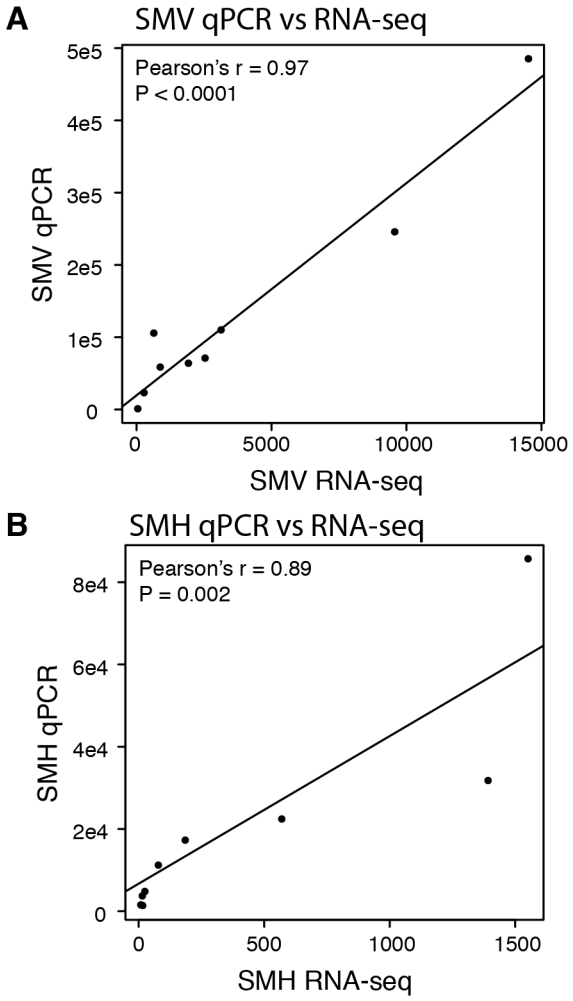

Figure S1
QPCR validation of RNAseq candidate gene expression. A) SMV qPCR values (copy numbers normalized by a reference gene) for nine candidate genes are significantly correlated with RNA-seq predicted values (FPKM). **B)** SMH qPCR values (copy numbers normalized by a reference gene) for nine candidate genes are significantly correlated with RNA-seq predicted values (FPKM).

Appendix (continued)

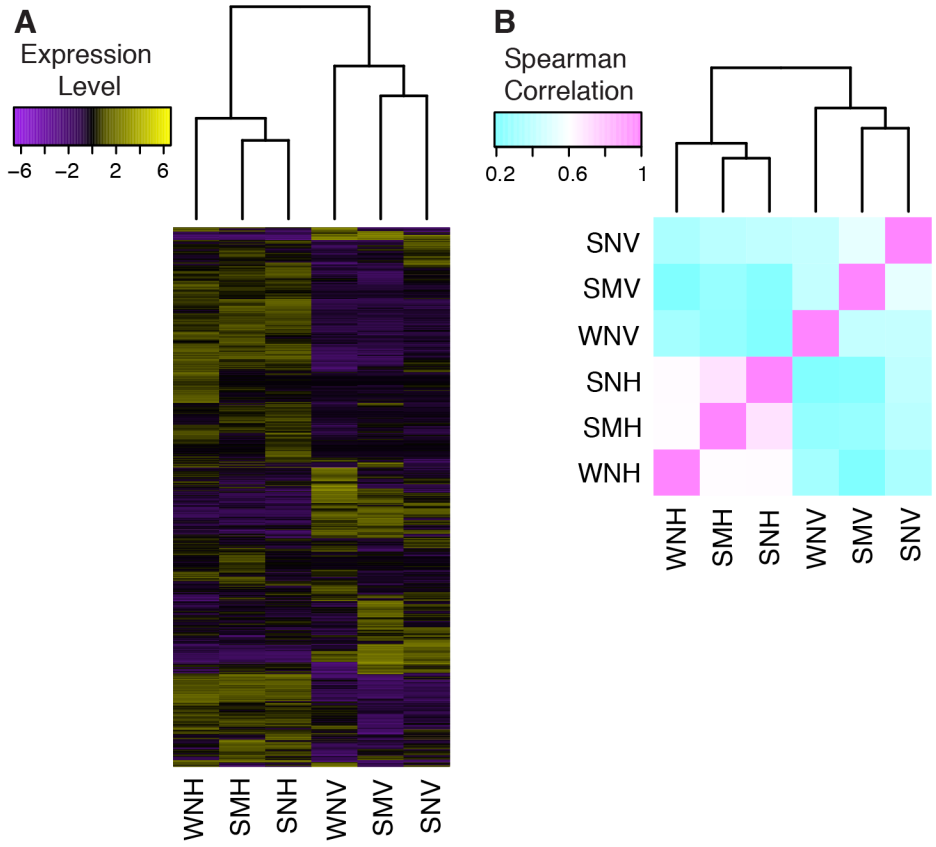

Figure S2
A) Heatmap of hierarchically clustered expression levels (median centered FPKM +1) of significantly differentially expressed transcripts based on the TMM-normalized dataset. Each line is a transcript, and each column is a sample group. Sample groups are hierarchically clustered based on their spearman correlation coefficients. **B)** Heatmap of pairwise Spearman correlation coefficients. Hindbrain sample groups show higher correlation of transcript expression patterns than VMN sample groups. See Fig. 4.1C for explanation of sample group abbreviations.